Biofidelity Report of the THOR 5th Percentile Anthropomorphic Test Device

Z. Jerry Wang

John Below

Brian Loeber

Breanna Greenlees

Humanetics Innovative Solutions, Inc.

July 30, 2018

NHTSA Contract number: DTNH2213D00301L/0045

Acknowledgements: John Bolte IV and Rakshit Ramachandra of Ohio State University

Jason Jenkins, Austin Kelly, Hyunjung Kwon of Transportation Research Center

Jason Luck of Duke University

REPORT DOCUMENTATION PAGE		Form Approved OMB No. 0704-0188
1. AGENCY USE ONLY (Leave blank)	2. REPORT DATE July 2018	3. REPORT TYPE AND DATES COVERED September 2015 – July 2018
4. TITLE AND SUBTITLE Biofidelity Report of the THOR 5th Percentile Anthropomorphic Test Device		5. FUNDING NUMBERS DTNH2213D00301L/0045
6. AUTHOR(S) Z. Jerry Wang, John Below, Brian Loeber, Breanna Greenlees		
7. PERFORMING ORGANIZATION NAME(S) AND ADDRESS(ES) Humanetics Innovative Solutions, Inc.		8. PERFORMING ORGANIZATION REPORT NUMBER
9. SPONSORING/MONITORING AGENCY NAME(S) AND ADDRESS(ES) U.S. Department of Transportation National Highway Traffic Safety Administration 1200 New Jersey Avenue, SE Washington, DC 20590		10. SPONSORING/MONITORING AGENCY REPORT NUMBER
11. SUPPLEMENTARY NOTES The Contract Officer Representative is Ellen Lee.		
12a. DISTRIBUTION/AVAILABILITY STATEMENT This document is available to the public through the National Technical Information Service, Springfield, VA 22161.		12b. DISTRIBUTION CODE

13. ABSTRACT (Maximum 200 words)

Three prototype anthropomorphic test devices (ATD) were fabricated in order to evaluate the biofidelity of a newly design THOR 5th percentile female ATD. This paper focuses on the biofidelity responses derived from testing one of these ATDs. There were a total of twenty-three biofidelity test conditions that included the head, neck, shoulder, thorax, abdomen, knee-thigh-hip complex, and lower extremity. Three repeated tests were conducted on a single ATD for each test condition. The biofidelity was objectively scored in accordance with NHTSA's Biofidelity Ranking System (BioRank). The BioRank score of each body region was scored and the overall BioRank score of the dummy (i.e. the average of all body regions) was less than 2.0, corresponding to "good" biofidelity.

14. SUBJECT TERMS			15. NUMBER OF PAGES 16. PRICE CODE
17. SECURITY CLASSIFICATION OF REPORT Unclassified	18. SECURITY CLASSIFICATION OF THIS PAGE Unclassified	19. SECURITY CLASSIFICATION OF ABSTRACT	20. LIMITATION OF ABSTRACT

EXECUTIVE SUMMARY

The Test Device for Human Occupant Restraint Fifth Female (THOR-05F) was developed by the National Highway Traffic Safety Administration (NHTSA) as an advanced frontal impact anthropomorphic test device (ATD), to address the ongoing problem of fatalities and injuries experienced by small female occupants in motor vehicles with modern restraints, such as airbags and force-limited seatbelts. The design of the THOR-05F was based on the design of the THOR-50M (50th percentile male advanced ATD), with some changes and new concepts that were described by Wang et al. (2017).

Biofidelity of a test dummy is a measure of the dummy's ability to mimic a human-like response in a crash environment. An assessment of biofidelity includes, but is not limited to, anthropometry, mass properties, joint properties (e.g., range of motion), and biomechanical response to impact. Impact biofidelity targets were established for the THOR-05F (Lee et al. 2019) to both guide the design of the hardware and assess the response of the ATD. The purpose of this report is to describe the methods used to conduct the biofidelity assessment as well as the results of those tests.

Twenty-three test conditions were evaluated, covering the head, neck, shoulder, thorax, abdomen, knee-thigh-hip (KTH) and lower extremities (Table 1). Multiple tests on a single THOR-05F ATD were used to evaluate each test condition. The biofidelity was objectively scored using NHTSA's Biofidelity Ranking System (BioRank).

Table 1. Biofidelity test matrix with test conditions appropriate for the THOR-05F

Body Region	Test	Impact Velocity	Impactor Mass	Impactor Face
Head	Head Impact	2.0 m/s	19.2 kg	152.4 mm disk
	Face Rigid Bar Impact	3.6 m/s	26.2 kg	Rigid Bar, Diameter 25 mm
	Face Rigid Disk Impact	6.7 m/s	10.7 kg	152.4 mm disk
Neck	Neck Frontal Flexion Response	15G Sled Acceleration		
	Neck Lateral Flexion Response (L & R)	7G Sled Acceleration		
	Torsion	500°/sec		
Thorax	Upper Ribcage Central Impact	4.3 m/s	14.0 kg	152.4 mm disk
	Lower Ribcage Oblique Impact (L & R)	4.3 m/s	14.0 kg	152.4 mm disk w/pad
Shoulder	Range of Motion/Stiffness Test	-	-	-
Abdomen	Upper Abdomen Impact	6.7 m/s	9.0 kg	Steering Wheel, Diameter 26.7 mm
	Lower Abdomen Impact	6.1 m/s	16.0 kg	Rigid Bar, Diameter 25 mm
	Belt Loading	4 m/s	-	-
Lumbar Spine	Flexion Pendulum Test	2.0 m/s	-	-
Knee-Thigh-Hip (KTH)	KTH Isolated Impact (L & R)	1.2 m/s	250 kg ram	Molded knee interface w/pad
	Whole Body KTH Impact	3.5 m/s	255 kg ram	Padded knee interface
	Knee Slider Impact (L & R)	2.15 m/s	7.26 kg	76.2 mm disk
Leg-Foot-Ankle	Axial Heel Impact (L & R)	3.1 m/s	28.4 kg	Padded Footplate
	Dynamic Dorsiflexion (L & R)	5.0 m/s	3.0 kg	NHTSA Impactor
	Inversion/Eversion (L & R)	1000°/sec	-	-
Full Body	Frontal sled test	30 km/h with 2 kN force-limiting belt		

BioRank for each test measurement was calculated and averaged when multiple repeat tests were conducted. An average of all ranked parameters in each test is the BioRank in that test condition. An average of all test conditions for each body region is the BioRank for that specific body region. The THOR-05F overall BioRank is the average of the BioRank of all body regions. The THOR-05F body regions were defined as head, neck, shoulder,

thorax, abdomen, knee-thigh-hip, and lower extremity. Results (Table 2) demonstrated overall "good" biofidelity according to the BioRank (BioRank between 1.0 and 2.0 is "good").

Table 2. Summary of body region BioRank

Body Region	BioRank	Biofidelity
Head	1.43	Good
Neck	2.20	Marginal
Shoulder	0.81	Excellent
Thorax	1.42	Good
Abdomen	2.03	Marginal
Knee-Thigh-Hip	1.31	Good
Lower	1.47	Good
Overall	**1.52**	**Good**

Table of Contents

1 Introduction

The Test Device for Human Occupant Restraint Fifth Female (THOR-05F) was developed by the National Highway Traffic Safety Administration (NHTSA) as an advanced frontal impact anthropomorphic test device (ATD), to address the ongoing problem of fatalities and injuries experienced by small female occupants in motor vehicles with modern restraints, such as airbags and force-limited seatbelts. The design of the THOR-05F was based on the design of the THOR-50M (50th percentile male advanced ATD), with some changes and new concepts that were described by Wang et al. (2017).

The final dummy design is described by a Drawing Package dated September 2019. One notable difference between the final dummy design described in the Drawing Package and the design described in Wang et al. (2017) is in the abdomen. The split abdomen described by Wang et al. (2017) was replaced by a single piece abdomen foam insert, due to issues with separation between the two original pieces. In this report, the ATDs and parts used in the biofidelity testing represent the final design documented in the September 2019 Drawing Package, except where noted.

The purpose of this report is to assess the impact biofidelity of the THOR-05F against the THOR-05F biomechanical response targets described in Lee et al. (2019). Lee et al. (2019) also described the mass and anthropometry specifications for the dummy. Those were assessed in Wang et al. (2017) and are not assessed in this report. For the ATD tests described in this report, the attempt was made to mimic the original human-based test conditions as closely as possible. Where possible, additional ATD setup and test procedures were also based on the appropriate qualification test procedures from the THOR-50M ATD. This report attempts to precisely document what was done in each test condition.

2 Biofidelity ranking procedures

ATD Biofidelity is evaluated by comparing the ATD responses against that of Post Mortem Human Subject (PMHS) or volunteers under various test conditions. The responses of the PMHS or volunteers were used to generate biofidelity corridors for multiple test modes. The 5th percentile female corridors were scaled from 50th percentile male when the responses of the female data were not available. The mean of the responses plus one standard deviation is defined as the upper biofidelity corridor, while the mean minus one standard deviation is defined as the lower corridor. The basis for the biofidelity corridors, and scaling where applicable, is documented in Lee et al. (2019). For BioRank evaluation, time zero was aligned with the method used to establish time zero in the original PMHS test data. In some cases, this resulted in a different definition of time zero than was used during the data collection procedure.

A score is given to each measured ATD response depending how well it matches the biofidelity corridor. To evaluate the ATD biofidelity, several approaches were developed in the past, such as ISO TR9790 method, CORA method and NHTSA method. The ISO TR9790 provided a guidance to calculate the biofidelity scores. If the ATD response is within the mean plus/minus one standard deviation of the biofidelity corridor, a score of 10 is given to such ATD response, 5 when it is within the mean plus/minus two standard deviations, and zero if it is beyond the mean plus/minus the two standard deviations. Gehre et al. (2009) introduced an alternative objective rating method of signals known as Correlation and Analysis (CORA). The method compares ATD responses against the biofidelity corridor which is comprised of inner and outer corridors. If the ATD response lies within the inner corridor, a score of 1 is assigned. A score of zero is assigned if the response lies outside the outer corridor. Between the two cases, linear, quadratic or cubic interpolation can be selected for its BioRank calculation. Rhule et al. proposed a method to calculate the BioRank in 2002 (NHTSA method) which included a weighting factor based on

injury priority. In 2009, Rhule et al. removed the weighting factor and began calculating the average BioRank by body segment. Then, an overall ATD BioRank could be determined by taking the average of all body segments. In 2013, Rhule et al introduced the phase into the BioRank calculation in addition to the shape of the response curve.

In this report, the method used in Rhule et al 2013 was chosen as the base for the BioRank calculation. This method includes ranks of shape and magnitude (SM), phase (P) and a composite score of both using a root mean square (RMS). In Rhule's calculation, only the upper 80% of the biofidelity corridor was used. Because this can eliminate important data in some cases, such as the toe-region of the knee slider response, it was proposed to include the entire time history of data. It was also observed in the data processing that cross correlation does not provide a meaningful result when the two data curves are not similar. To address this issue, a repetitive shift method was proposed. The repetitive shift method was used to find the Lowest Root Mean Square (LRMS) value. In summary, the following changes are made to the Rhule 2013 method (referred as Rhule 2013+).

1) Repetitive shift method was used to determine the Lowest Root Mean Square (LRMS) score instead of cross-correlation method.
2) All data were used in the BioRank calculation instead of upper 80% of the data.
3) Force vs deflection and/or moment vs rotation corridor was included in the BioRank calculation. The deflection and rotation was treated like time in the numerical calculation. The data was resampled with 0.1 mm or 0.1 degree interval before the calculation was carried out. Phase-shifting was not performed for force vs. deflection or moment vs rotation data (only SM score was calculated).
4) As part of the phase comparison (P value), the Acceptable Lag is found by shifting the PMHS mean curve in time with respect to itself. At each shift, the differences between the shifted curve and unshifted curve are calculated at the overlapping regions and summed. The phase shift required for the sum to exceed CCSD (Cadaver Cumulative Standard Deviation) is the Acceptable Lag. Since the PMHS mean curve has a finite length, the length of the overlapping regions between the shifted and unshifted curves decreases by two samples with each time shift. Therefore, in order to maintain the original PMHS curve length in the overlapping regions of the shifted and unshifted curves, the PMHS mean curve must be padded prior to shifting. The beginning of the curve is padded with the value of the first data point and the end of the curve is padded with the last data point.

The biofidelity was assessed based on the BioRank scores calculated according to the procedures above and summarized in Table 3.

Table 3. Biofidelity definition based on the BioRank score

Biofidelity	BioRank Score	Statistics Meaning
Excellent	BioRank ≤ 1.0	within ± 1 SD
Good	1.0 < BioRank ≤ 2.0	between ±1 SD and ±2 SD
Marginal	2.0 < BioRank ≤ 3.0	between ±2 SD and ±3 SD
Poor	BioRank > 3.0	outside ±3 SD

In the following sections, the BioRank test procedure and scores are presented by body segments. BioRank scores for each test metric were averaged to yield an overall test condition BioRank score. All test condition BioRank scores within a body segment were averaged to produce an overall body region BioRank. Accompanying plots showing comparison of test data to the biofidelity corridors are shown for each condition. In all subsequent plots, corridors are shown in black, while test data are shown in color (i.e. blue, red, green, yellow).

There are a few test conditions reported herein in which BioRank was not performed, specifically the neck frontal and lateral pendulum tests, neck torsion test, lumbar test, and full body sled test. The neck pendulum and torsion tests targets were derived from human-based data (Lee et al., 2019), but the available corridors did not represent a one standard deviation upper and lower bound. As this is a requirement for a meaningful BioRank score, these tests were excluded from the BioRank calculations. For the lumbar spine, no dynamic biofidelity data was available (Lee et al., 2019) and therefore targets were scaled from tests on the THOR-50M ATD. Again, BioRank is only meaningful when the ATD response is compared to a human-based response. Finally, the full body sled test was performed only to assess durability of the ATD. BioRank assessment for this condition may be made in the future but was not performed for this effort.

3 Head

Three tests were conducted for evaluation of the THOR-05F head: a frontal impact to the forehead by a rigid impactor, an impact to the face with a rigid bar at 3.6 m/s, and an impact to the face with a 152.4 mm rigid disk at 6.7 m/s.

Table 4. Summary of head test conditions

Test Condition	Input	ATD Identifier
Head	2.0 m/s, 19.2 kg mass, 152.4 mm diameter Impact point: 26 mm above nasion	Serial No. ED7441 Neck: REE2122*
Face Rigid Bar	3.6 m/s, 26.2 kg mass 25 mm diameter x 30 cm length Impact point: mid-line of left and right maxilla	Serial No. ED7448 Face: EJ2610 Neck: ED6992R
Face Disk	6.7 m/s, mass 10.7 kg 152.4 mm diameter, 12 mm edge radius Impact point: cheek and chin plates	Serial No. ED7448 Face: EJ2610 Neck: ED6992R

* **Note:** The neck rubber material used during the head impact test (serial no. REE2122) was natural rubber. Later in the program, the neck was changed to Butyl rubber due to the manufacturing difficulties. The later manufactured Butyl rubber neck had similar biofidelity responses to the natural rubber neck in sled test conditions. However, the head impact tests were not conducted with the final butyl neck due to the constraint of the program schedule.

3.1 Head Impact

3.1.1 Methods

3.1.1.1 Materials used

1. Fully assembled THOR-05F dummy
2. Impact probe with a mass of 19.207 kg, which included all attached hardware and 1/3 of the weight of the suspension cables. The impacting end of the probe, perpendicular and concentric with the longitudinal axis of the probe, had a flat, continuous, and non-deformable 152.4 mm diameter impact face with an edge radius of 12.7 mm.

3.1.1.2 Instrumentation

1. Impact velocity measuring instrumentation consists of a light trap and evenly spaced mechanical vanes that can generate square electrical pulse for velocity calculation.
2. Accelerometer for measuring the impactor acceleration; mounted to the probe with its sensitive axis in line with the longitudinal centerline of the test probe.
3. (3) Head accelerometers (A_X, A_Y, A_Z), mounted at the Center of Gravity (CG) of the head.
4. Tilt sensors mounted in the head to measure the initial angle about “X” and “Y” axis.
5. Tilt sensors mounting in the pelvis to measure the initial angle about “X” and “Y” axis.

3.1.1.3 Test Procedure

1. The head and neck assembly were inspected for wear, tears, or other damage.

2. Dummy was soaked in a controlled environment at a temperature between 20.6° to 22.2°C (69° to 72°F) and a relative humidity from 10 to 70% for a period of at least 4 hours prior to testing. The test environment had the same temperature and humidity as the soak environment.
3. The neck pitch change joint was kept in the neutral position.
4. The lower thoracic spine (LTS) pitch change joint was set to the slouched posture (Figure 1).

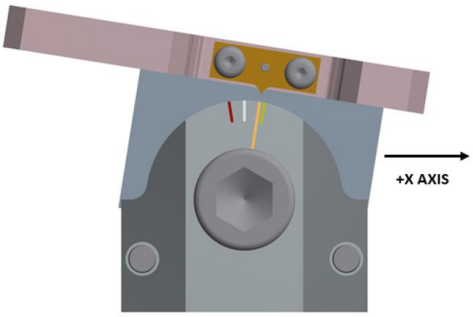

COLOR	RED	WHITE	ORANGE	YELLOW
POSTURE	ERECT	NEUTRAL	SLOUCHED	SUPER SLOUCHED
ANGLE	9°	0°	-9°	-12°

Figure 1. LTS Posture Setting

5. Joints were set to 1-2g setting.
6. Dummy was seated on a steel, horizontal surface (± 0.5°) that is flat, smooth, rigid, clean, and dry with no back support.
7. All limbs were extended forward in front of the torso. The arms were within ± 1° from horizontal. Arms were positioned so they did not interfere with the impact probe or suspension cables. Arm supports were used to help support the dummy.
8. The pelvis was set so the angle measured by the pelvis tilt sensor was approximately 8° in the Y-axis (rearward tilt about the Y-axis) and 0° laterally (about the X-axis). Target tilt angles were based on qualification tests using THOR-50M. Test setup parameters are shown in Table 6.
9. The impactor was placed so its longitudinal axis is aiming at a point on the forehead on the midsagittal plane and the head tipped forward approximately -29° (Figure 3), so the forehead plane was normal to the impact axis, and the axis passed through the head center-of-gravity as indicated by the notch on the side of the head skin.
10. The dummy was positioned so the head was just barely touching the impact probe with the probe at rest. ***NOTE:*** *Test probe centerline was horizontal (± 0.5°) at impact.*
11. At least 20 milliseconds of pre-time zero data and 20 milliseconds of post-time zero data was recorded.
12. The motion of the impactor was constrained so that there was no significant lateral, vertical, or rotational movement.
13. At least 60 minutes had passed since the last head, face, or neck test.
14. The probe was raised ~8” above the resting position to generate an impact velocity of 2 m/s. Actual impact velocities achieved are shown in Table 5.

Table 5. Velocities achieved in the three head impact tests

Test ID	610	612	613
Impact velocity	1.97 m/s	1.99 m/s	1.99 m/s

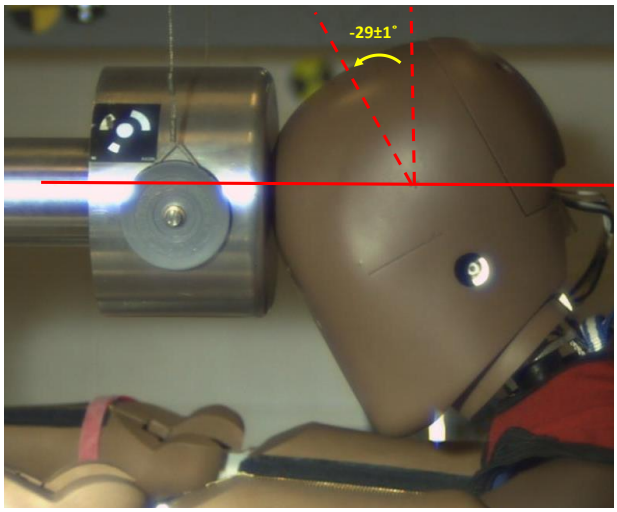

Figure 2. Setup for head impact

Table 6. Test setup parameters for head and face impacts

Parameter	Head Impact		Face Bar Impact		Face Disk Impact	
Neck Pitch Change Setting	"Neutral"		"Neutral"		"Neutral"	
LTS Pitch Change Setting	"Slouched"		"Erect"		"Erect"	
	X	Y	X	Y	X	Y
	-0.6°	-29.0	0.3	0.3	0.0	0.7
Head Tilt Sensor Reading(s)	0.5	-29.5	0.3	0.3	0.7	0.6
[in each of the three tests]:	0.5	-29.1	-0.4	0.5	-0.2	-0.5
	X	Y	X	Y	X	Y
Pelvis Tilt Sensor Reading(s)	-0.6	9.5	0.4	11.1	0.8	10.0
[in each of the three tests]::	0.2	7.1	0.4	11.1	0.1	9.8
	0.0	8.3	0.3	10.7	-0.5	9.5
Teflon® Sheeting on Test Bed?	No		No		No	
Dummy Clothing?	Jacket		Jacket		Jacket	
Wait Time Between Tests	60 minutes		30 minutes		30 minutes	

3.1.1.4 Data Processing

1. The polarity conventions and data acquisition system conformed to the latest requirements of SAE Recommended Practice J211.
2. Data channel offset removed per SAE J211 Section 8.4.3
3. Time zero (T_0) was defined when the accelerometer with a CFC-1000 response mounted on the probe rises through the 1g level. Note: Establishing time zero in a consistent manner for the test procedures allowed proper alignment and syncing of all data. For subsequent BioRank calculations, time zero was adjusted to align with how the original PMHS study defined time zero.
4. Channels were filtered based on the CFC filter classes listed in Table 7.

5. Time history of the Probe Force was calculated using the Probe Acceleration at each time step:

$$Force_{Probe}(N) = Acceleration_{Probe}(m/s^2) * Mass_{Probe}(kg)$$

6. Time history of the Head CG Resultant Acceleration was calculated using the acceleration components at each time step:

$$Head\ CG\ Resultant\ Acceleration = \sqrt{A_X^2 + A_Y^2 + A_Z^2}$$

Table 7. Head impact data channels

Item #	Channel Description	Filter Class	Comments
1	Probe Accelerometer	CFC-180	
2	Head CG Accelerometer, X-axis	CFC-1000	
3	Head CG Accelerometer, Y-axis	CFC-1000	
4	Head CG Accelerometer, Z-axis	CFC-1000	
5	Probe Force	N/A	Calculated
6	Head CG Resultant Acceleration	N/A	Calculated

3.1.2 Results

For the head impact test, the time zero, which was defined by the original PMHS study as the contact time between the impactor and the head, could not be determined precisely. The filtered data near time zero was distorted and made it impossible to determine the time zero. Multiple methods were considered for establishing time zero, including manual eyeball processing, 1g probe acceleration as time zero and align the peak with the middle point of the corridor. No significant difference was found between the manual processing and the peak alignment methods. The peak alignment method was selected to automate the process.

The head impact test result is shown in Figure 3. Due to the lack of corridor time history data, the peak value was used for the BioRank calculation. The BioRank for this test condition is 0.92, corresponding to "excellent" biofidelity.

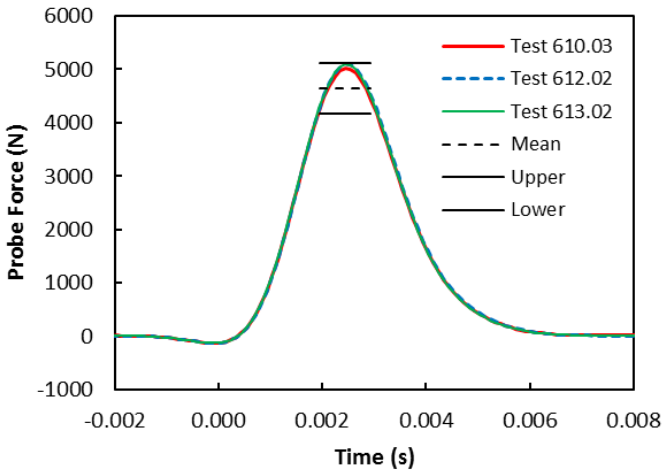

Figure 3. Probe force time history of head impact.

3.2 Face Rigid Bar Impact

3.2.1 Methods

3.2.1.1 Materials used

1. Fully assembled THOR-05F dummy
2. Impact probe with a mass of 26.192 kg, which includes all attached hardware and 1/3 of the weight of the suspension cables. The impacting end of the probe consisted of a rigid cylindrical impactor with a diameter of 25 mm and length of 300 mm.

3.2.1.2 Instrumentation

1. Instrumentation to measure impact velocity consists of a light trap and evenly spaced mechanical vanes that generate square electrical pulses for velocity calculation.
2. Accelerometer for measuring the impactor acceleration, mounted to the probe with its sensitive axis in line with its longitudinal centerline.
3. (3) Head accelerometers (A_x, A_y, A_z), mounted at the Center of Gravity (CG) of the head.
4. A dual-axis tilt sensor in the head to measure initial angles about the "X" and "Y" axes.
5. A dual-axis tilt sensor in the pelvis to measure initial angles about the "X" and "Y" axes.

3.2.1.3 Test Procedure

1. The face skin, the face element, and the head skin were inspected for wear, tears, or other damage.
2. Dummy was soaked in a controlled environment at a temperature between 20.6° to 22.2°C (69° to 72°F) and a relative humidity from 10 to 70% for a period of at least 4 hours prior to testing. The test environment had the same temperature and humidity as the soak environment.
3. The neck pitch change joint was kept in the neutral position.
4. The lower thoracic spine (LTS) pitch change joint was set to the erect posture position.
5. Joints were set to 1-2g setting.
6. The dummy was seated on a steel, horizontal surface (± 0.5°) that is flat, smooth, rigid, clean, and dry with no back support.
7. All limbs were extended horizontally and forward to the midsagittal plane (median plane) with the midsagittal plane vertical within ± 1°. Arms were positioned so they did not interfere with the impact probe or suspension cables. Arm supports were used to help support the dummy.
8. The head angle was positioned such that it was approximately 0° about the X and Y axis. Target tilt angles were based on qualification tests using THOR-50M. Test setup parameters are shown in Table 6.
9. The dummy was positioned so the centerline of the probe axis aligned with the dummy's midsagittal plane.
10. The dummy was adjusted so the impactor was centered at the mid-line of the left and right maxilla plates on face (Figure 4). This location is 43.0 mm below the head CG location. The face load cell plates (under the head skin) should be perpendicular to the impact direction.
11. The dummy was positioned so the face was just barely touching the impact probe with the probe at rest. The dummy was seated so the centerline of the probe axis aligned with the dummy's midsagittal plane. ***NOTE:*** *Test probe centerline was horizontal (± 0.5°) at impact*
12. At least 20 milliseconds of pre-time zero data and 20 milliseconds of post-time zero data was recorded.
13. The motion of the impactor was constrained so that there is no significant lateral, vertical, or rotational movement.
14. At least 30 minutes had passed since the last face, head, or neck test.

15. The probe was raised ~26” above the resting position to generate an impact velocity of 3.6 m/s. Actual velocities achieved are shown in Table 8.

Table 8. Velocities achieved in the face rigid bar impact tests

Test ID	1446	1447	1448
Impact velocity	3.60 m/s	3.60 m/s	3.64 m/s

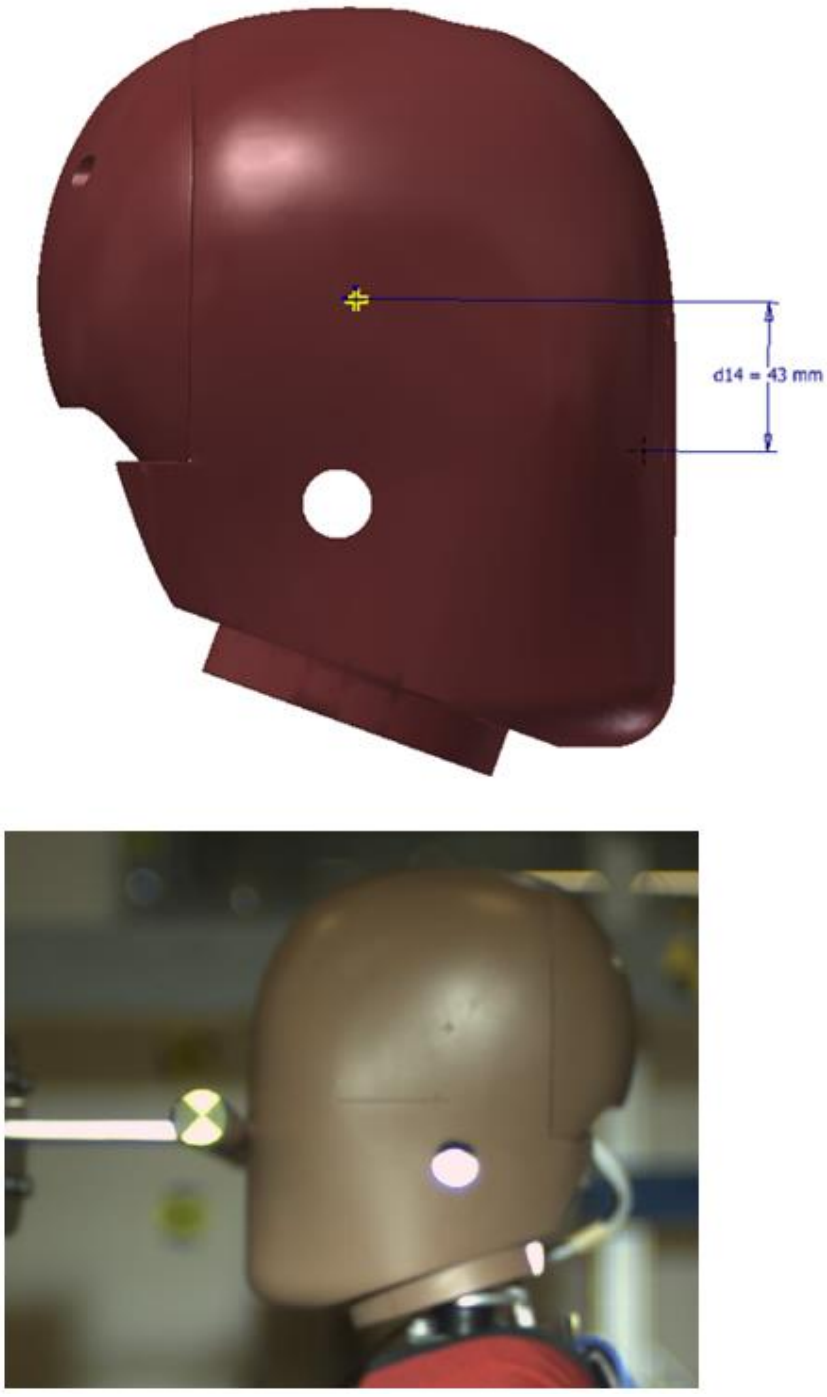

Figure 4. Setup of face impact test with rigid bar

3.2.1.4 Data Processing

1. The polarity conventions and data acquisition system conformed to the latest requirements of SAE Recommended Practice J1733 and J211 respectively.
2. Data channel offset removed per SAE J211 Section 8.4.3
3. Time zero (T_0) was defined when the accelerometer with a CFC-1000 response mounted on the probe rises through the 1g level.
4. Channels were filtered based on the CFC filter classes listed in Table 9.
5. Time history of the Probe Force was calculated using the Probe Acceleration at each time step:

$$Force_{Probe}(N) = Acceleration_{Probe}(m/s^2) * Mass_{Probe}(kg)$$

6. Time history of the Head CG Resultant Acceleration was calculated using the Acceleration components at each time step:

$$Head\ CG\ Resultant\ Acceleration = \sqrt{A_X^2 + A_Y^2 + A_Z^2}$$

Table 9. Face rigid bar impact data channels

Item #	Channel Description	Filter Class	Comments
1	Probe Accelerometer	CFC-180	
2	Head CG Accelerometer, X-axis	CFC-1000	
3	Head CG Accelerometer, Y-axis	CFC-1000	
4	Head CG Accelerometer, Z-axis	CFC-1000	
5	Probe Force	N/A	Calculated
6	Head CG Resultant Acceleration	N/A	Calculated

3.2.2 Results

Since the corridor is not a time history corridor, only the peak probe force value was used for this test condition. Response of the face bar impact test is shown in Figure 5. The BioRank for this test condition is 1.94, corresponding to “good” biofidelity.

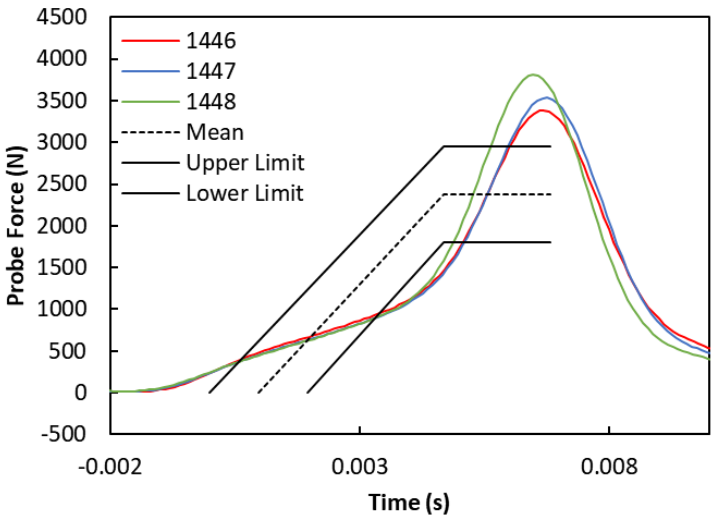

Figure 5. Probe force time history of facial bar impact.

3.3 Face Rigid Disk Impact

3.3.1 Methods

3.3.1.1 Materials used

1. Fully assembled THOR-05F dummy.
2. Impact probe with a mass of 10.708 kg, which includes all attached hardware and 1/3 of the weight of the suspension cables. The impact face was perpendicular and concentric with the longitudinal axis of the probe having a flat, continuous, and non-deformable 152.4 mm diameter impact face and an edge radius of 12.7 mm.

3.3.1.2 Instrumentation

1. Instrumentation to measure impact velocity consists of a light trap and evenly spaced mechanical vanes that generate square electrical pulses for velocity calculation.
2. Accelerometer for measuring the impactor acceleration, mounted to the probe with its sensitive axis in line with its longitudinal centerline.
3. (3) Head accelerometers (A_x, A_y, A_z), mounted at the Center of Gravity (CG) of the head.
4. A dual-axis tilt sensor in the head to measure initial angles about the “X” and “Y” axes.
5. A dual-axis tilt sensor in the pelvis to measure initial angles about the “X” and “Y” axes.

3.3.1.3 Test Procedure

1. The face skin, the face element, and the head skin were inspected for wear, tears, or other damage.
2. Dummy was soaked in a controlled environment at a temperature between 20.6° to 22.2°C (69° to 72°F) and a relative humidity from 10 to 70% for a period of at least 4 hours prior to testing. The test environment had the same temperature and humidity as the soak environment.
3. The neck pitch change joint was kept in the neutral position.
4. The lower thoracic spine (LTS) pitch change joint was set to the erect posture position.
5. Joints were set to 1-2g setting.
6. Dummy was seated on a steel, horizontal surface (± 0.5°) that is flat, smooth, rigid, clean, and dry with no back support.

7. All limbs were extended horizontally and forward to the midsagittal plane (median plane) with the midsagittal plane vertical within ± 1°. Arms were positioned so they did not interfere with the impact probe or suspension cables. Arm supports were used to help support the dummy.
8. The head angle was positioned such that it was approximately 0° about the X and Y axis. Target tilt angles were based on qualification tests using THOR-50M. Test setup parameters are shown in Table 6.
9. The dummy was positioned so the centerline of the probe axis aligned with the dummy's midsagittal plane.
10. The dummy was adjusted such that the center axis of the impact probe impacted between the cheek and chin while maintaining the setup angles for impact position. This location is 61.8 mm below the head CG location. The face load cells were parallel to the disk at point of contact (Figure 6).
11. The dummy was positioned so the face was just barely touching the impact probe with the probe at rest. ***NOTE:*** *Test probe centerline was horizontal (± 0.5°) at impact.*
12. At least 20 milliseconds of pre-time zero data and 20 milliseconds of post-time zero data was recorded.
13. The motion of the impactor was constrained so that there is no significant lateral, vertical, or rotational movement.

At least 30 minutes had passed since the last face, head, or neck test. The probe was raised ~91" above the resting position to generate an impact velocity of 6.7 m/s. Actual velocities achieved are shown in

14. Table 10.

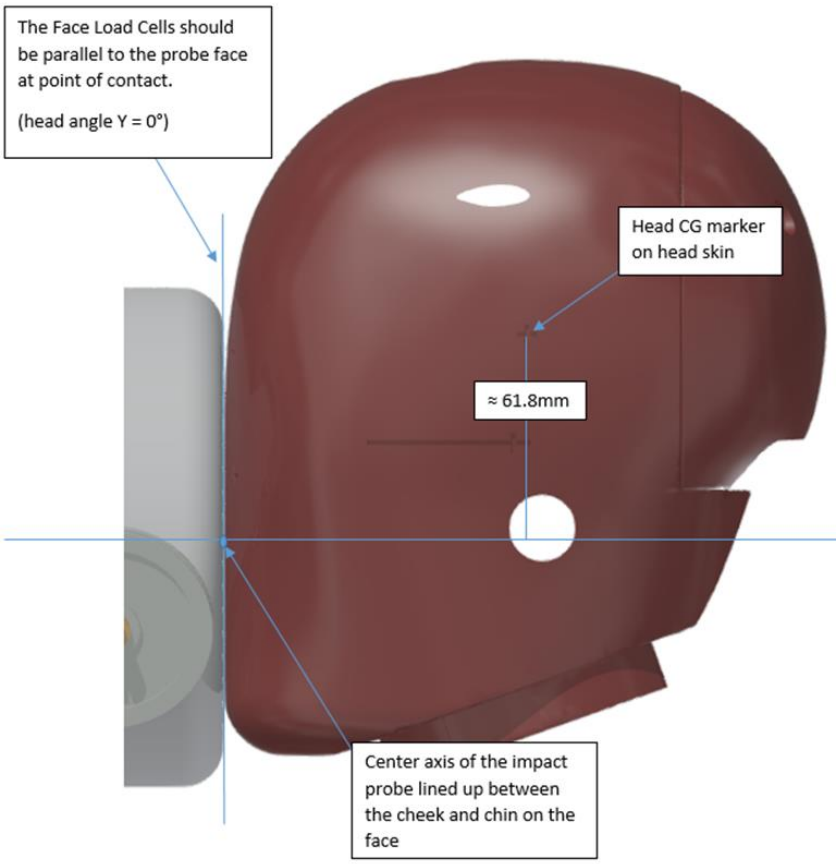

Figure 6. Setup for face rigid disk impact test

Table 10. Velocities achieved in the face rigid disk impact tests

Test ID	1435	1436	1437
Impact velocity	6.70 m/s	6.70 m/s	6.71 m/s

3.3.1.4 Data Processing

1. The polarity conventions and data acquisition system must conform to the latest requirements of SAE Recommended Practice J211.
2. Remove data channel offset per SAE J211 Section 8.4.3
3. Time zero (T_0) is defined when the accelerometer with a CFC-1000 response mounted on the probe rises through the 1g level.
4. Filter channels based on the CFC filter classes listed in Table 9.
5. Calculate the time history of the Probe Force using the Probe Acceleration at each time step:

$$Force_{Probe}(N) = Acceleration_{Probe}(m/s^2) * Mass_{Probe}(kg)$$

6. Calculate the time history of the Head CG Resultant Acceleration using the Acceleration components at each time step:

$$Head\ CG\ Resultant\ Acceleration = \sqrt{A_X^2 + A_Y^2 + A_Z^2}$$

Table 11. Face rigid disk impact data channels

Item #	Channel Description	Filter Class	Comments
1	Probe Accelerometer	CFC-180	
2	Head CG Accelerometer, X-axis	CFC-1000	
3	Head CG Accelerometer, Y-axis	CFC-1000	
4	Head CG Accelerometer, Z-axis	CFC-1000	
5	Probe Force	N/A	Calculated
6	Head CG Resultant Acceleration	N/A	Calculated

3.3.2 Results

Similar to the Face Bar Impact test, the peak probe force value was used for the BioRank calculation. The response of the face disk impact test is shown in Figure 7. The BioRank for this test is 1.42, corresponding to "good" biofidelity.

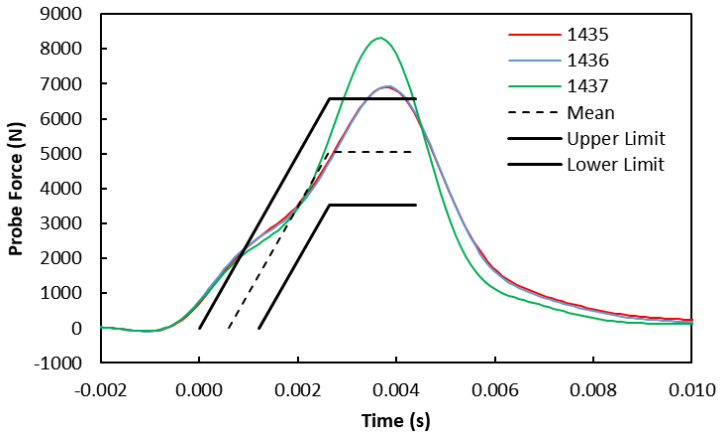

Figure 7. Probe force of the face disk impact test

3.4 Head Biofidelity Summary

The head BioRank scores are summarized in Table 12. The SM is the Shape and Magnitude BioRank, the P is the Phase BioRank and RMS is the Root Mean Square of SM and P as defined in Rhule et al. (2013). The head overall BioRank, an average of the scores from all test conditions, is 1.32, corresponding to "good" biofidelity.

Table 12. Head biofidelity summary

Test Condition	SM	P	RMS
Head Impact	0.92	N/A	0.92
Face Bar Impact	1.94	N/A	1.94
Face Disk Impact	1.42	N/A	1.42
Head Overall			**1.43**

4 Neck

There were multiple tests used for evaluating the biofidelity of the neck. The first were two mini-sled tests evaluating the forward flexion and lateral flexion of the neck. Two other tests utilized the neck and head assembly attached to the standard head-neck pendulum as defined in CFR Title 49, Part 572. The first pendulum test was a dynamic forward (flexion) bending of the head neck assembly about the local Y-axis. The second was a dynamic lateral flexion of the head neck assembly about the local X-axis. The final neck test, a torsion test, which is unique to THOR but similar to that of the Q3s, was conducted in the left and right directions to assess the response of the neck in dynamic rotation about its Z-axis.

Table 13. Summary of the neck biofidelity test conditions

Test Condition	Input	ATD Identifier
Frontal Sled	T1 acceleration Head is horizontal with 10° wedge at the mounting base to level the head	Neck: EH0497
Lateral Sled	T1 acceleration Head is horizontal with 10° wedge at the mount base	Neck: EH0497
Pendulum Flexion	5.0 m/s, Part 572 pendulum	Neck: EH0497
Pendulum Lateral	3.4 m/s, Part 572 pendulum	Neck: EH0497
Torsion	500° /sec, max rotation 95°	Neck: REE2122*

* **Note:** The neck rubber material used during the torsion test was the earlier natural rubber, which was not the final neck design. The natural rubber and Butyl rubber necks yielded similar response in the torsion qualification test and therefore the torsion biofidelity tests were not repeated on the Butyl rubber neck. The torsion qualification test was based on the THOR-50M torsion qualification test and is a different test procedure from the biofidelity test described herein.

4.1 Neck Setup Procedure

4.1.1.1 Description

Before the neck evaluation procedures were performed, the neck spring towers were properly installed, adjusted, and locked in place using the jam nuts at the top of the front and rear towers.

4.1.1.2 Materials

1. Fully assembled neck assembly (474-2000)
2. Fully assembled head assembly (474-1000)
3. Neck pendulum (as defined in CFR Title 49, Part 572)
4. Neck mounting plate with 10° offset to attach the lower neck load cell (or structural replacement) to the pendulum Figure 8.
5. 6" aluminum honeycomb hex cell 28.8kg/m^3 (1.8lb/ft^3) or equivalent used for decelerating the pendulum in flexion and extension
6. 3" aluminum honeycomb hex cell 28.8kg/m^3 (1.8lb/ft^3) or equivalent used for decelerating the pendulum in lateral and torsion

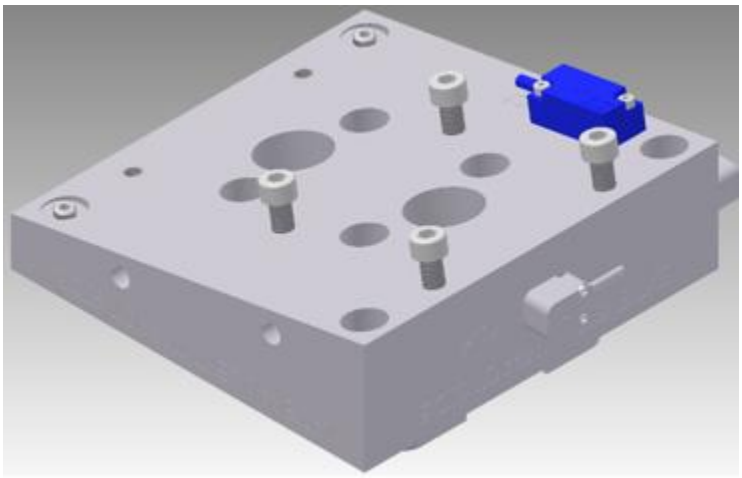

Figure 8. Neck mounting plate with 10° offset

4.1.1.3 Instrumentation

1. Instrumentation to measure impact velocity consists of a light trap and evenly spaced mechanical vanes that can generate square electrical pulse for velocity calculation.
2. Accelerometer for measuring the deceleration of the pendulum, mounted on pendulum as described in CFR Title 49, Part 572.
3. Angular rate sensor (ARS) mounted rigidly to the end of the pendulum arm such that it is perpendicular to the plane of motion of the pendulum's longitudinal axis (global Y-axis is recorded).
4. Head angular rate sensor (ARS) to measure ω_x (lateral), ω_y (flexion)
5. Upper neck load cell (F_x,F_z, M_x, M_y) (IH-11610J)
6. (2) Skull spring force load cells (Anterior and Posterior) in the neck (10386JS1I4)
7. Condyle potentiometer (9945)

4.1.1.4 Neck Pre-Test Setup Procedure

1. If necessary, remove the following:
   i. Head from the neck (474-1000)
   ii. Front and rear spring tubes (474-2303)
   iii. M5 x 0.8 thin profile jam nuts from the top of the front and rear spring cables
   iv. Stop assembly (474-2115)
2. Inspect the following components and replace or refurbish before proceeding with the assembly:
   i. Molded neck for tearing, debonding, or deformation
   ii. Front and rear cables for excessive fraying or kinks
   iii. Cable guides are intact and installed correctly

iv. Stop assembly rubber bumpers for excessive wear or other damage
v. Spring elements for wear

3. Place the neck mounting plate on a level surface.
4. Attach the neck assembly to the neck mounting plate.
5. Install 474-1031 sensor mounting plate from the head assembly onto the top of the neck assembly (without 474-2115 stop assembly).
6. Install a tilt sensor onto each of the following:
   i. Neck mounting plate
   ii. Upper neck plate
   iii. Head sensor mounting plate
7. Loosen both M5 x 0.8 thin profile adjustment nuts at the top of the front and rear spring cables until both springs are no longer under compression and the 474-2302 neck mounting platform is mostly free to rotate about the OC.
8. Adjust and stabilize the neck mounting plate so the tilt sensor reads 10.0 ± 0.2° about the Y-axis and 0 ± 0.5° about the X-axis
9. Manipulate the neck bend and adjust the 474-2302 neck mounting platform until both sensors are reading 0 ± 0.2° about the Y-axis and 0 ± 0.5° about the X-axis. Gently tighten the front and rear adjustment nuts to temporarily hold mounting platform orientation. ***NOTE:*** *Make sure neck bend is stable before continuing.*
10. Gently remove the 474-1031 head sensor mounting plate, install the 474-2115 stop assembly, and reattach the 474-1031 head sensor mounting plate.
11. Back off the front and rear adjustment nuts so there is no spring compression and confirm that the head and neck tilt sensors about the Y-axis are still 0 ± 0.2°. If not, repeat steps 7 and 8.
12. With zero compression on the front and rear neck cable load cells, acquire voltages for the front and rear skull spring load cells. ***NOTE*****:** *Load cells must have no applied pressure before balancing or else the output will be unintentionally offset.*
13. Gently tighten the front and rear adjustment nuts evenly until they both have 0.5-1.5 lbs (2.2-6.7 N) of applied force.
14. Reinstall front and rear jam nuts to lock adjustment nut position. ***NOTE:*** *Adjustment nut may move while jamming. Confirm that applied compression on both spring load cells is 0.5-1.5lbs (2.2-6.7N) with the head and neck Y-axis tilts still at 0 ± 0.2°.*
15. Remove the 474-1031 neck mounting platform and reinstall the 474-2303 spring tubes. Neck setup is complete (Figure 9 and Figure 10).

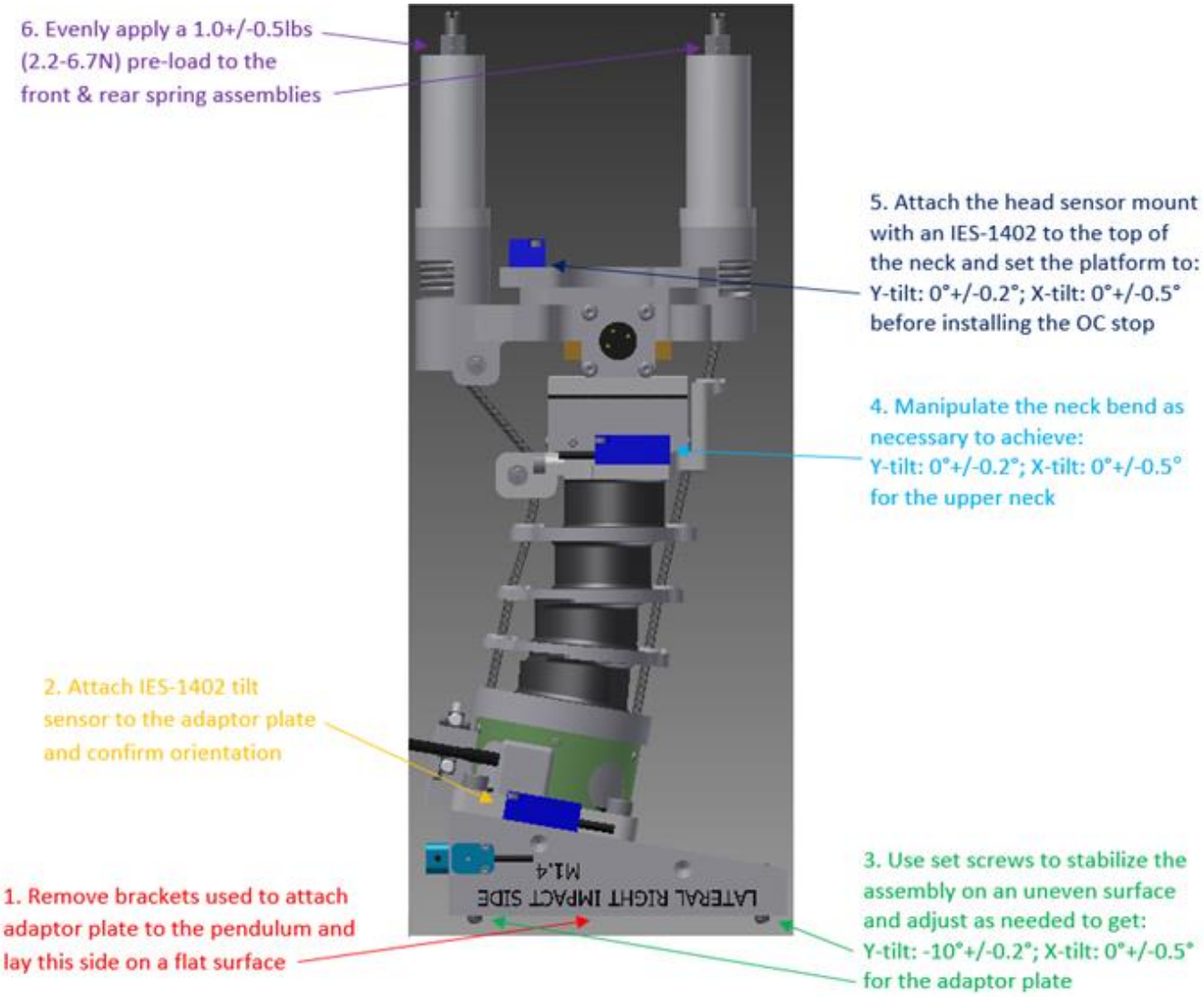

Figure 9. Visual summary of neck setup process using neck mounting plate with 10° offset

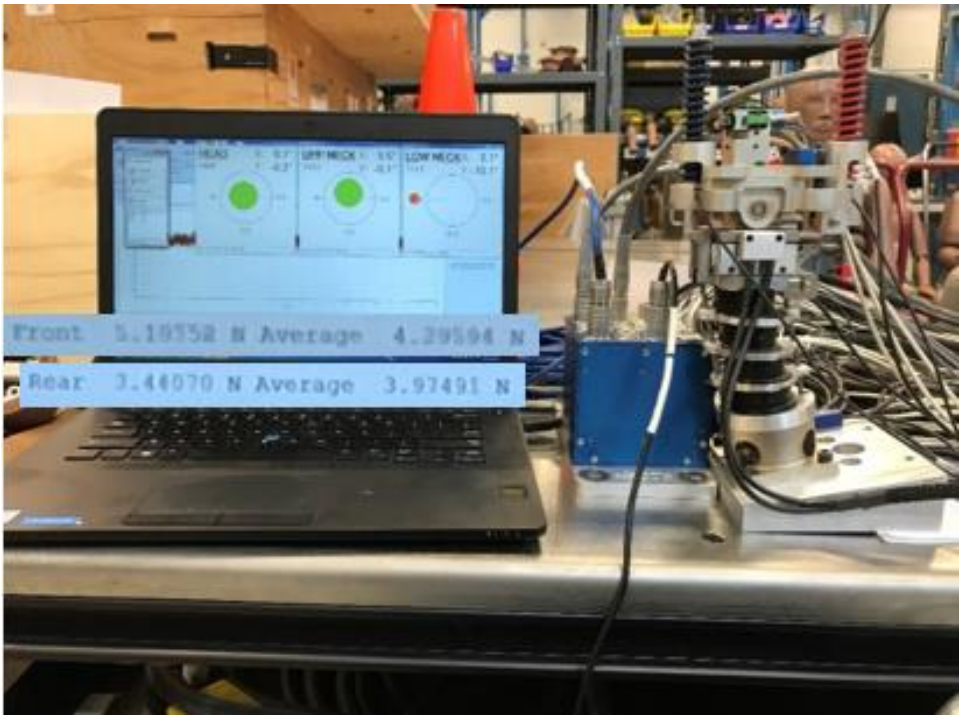

Figure 10. Complete neck setup

4.2 Neck Flexion and Neck Lateral Mini-Sled Tests

4.2.1 Methods

4.2.1.1 Materials

1. THOR-05F neck-head assembly (474-2000 and 474-1000)
2. Automated horizontal sled with programmable motion profiles
3. Lower neck-sled mounting adaptor
4. Cable spools
5. 3D position measuring device
6. Quadrant tracking stickers
7. Head restraint apparatus
8. Two high-speed cameras (at least 1000fps)
9. Light fixtures

4.2.1.2 Instrumentation

1. X, Y, Z-axis accelerometers for measuring the sled acceleration near the base of the neck.
2. (3) Head accelerometers (A_x, A_y, A_z), mounted at the Center of Gravity (CG) of the head.
3. (3) Head angular rate sensors (ω_x, ω_y, ω_z) mounted inside the head.
4. A dual-axis tilt sensor in the head to measure initial angles about the “X” and “Y” axes.
5. A dual-axis tilt sensor on the upper neck to measure initial angles about the “X” and “Y” axes.

4.2.1.3 Test Procedure

1. The neck assembly was soaked in a controlled environment at a temperature between 20.6° to 22.2°C (69° to 72°F) and a relative humidity from 10 to 70% for a period of at least 4 hours prior to testing. The test environment had the same temperature and humidity as the soak environment.

2. The 474-2000 neck assembly was mounted onto the center of the carriage using a 10° angled wedge. ***NOTE:*** *Upper neck was horizontal.*
3. If necessary, perform the THOR-05F Neck Setup Procedure.
4. Head and neck IES-1402 tilt sensors were installed.
5. The 474-1000 head assembly was installed onto the 474-2000 neck assembly with all desired instrumentation.
6. Cable spools were mounted to one end of the carriage using provided shoulder bolts. ***NOTE:*** *Exact placement is not important, but utilizing as much of the available space and evenly distributing the spools is generally most effective.*
7. On the other end of the carriage, the data acquisition system (DAS) was mounted and grounded.
8. The location of coordinate system defining targets about 3D space was accurately measured. ***NOTE:*** *These values were used to calibrate the high-speed camera video analysis.*
9. One quadrant tracker was placed sticker on the CG of the head, one at the OC, and two across the sled to form a horizontal reference line.
10. Some slack was left in the cables near the head so it could rotate freely. The extra cable lengths were secured using the spools, carriage anchors, and cable ties including any necessary adaptor cables.
11. For the flexion test, the head restraint apparatus was installed (Figure 11)

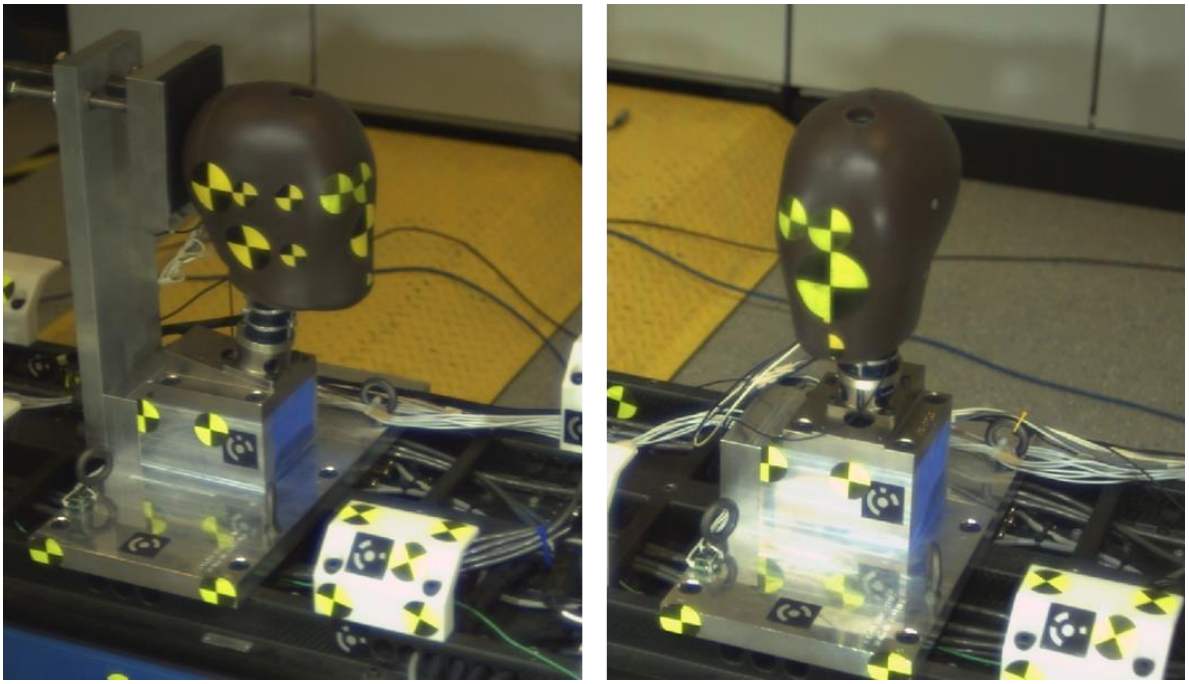

Figure 11. Neck sled test setup: Flexion has an installed head restraint (left); Lateral bending tested without head restraint (right).

12. Power and communication cables were plugged into the DAS.
13. The two high-speed cameras and light fixtures were powered up.
14. The position and angle of the cameras and lights were adjusted so the full range of motion for the test profile was visible with both cameras approximately 45° apart. Focus on the cameras was adjusted to achieve optimum clarity.
15. The high-speed cameras were set to 1000 frame per second (fps) with a 'START' trigger.

16. The cameras were armed using a trigger that sent a signal to the DAS. ***NOTE:*** *Camera trigger signal was used for syncing camera images to data collected by DAS.*
17. The initial head tilt angles were adjusted to meet the following requirements and record values:

Flexion

About X: 0 ± 1°

About Y: 0 ± 1° (when head is pressed against the head restraint)

Lateral

About X: 0 ± 1°

About Y: N/A (Head leans slightly forward due to weight of head assembly)

18. At least one second of pre-trigger and five seconds of post-trigger data collection was recorded.
19. Once the DAS was waiting for trigger, the tilt sensors cables and the power/communication cables were disconnected from the DAS.
20. The sled test input configuration shown below was loaded (Figure 12):

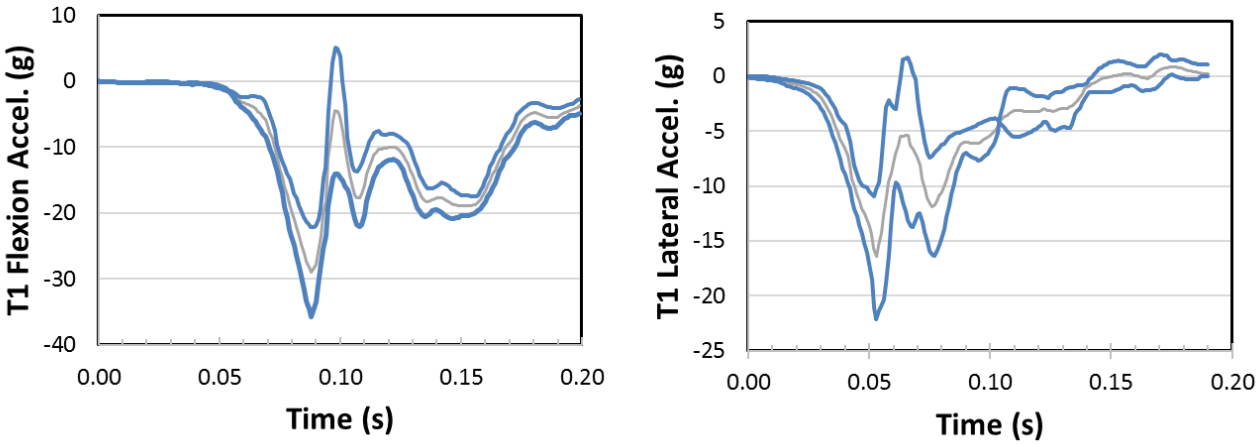

Figure 12. Neck flexion pulse (left) and Neck lateral flexion pulse (right)

21. The sled launch sequence began; cameras were triggered when the countdown reached one second.
22. At least 30 minutes elapsed between tests on the same neck.

4.2.1.4 Data Processing

1. The polarity conventions and data acquisition system conformed to the latest requirements of SAE Recommended Practice J211.
2. Data channel offset removed per SAE J211 Section 8.4.3
3. Time zero (T0) was defined when the target motion profile begins.
4. Channels filtered based on the CFC filter classes listed in **Table 14**.
5. Time history of the Head CG Resultant Acceleration was calculated:

$$Head\ CG\ Resultant\ Acceleration = \sqrt{A_X^2 + A_Y^2 + A_Z^2}$$

Table 14. Neck sled test data channels

Item #	Channel Description	Filter Class	Comments
1	T1 Accelerometer, X-axis	CFC-1000	
2	T1 Accelerometer, Y-axis	CFC-1000	
3	T1 Accelerometer, Z-axis	CFC-1000	
4	Head CG Accelerometer, X-axis	CFC-1000	
5	Head CG Accelerometer, Y-axis	CFC-1000	
6	Head CG Accelerometer, Z-axis	CFC-1000	
7	Head Angular Velocity about X-axis	N/A	
8	Head Angular Velocity about Y-axis	N/A	
9	Head CG Resultant Acceleration	N/A	Calculated

4.2.2 Frontal Mini-sled Results

To determine the time zero for this test mode, the T1 sled pulse was aligned in time with the T1 corridor mean at -10g. The time coincident with the corridor time zero was defined as the time zero for all test data channels. The displacement magnitude was adjusted so that its value at time zero matches the initial value of the corresponding corridor mean before the BioRank was calculated. The head motions, including the head linkage angle, the neck linkage angle, and the head center of gravity (CG) motion were analyzed from the video. No filter was applied to the video data. The head linkage angle was calculated using targets placed at the head CG and the occipital condyle (OC). The neck linkage angle could not be calculated directly because, unlike the volunteer human subject testing, a target could not be placed exactly at the T1 location for motion analysis (this would be on the rubber portion of the neck). Instead, the coordinates at the OC were used to calculate the neck linkage angle.

The anatomical landmarks used to measure neck response variables differs between the volunteer/PMHS study (Thunnissen et al. 1995) and the THOR-05F. The THOR-05F was designed according to the UMTRI AMVO 5th percentile female anthropometry specification (Schneider et al. 1983). To compare the data, the head CGs were aligned and the coordinates were mapped into a coordinate system with origin at T1 of the volunteer/PMHS samples. The coordinates of Thunnissen et al 1995 and the AMVO (Schneider et al. 1983) are shown in

Table 15. Since it is reasonable to assume there is no motion before the pulse is applied, the initial position is used to locate the head CG in the Thunnissen T1 coordinate system.

Table 15. Coordinates of the landmarks in head and neck

UMTRI Coordinate System	X	Y	Z
OC	-189	0	519
Head CG	-184	0	578
T1	-183	0	429
UMTRI T1 to UMTRI CG	1	0	-149
UMTRI OC to UMTRI CG	-5	0	-59
Thunnissen T1 to Thunnissen CG	-27.9	0	-166.9
Coordinates After Aligning Thunnissen Head CG with UMTRI Head CG			
UMTRI T1 to Thunnissen T1	28.9	0	17.9
UMTRI OC to Thunnissen T1	22.9	0	107.9
CG to Thunnissen T1	27.9	0	166.9

After aligning the two datasets at the head CG, the Thunnissen T1 location in the UMTRI AMVO coordinate system is shown in Figure 13.

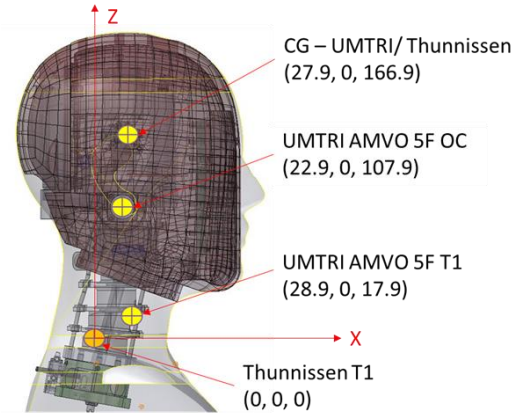

Figure 13. Landmarks overlay of scaled Thunnissen et al 1995 and UMTRI AMVO 5F with CG aligned

Due to the difficulty of physically attaching a target on the T1 location, the neck linkage angle could not be measured from the video analysis. Instead, the OC coordinates are calculated in reference to the Thunnissen T1 coordinate system. The rotation angle is calculated with the following formula.

$$\theta_y = \arctan(z/x)$$

For the neck frontal sled tests, the resultant acceleration of head center of gravity (CG), head linkage angle (head CG to occipital condyle), neck linkage angle (occipital condyle to T1), CG displacement in both x and z directions were evaluated. The sled input achieved is shown in Figure 14 and the responses of the neck are shown in Figure 15 through Figure 20. In the test, a head rest was needed to keep head in position during the pretest motion. During rebound, the head hit the head rest, which caused a spike in the head acceleration, see Figure 20. The BioRank calculation for the head acceleration was carried out only to the 0.22 millisecond to exclude the acceleration spikes.

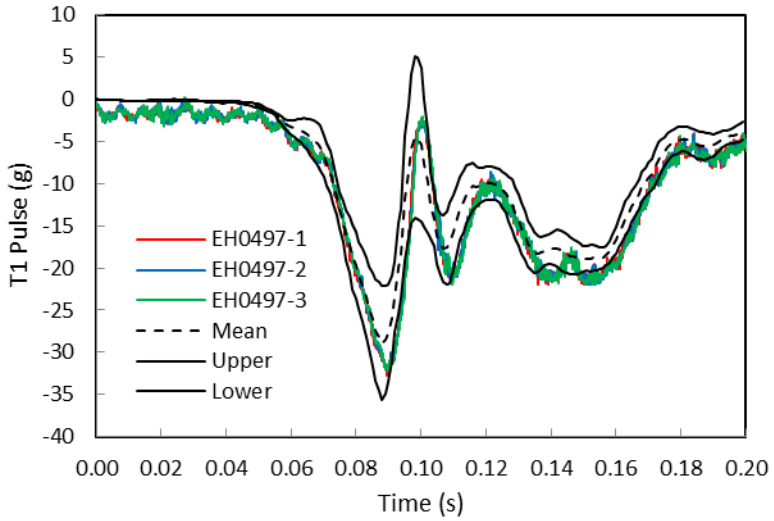

Figure 14. Neck frontal sled pulse (T1 pulse from NBDL test)

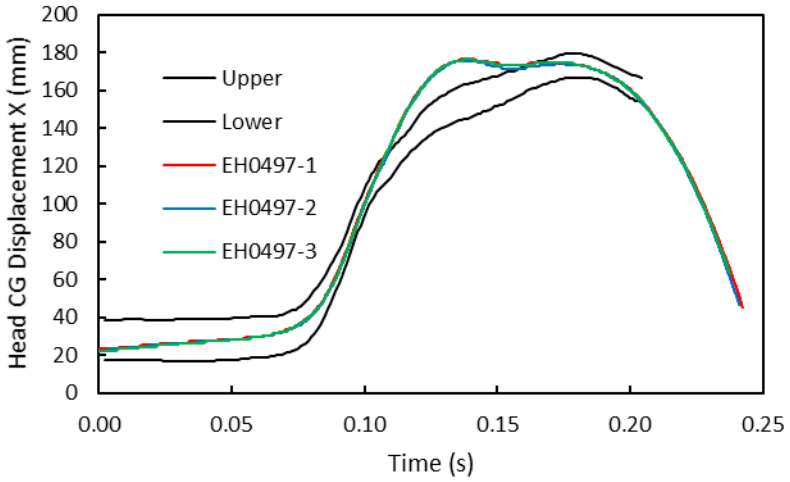

Figure 15. Head CG displacement in x direction of the neck frontal sled test

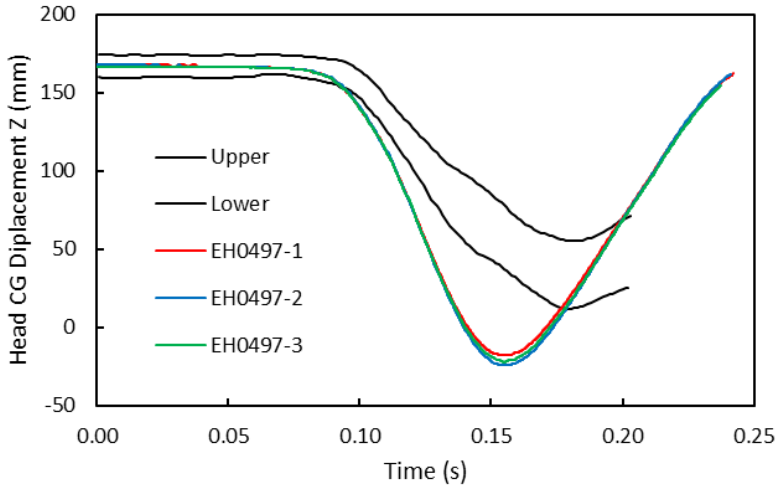

Figure 16. Head CG displacement in z direction of the neck frontal sled test

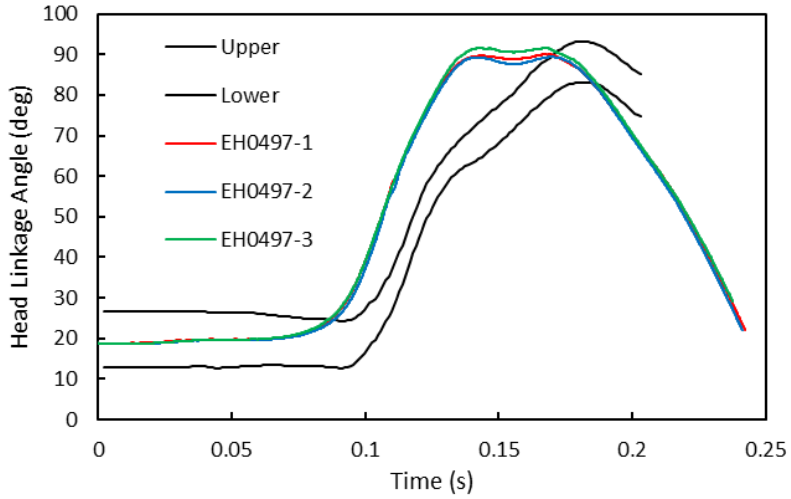

Figure 17. Head linkage angle of the neck frontal sled test

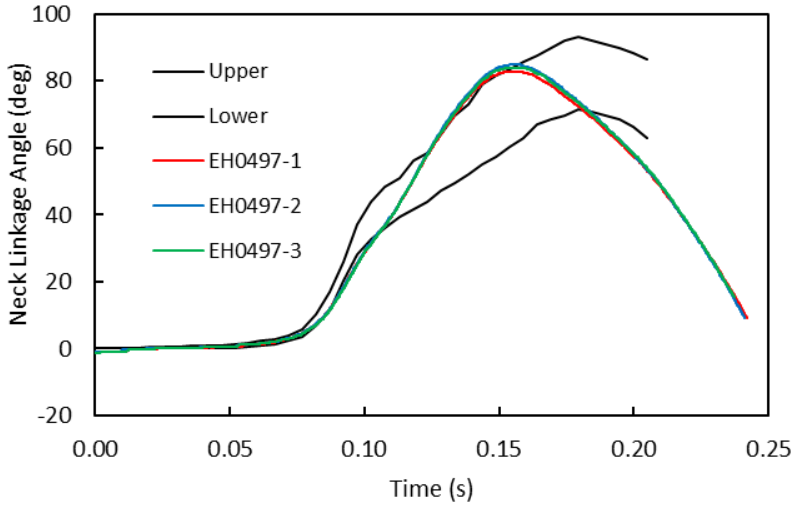

Figure 18. Neck linkage angle of the neck frontal sled test

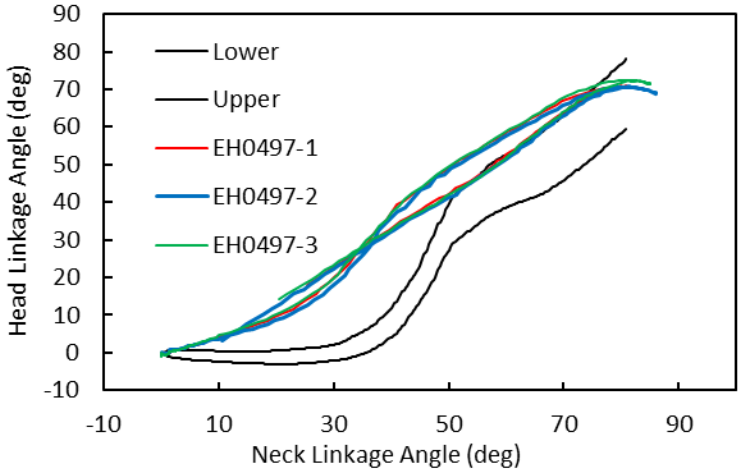

Figure 19. Head linkage angle vs neck linkage angle of the neck frontal sled test

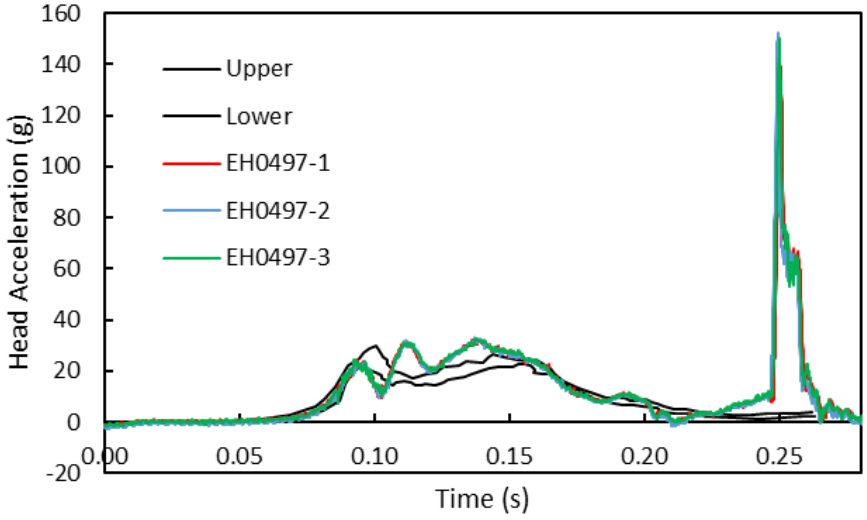

Figure 20. Head resultant acceleration of the neck frontal sled test

4.2.3 Lateral Mini-sled Results

For the neck lateral sled test, head CG displacements in y and z directions, and head linkage angle (head CG to OC joint) were evaluated. The test time zero was determined with the same method used in neck frontal sled test. The sled input achieved is shown in Figure 21 and the responses of the neck are shown in Figure 22 through Figure 24.

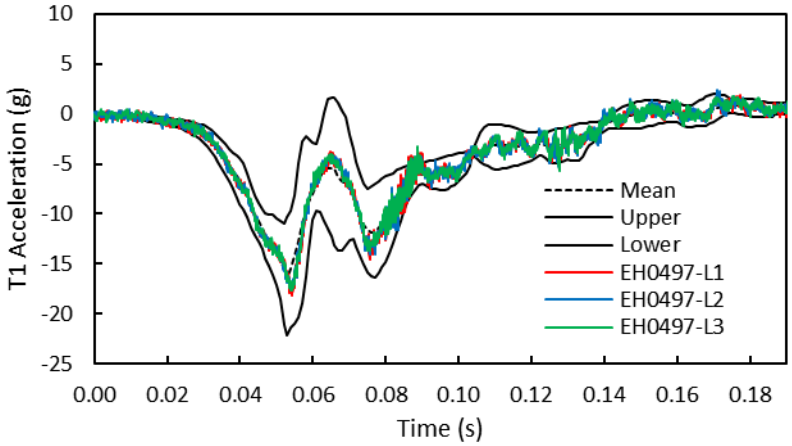

Figure 21. Sled pulse of neck lateral sled test (NBDL T1 pulse)

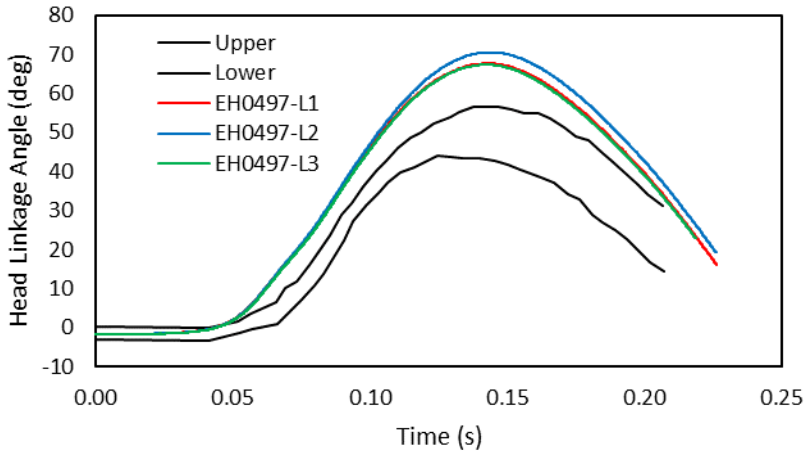

Figure 22. Head linkage angle of neck lateral sled test

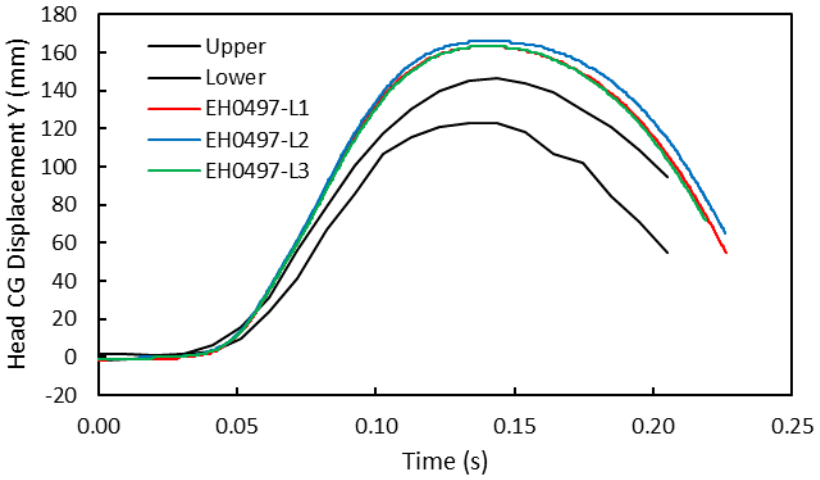

Figure 23. Head CG displacement in y direction of neck lateral sled test

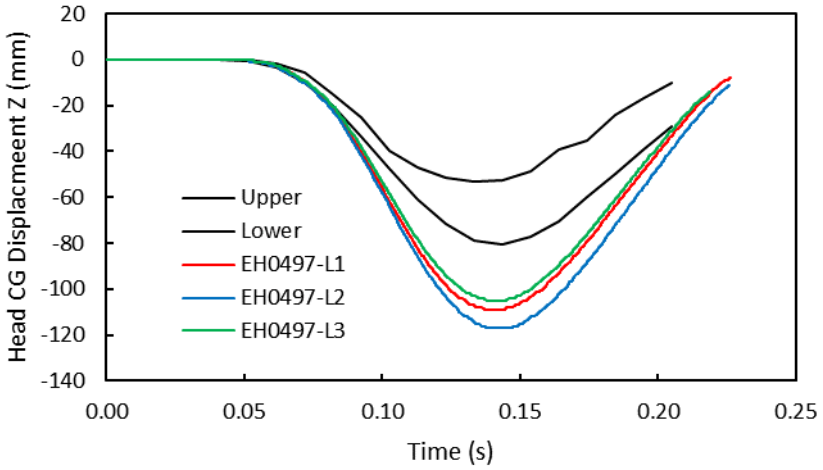

Figure 24. Head CG displacement in z direction of neck lateral sled test

4.3 Neck Flexion Dynamic Response with Pendulum

4.3.1 Methods

4.3.1.1 Test Procedure

1. Neck assembly was soaked in a controlled environment at a temperature between 20.6° to 22.2°C (69° to 72°F) and a relative humidity from 10 to 70% for a period of at least 4 hours prior to testing. The test environment had the same temperature and humidity as the soak environment.
2. The “Neck Pre-Test Setup Procedure” was completed.
3. The head assembly was installed onto the neck.
4. The neck mounting plate was attached to the bottom of the pendulum arm such that the thickest side of the wedge was facing away from the direction of impact.
5. The head-neck assembly was rigidly attached to the neck mounting plate such that the front edge of the lower neck was aligned with the leading edge of the pendulum arm with the forehead facing the direction of impact (Figure 25).
6. The neck instrumentation cables were mounted to the pendulum with sufficient slack so the cables did not become taut during the test and did not interfere with the motion of the head.

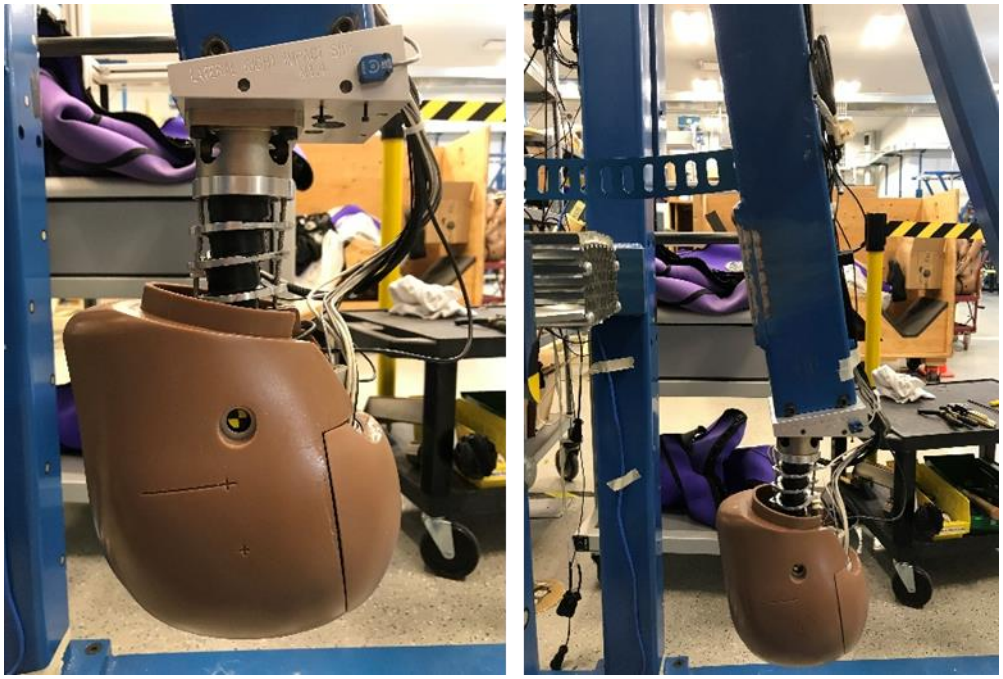

Figure 25. Neck flexion neck to neck plate alignment (left); Neck flexion test setup (right)

7. The 6" aluminum honeycomb (hex cell) used to decelerate the pendulum was mounted. The pulse criteria targets are specified in Table 16, along with the actual velocities achieved in the three tests. Time zero (T_0) defined as when the accelerometer with a CFC-1000 response mounted on the pendulum rose through the 1g level.

Table 16. Neck flexion deceleration pulse targets and values achieved in the three tests

Parameter	Target (m/s)	Achieved
Pendulum Velocity at 8ms after T0	1.62	1.38 1.46 1.36
Pendulum Velocity at 16ms after T0	3.33	3.05 3.05 2.94
Pendulum Velocity at 24ms after T0	4.83	4.52 4.54 4.40

8. At least 20 milliseconds of pre-time zero data and 200 milliseconds of post-time zero data were recorded.
9. At least 30 minutes had passed since the last face, head, or neck test.
10. The pendulum was raised ~75° from vertical to generate an impact velocity of 5.0 m/s. Actual impact velocity achieved are shown in Table 17. ***NOTE:*** *After the test was complete, the pendulum was allowed to hang close to vertical until the next test was ready to be run. This prevents the neck from experiencing undesired bending.*

Table 17. Impact velocities achieved in the neck flexion pendulum tests

Test ID	1336	1337	1338
Impact velocity	5.03 m/s	5.03 m/s	5.03 m/s

4.3.1.2 Data Processing

1. The polarity conventions and data acquisition system conformed to the latest requirements of SAE Recommended Practice J211.
2. Data channel offset removed per SAE J211 Section 8.4.3.
3. The polarity of the pendulum ARS was set such that the angular velocity of the pendulum as it fell towards the decelerator was positive.
4. Channels were filtered based on the CFC filter classes listed in Table 18.
5. Pendulum velocity was calculated using the pendulum accelerometer:

$$Pendulum\ X\ Velocity = \int_{t_0}^{t_f} Pend_{X\ ACCEL} dt$$

$where\ t_0\ and\ t_f\ are\ the\ first\ and\ last\ time\ points, respectively, for\ data\ collection.$

6. Head rotation relative to the pendulum was calculated:

$$Head\ Rotation = \int_{t_0}^{t_f} Head_{VY} - Pend_{VY} dt$$

$where\ t_0\ and\ t_f\ are\ the\ first\ and\ last\ time\ points, respectively, for\ data\ collection$

7. Neck moment about the OC was calculated: See calculation in Appendix 1 (14.1).

Table 18. Neck flexion data channels

Item #	Channel Description	Filter Class	Comments
1	Pendulum Accelerometer	CFC-60	
2	Pendulum Angular Velocity	CFC-60	
3	Head Angular Velocity about Y-axis	CFC-60	
4	Upper Neck Force, X-axis	CFC-1000	
5	Upper Neck Force, Z-axis	CFC-1000	
6	Upper Neck Moment, Y-axis	CFC-600	
7	Posterior Skull Spring, Z-axis	CFC-1000	
8	Occipital Condyle (OC) Potentiometer	CFC-180	
9	Head Rotation	N/A	Calculated
10	Pendulum Velocity	N/A	Calculated
11	Moment about OC	N/A	Calculated

4.3.2 Results

The neck pendulum test moment vs rotation responses for frontal flexion is shown in Figure 26.

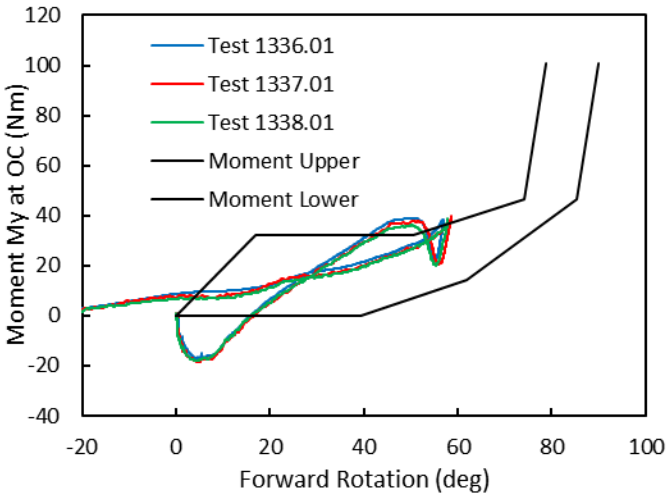

Figure 26. Moment vs head rotation of neck frontal flexion pendulum test

4.4 Neck Lateral Flexion Dynamic Response with Pendulum

4.4.1 Methods

4.4.1.1 Test Procedure

1. The neck assembly was soaked in a controlled environment at a temperature between 20.6° to 22.2°C (69° to 72°F) and a relative humidity from 10 to 70% for a period of at least 4 hours prior to testing. The test environment had the same temperature and humidity as the soak environment.
2. The "Neck Pre-Test Setup Procedure" was completed.
3. The head assembly was installed onto the neck.
4. The neck mounting plate was attached to the bottom of the pendulum arm such that the thickest side of the wedge was facing 90 ± 0.5° offset from the direction of impact (Figure 27).
5. The head-neck assembly was rigidly attached to the neck mounting plate such that the rear edge of the lower neck was aligned with the thickest side of the wedge. ***NOTE:*** *OC was aligned with the longitudinal centerline of the pendulum arm*.
6. The neck instrumentation cables was secured to the pendulum with sufficient slack so the cables did not become taut during the test, but did not interfere with the motion of the head.

The 3" aluminum honeycomb (hex cell) used to decelerate the pendulum was mounted. Pulse criteria targets are specified in

7. Table 19, along with the actual velocities achieved in the three left lateral tests and three right lateral tests. Time zero (T_0) defined as when the accelerometer with a CFC-1000 response mounted on the pendulum rises through the 1g level.

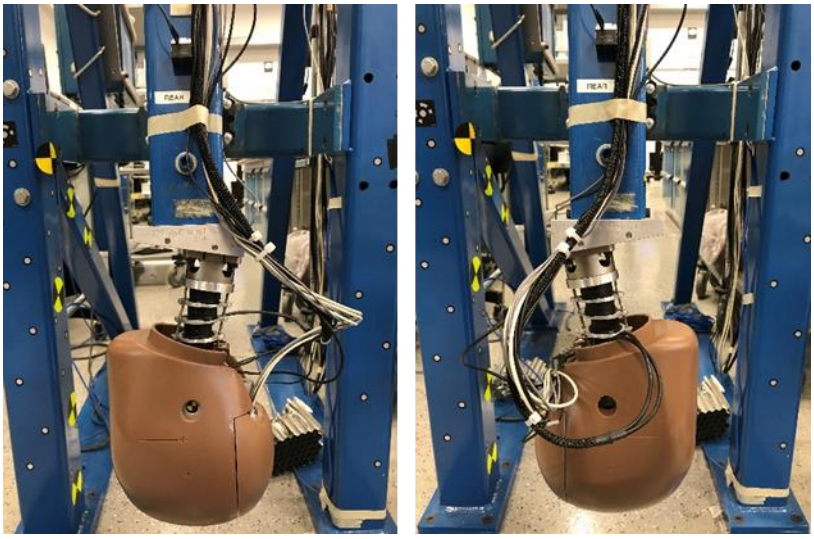

Figure 27. Neck lateral flexion setup

Table 19. Neck lateral flexion deceleration pulse targets and actual values achieved in the tests

Parameter	Target (m/s)	Achieved, left tests	Achieved, right tests
Pendulum Velocity at 5ms after T0	0.86	0.73 0.81 0.78	0.71 0.84 0.82
Pendulum Velocity at 10ms after T0	2.07	1.73 1.82 1.78	1.68 1.86 1.87
Pendulum Velocity at 15ms after T0	3.19	2.71 2.77 2.70	2.65 2.91 2.90

8. At least 20 milliseconds of pre-time zero data and 200 milliseconds of post-time zero data were recorded.
9. At least 30 minutes had passed since the last face, head, or neck test.
10. The pendulum was raised ~49° from vertical to generate an impact velocity of 3.4 m/s. Actual impact velocity achieved is shown in Table 20. ***NOTE:*** *After the test was complete, the pendulum was allowed to hang close to vertical until the next test was ready to be run. This prevents the neck from experiencing undesired bending.*

Table 20. Impact velocities achieved in the neck lateral bending pendulum tests

Test ID	1342	1344	1345	1346	1347	1348
Impact velocity	3.40 m/s	3.40 m/s	3.40 m/s	3.40 m/s	3.40 m/s	3.40 m/s
Direction	Left	Left	Left	Right	Right	Right

4.4.1.2 Data Processing

1. The polarity conventions and data acquisition system conformed to the latest requirements of SAE Recommended Practice J211.
2. Data channel offset removed per SAE J211 Section 8.4.3
3. The polarity of the pendulum ARS was set such that the angular velocity of the pendulum as it fell towards the decelerator was positive.
4. Channels were filtered based on the CFC filter classes listed in Table 21.
5. The pendulum velocity was calculated using the pendulum accelerometer:

$$Pendulum\ X\ Velocity = \int_{t_0}^{t_f} Pend_{X\ ACCEL} dt$$

$$where\ t_0\ and\ t_f\ are\ the\ first\ and\ last\ time\ points, respectively, for\ data\ collection.$$

6. The head rotation relative to the pendulum was calculated:

$$Head\ Rotation = \int_{t_0}^{t_f} Head_{VY} - Pend_{VY} dt$$

$$where\ t_0\ and\ t_f\ are\ the\ first\ and\ last\ time\ points, respectively, for\ data\ collection.$$

Table 21. Neck lateral flexion data channels

Item #	Channel Description	Filter Class	Comments
1	Pendulum Accelerometer	CFC-60	
2	Pendulum Angular Velocity	CFC-60	
3	Head Angular Velocity about X-axis	CFC-60	
4	Upper Neck Moment, X-axis	CFC-600	
5	Head Rotation	N/A	Calculated
6	Pendulum Velocity	N/A	Calculated

4.4.2 Results

The neck pendulum test moment vs rotation responses for lateral bending is shown in

Figure 28.

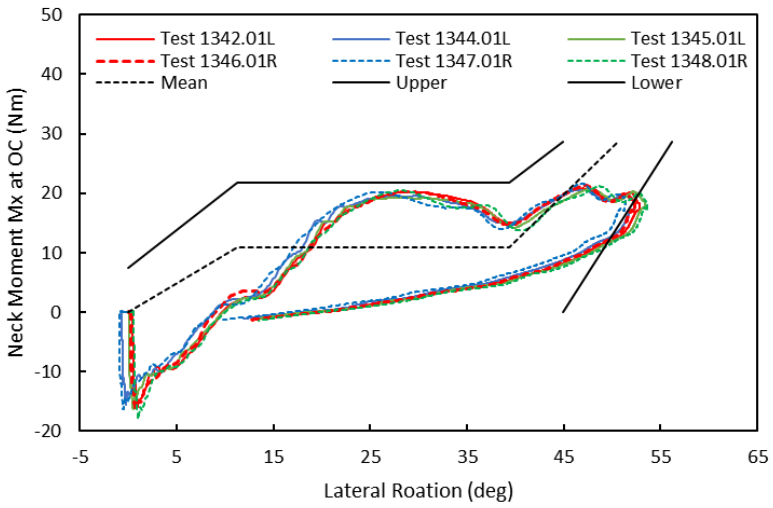

Figure 28. Moment vs head rotation of the neck lateral flexion pendulum test

4.5 Neck Torsion Dynamic Response

4.5.1 Methods

4.5.1.1 Test Procedure

The THOR-05F neck was rigidly fixed to a testing fixture (Figure 29) capable of applying torsional loading regimes to human surrogates. A six-axis Denton load cell (Bottom Load Cell) coupled the caudal end of the spinal segment (ATD) to a fixed boundary condition. The cranial portion of the ATD neck was rigidly fixed to an MTS rotary servo-hydraulic actuator to provide angular displacement input waveforms. The test fixture allowed for rotation about the Z axis of the neck and elongation/contraction translation along the Z axis (superior to inferior). A rotary potentiometer aligned with the rotary actuator quantified head rotation, while an LVDT aligned with the Z axis quantified elongation or contraction of the neck. Data were collected using two digital data acquisition systems (National Instruments; Austin, TX and Hi-Techniques, Inc.; Madison, WI). Test imaging was done in the coronal plane using a Phantom camera system at various frame rates.

The baseline condition CM (included neck muscle cables) was evaluated. Repeatability was evaluated through repeat tests that spanned the entire test matrix.

The test matrix included a total *of 8 individual tests* (Table 22). These 8 tests assessed both the right (4) and left (4) torsional response of the neck. A single complete test cycle included all 8 tests for the given muscle condition over both right and left rotation (left rotation followed by right rotation). Both slow rate (25 deg/sec) and high rate (500 deg/sec) simulations at both low (40 deg) and high (85 deg) amplitude were performed.

Table 22. Neck Torsion Test Matrix

Test Description	Test ID: Rotate Left	Test ID: Rotate Right	Peak (Degrees)	Rate (Deg/S)
Failure Simulation	LFAIL1	RFAIL1	40	25
	LFAIL2	RFAIL2	40	500
	LFAIL3	RFAIL3	85	25
	LFAIL4	RFAIL4	85	500

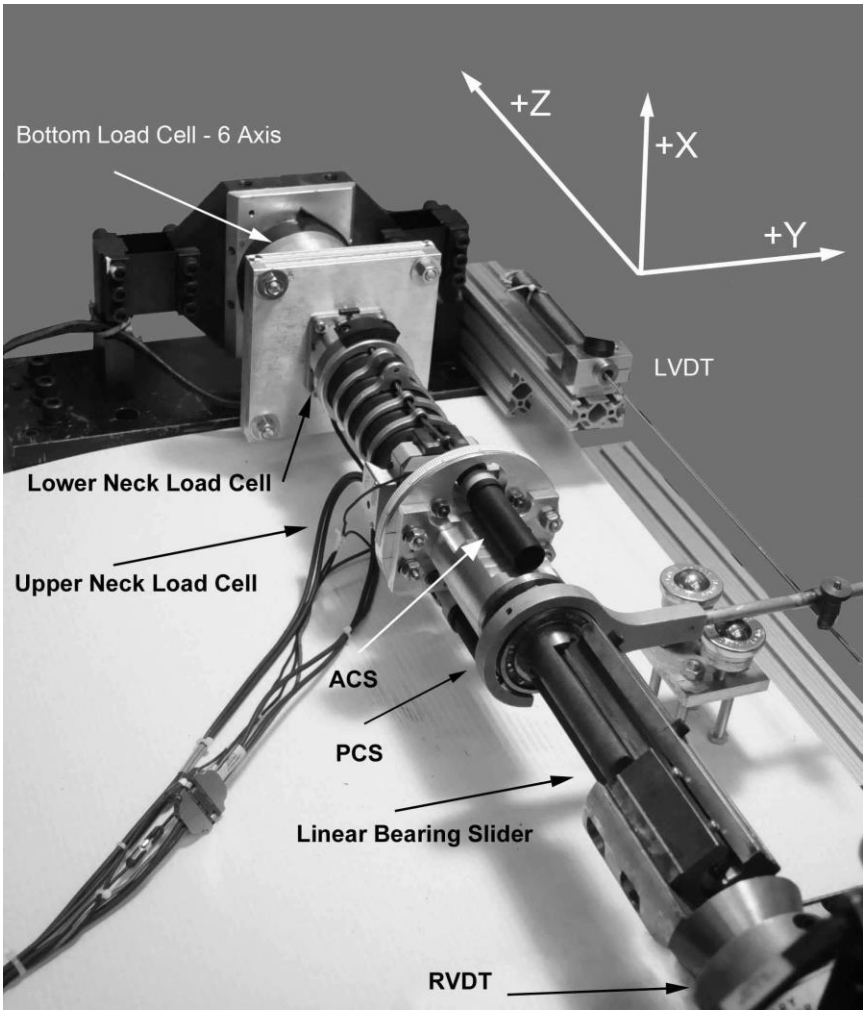

Figure 29. Neck Torsion Test Fixture

4.5.2 Results

Neck torsion and pendulum test responses were evaluated, but given the lack of a suitable corridor for BioRank analysis, their scores were not included in the overall neck BioRank calculation. The torsion response is shown in Figure 30. During the loading portion of the event (upper portion of curve shown in Figure 30), the response did not meet the target response (shown as a black box).

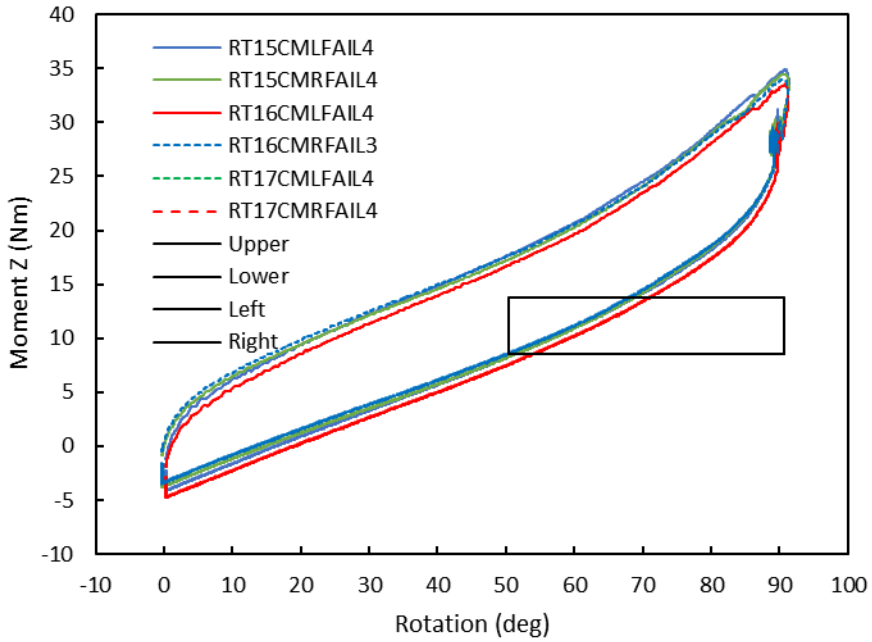

Figure 30. Neck torsion moment z vs rotation, three tests in clockwise rotation and three tests counter clockwise. The polarities were changed to overlay the data for better visual comparison. The upper portion of the plot is the loading curve.

4.6 Neck Biofidelity Summary

Since the neck pendulum test and torsion corridors were not established with the mean plus/minus one standard deviation method, the BioRank was not calculated for these test conditions. Instead, the test data was plotted against the corridors for qualitative comparison. The BioRank scores for the neck mini-sled tests are summarized in

Table 23. The neck has an overall BioRank of 2.20, which corresponds to "marginal" biofidelity. The neck frontal flexion sled test BioRank is 1.86 and the neck lateral sled test BioRank is 2.54, corresponding to "good" and "marginal" biofidelity respectively.

Table 23. Neck sled test biofidelity summary

	SM	***P***	***RMS***
Neck frontal sled test			**1.86**
Head resultant acceleration	2.45	0.32	2.47
Head linkage angle	1.31	1.01	1.65
Neck linkage angle	1.02	0.24	1.04
Head linkage vs neck linkage angle	2.86	N/A	2.86
Head CG displacement X	1.01	0.18	1.03
Head CG displacement Z	1.95	0.83	2.11
Neck lateral sled test			**2.54**
Head linkage angle	2.35	0.20	2.36
Head CG displacement Y	2.37	0.11	2.38
Head CG displacement Z	2.88	0.12	2.89

Neck Overall	**2.20**

5 Thorax

The two tests conducted to evaluate the response of the THOR-05F thorax were the central impact test to the sternum at 4.3 m/s and the oblique impact to the lower ribcage at 4.3 m/s.

Table 24. Summary of thorax test conditions

Test Condition	Input	ATD Identifier
Upper Thorax Central Impact	4.3 m/s, 14 kg mass	Serial No. ED2634
Oblique Lower Thorax Impact*	4.3 m/s, 14 kg mass; two pieces of 152 mm diameter x 9.5 mm thickness Rubatex® foam attached to the front of the probe; ATD was rotated ±15° along z axis through T1	Serial No. ED2634

* **Note:** The test procedure for the biofidelity test differs from the lower thorax qualification test that is currently used for THOR-50M and is likely to be used for THOR-05F.

5.1 Upper Ribcage Central Impact Test

5.1.1 Methods

5.1.1.1 Materials used

1. Fully assembled THOR-05F dummy with internal 3D IR-TRACC units
2. Impact probe with a mass of 13.99 kg, including instrumentation, rigid attachments, and the lower 1/3 of the suspension cable mass. The impacting end of the probe, perpendicular and concentric with the longitudinal axis of the probe, has a flat, continuous, and non-deformable 152.4 mm diameter impact face with an edge radius of 12.7 mm.
3. Targets for external displacement calculation using high-speed cameras.

5.1.1.2 Instrumentation

1. Instrumentation to measure impact velocity consists of a light trap and evenly spaced mechanical vanes that can generate square electrical pulses for velocity calculation.
2. Accelerometer for measuring the impactor acceleration, mounted to the probe with its sensitive axis in line with the longitudinal centerline of the test probe.
3. Two 3D IR-TRACC units (left and right side) attached to the standard upper thorax locations (IH-11620).
4. A dual-axis tilt sensor at T6 (middle thoracic spine or MTS) to measure initial angles about the “X” and “Y” axes.
5. A dual-axis tilt sensor in the pelvis to measure initial angles about the “X” and “Y” axes.
6. Contact switch for synchronizing external deflection with probe force.
7. Method for measuring external abdominal displacement (High-speed cameras)
8. Targets on impact probe, dummy and test fixture for external displacement calculations. Target must be attached to the local body segment being impacted.

5.1.1.3 Test Procedure

1. The ribcage, sternum, and jacket were inspected for wear, tears, or other damage.
2. Dummy was soaked in a controlled environment at a temperature between 20.6° to 22.2°C (69° to 72°F) and a relative humidity from 10 to 70% for a period of at least 4 hours prior to testing. The test environment had the same temperature and humidity as the soak environment.
3. The neck pitch change joint was kept in the neutral position.
4. The lower thoracic spine (LTS) pitch change joint was set to the slouched posture position. Joints were set to 1-2g setting.
5. Dummy was seated on a steel, horizontal surface (± 0.5°) that is flat, smooth, rigid, clean, and dry with no back support.
6. All limbs were extended forward in front of the torso. The arms were within ± 1° from horizontal. Arms were positioned so they did not interfere with the impact probe or suspension cables. Arm supports were used to help support the dummy.
7. Jacket was unzipped and the front panel was laid on the lap of dummy (it was not removed completely).

The pelvis was set so the angle measured by the pelvis tilt sensor was approximately 11° in the Y-axis (rearward tilt about the Y-axis) and 0° laterally (about the X-axis). The test setup parameters are shown in

8. Table 25.
9. The thorax was positioned so that the MTS (T6) tilt sensor read approximately 0° (about the Y-axis) and 0° laterally (about the X-axis).
10. The midsagittal plane was aligned with the probe longitudinal centerline (Figure 31). The midsagittal plane was visualized using the center of the bottom facial load cell (indicated by the detent on the head skin), the midpoint between the IRTRACC attachment bolts, the umbilicus detent on the abdomen, and the pelvis flesh at the pubic symphysis (Figure 32).

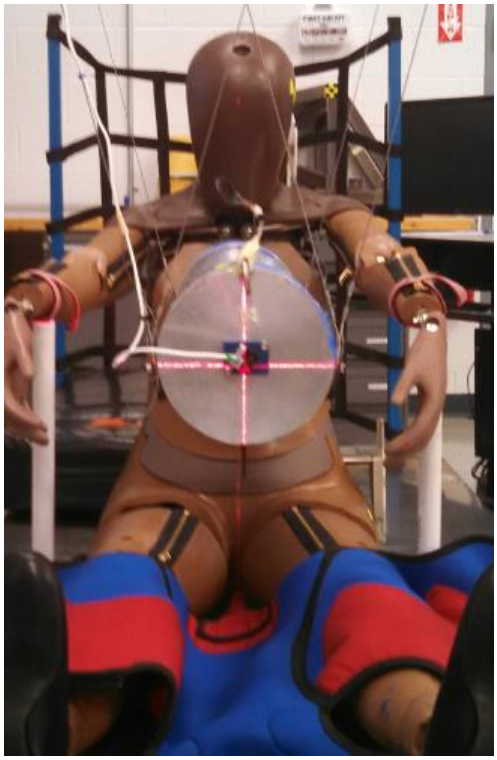

Figure 31. Lateral alignment of impact location

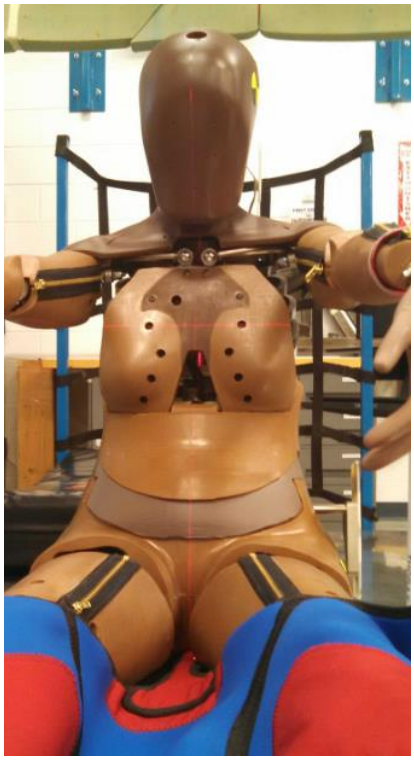

Figure 32. Midsagittal plane definition

11. The dummy was positioned in front of the impactor such that the centerline of the impactor was at the vertical level of rib #3, and positioned over the mid-line of the sternum. This position was at the middle of the line connecting the attachment nuts of the two upper chest deflection measurement systems (Figure 33).

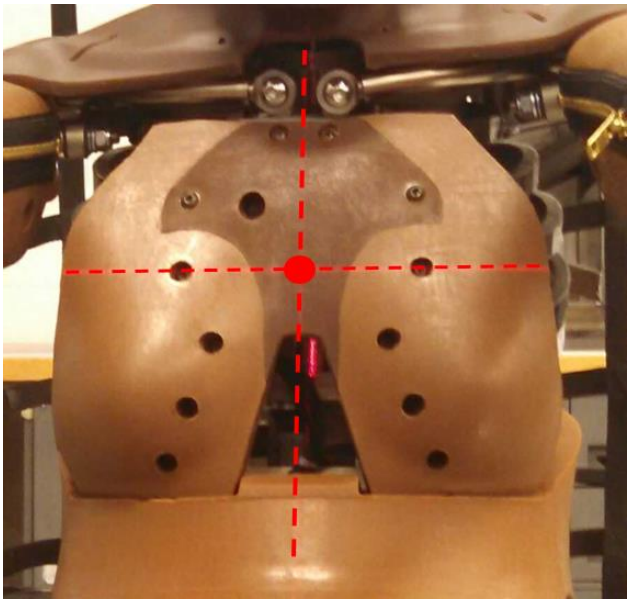

Figure 33. Vertical alignment of impact

12. The jacket was reattached once the dummy was in position by zipping up the back and shoulders.

13. Figure 34 shows a typical test setup with jacket installed (the cloth under the dummy seen in Figure 34 is removed prior to testing).

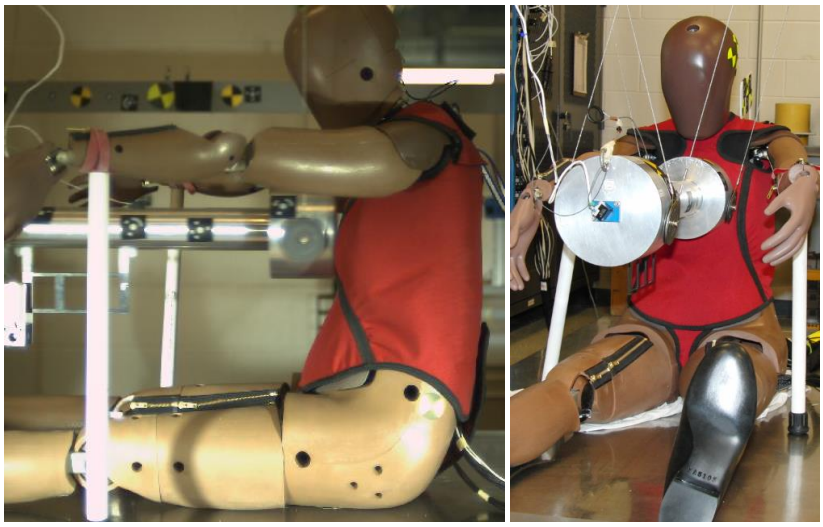

Figure 34. Setup of upper thorax central impact

14. The dummy was positioned so the chest was just barely touching the impact probe when the probe was at rest. ***NOTE:*** *Test probe centerline was horizontal (± 0.5°) at impact.*
15. At least 20 milliseconds of pre-time zero data and 200 milliseconds of post-time zero data was recorded.
16. The motion of the impactor was constrained so that there was no significant lateral, vertical, or rotational movement. At least 30 minutes have had passed since the last upper thorax or lower thorax test.

The probe was raised ~37" above the resting position to generate an impact velocity of 4.30 ± 0.05 m/s. Actual impact velocity achieved is shown in

17. Table 26.

Table 25. Upper thorax impact setup parameters

Parameter	Setting	
Neck Pitch Change Setting	"Neutral"	
LTS Pitch Change Setting	"Slouched"	
Mid Thorax (MTS) (T6) Tilt Sensor Reading(s):	X 0.0° 0.3° 0.1°	Y 0.0° -0.3° -0.1°
Pelvis Tilt Sensor Reading(s):	X 0.6° 0.6° 0.8°	Y 11.7° 10.1° 10.6°
Teflon® Sheeting on Test Bed?	No	
Dummy Clothing?	Jacket	
Wait Time Between Tests	30 minutes	

Table 26. Impact velocities achieved in the thorax impact tests

Test ID	1165	1167	1168
Impact velocity	4.28 m/s	4.30 m/s	4.28 m/s

5.1.1.4 Data Processing

1. The polarity conventions and data acquisition system conformed to the latest requirements of SAE Recommended Practice J211.
2. Data channel offset was removed, but the IR-TRACC and potentiometer channels were not *zeroed*; per SAE J211 Section 8.4.3, the normalized value of a stable pre-test section of data was set to the *proper* initial value for the transducer.
3. Time zero (T_0) was defined when the probe contacted the dummy (for BioRank) or when the accelerometer with a CFC-1000 response mounted on the probe rose through the 1g level.
4. **Channels were filtered based on the CFC filter classes listed in** Table 27.
5. Time history of the Probe Force was calculated using the Probe acceleration at each time step:

$$Force_{Probe}(N) = Acceleration_{Probe}(m/s^2) * Mass_{Probe}(kg)$$

6. Upper left and upper right resultant deflections were calculated in the *local spine coordinate system:*

$$Resultant\ Deflection = \sqrt{D_{AX}^2 + D_{AY}^2 + D_{AZ}^2}$$

7. External X-axis deflection was calculated from the high-speed video system (For biofidelity testing)

Table 27. Upper thorax impact data channels

Item #	Channel Description	Filter Class	Comments
1	Contact Switch	N/A	For BioRank
2	Probe Acceleration	CFC-600	
3	Upper Left IR-TRACC Tube	N/A	Internal Deflection
4	Upper Left Y-Axis Rotational Potentiometer	CFC-600	Internal Deflection
5	Upper Left Z-Axis Rotational Potentiometer	CFC-600	Internal Deflection
6	Upper Right IR-TRACC Tube	N/A	Internal Deflection
7	Upper Right Y-Axis Rotational Potentiometer	CFC-600	Internal Deflection
8	Upper Right Z-Axis Rotational Potentiometer	CFC-600	Internal Deflection
9	Probe Force	N/A	Calculated
10	Upper Left Resultant Deflection	N/A	Calculated
11	Upper Right Resultant Deflection	N/A	Calculated
12	Thorax X-Axis Deflection (External using High-speed Camera)	N/A	External Deflection

5.1.2 Results

For BioRank evaluation, the time zero was defined as contact time between the probe and the thorax with contact switch. An average of the two upper thoracic IR-TRACCs displacement were used as internal thoracic displacement with respect to the spine coordinate system. The displacement was then projected to the ground horizontal direction with the following formula.

$$Dxh = Dxavg * \cos(-16.6 + \theta_{tilt}) + Dzavg * \sin(-16.6 + \theta_{tilt})$$

where

Dxh is the displacement in horizontal plane

Dxavg is the average of the upper left and right IR-TRACCs displacement in x direction

DZavg is the average of the upper left and right IR-TRACCs displacement in z direction

The upper thoracic IR-TRACC and mid thoracic tilt sensor orientation is shown in Figure 35 following SAE J211 sign convention.

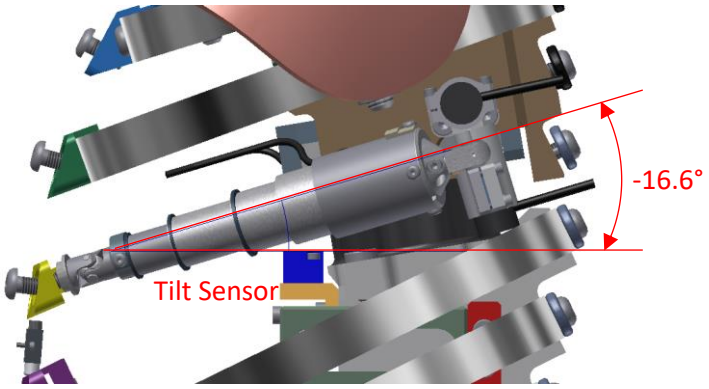

Figure 35. Upper thoracic IR-TRACC and the thoracic spine tilt sensor orientation

The upper thorax responses are shown in Figure 36 through Figure 39.

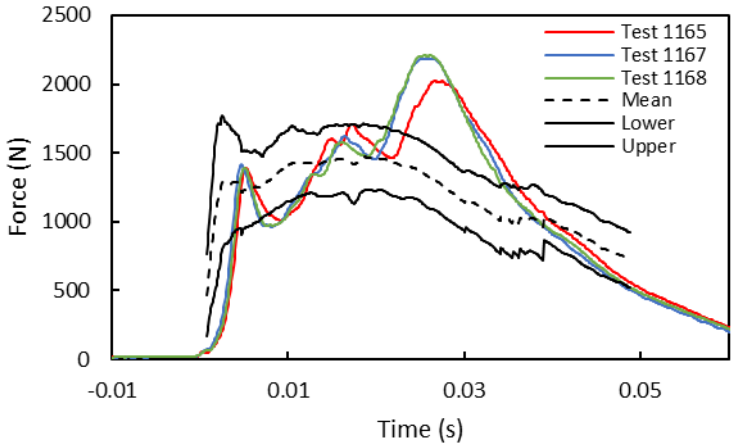

Figure 36. Force response of upper thorax impact test

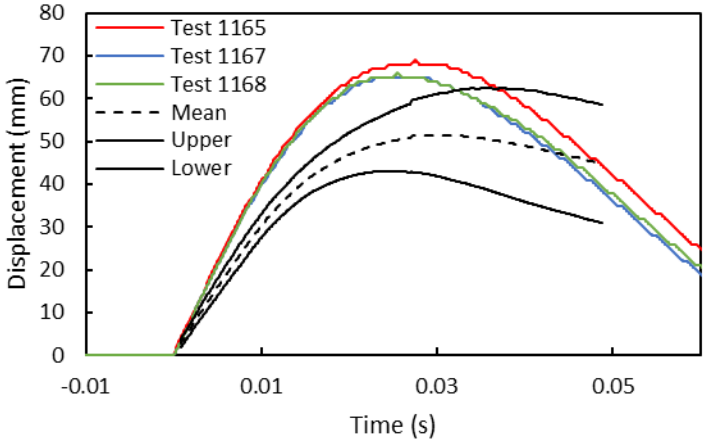

Figure 37. External deflection of upper thorax impact test

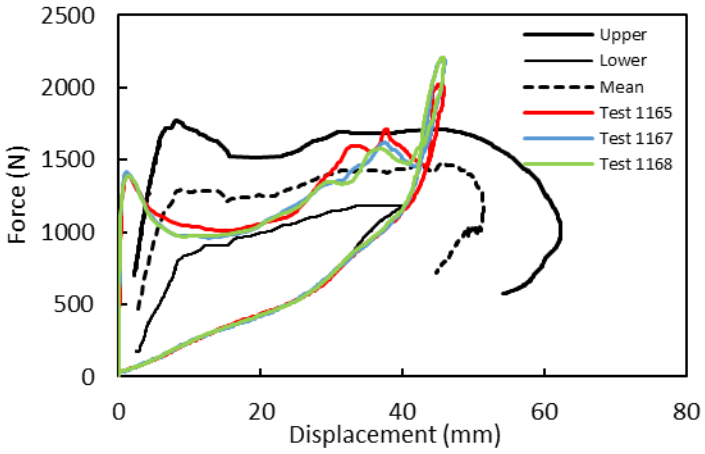

Figure 38. Force vs external displacement response of upper thorax impact test

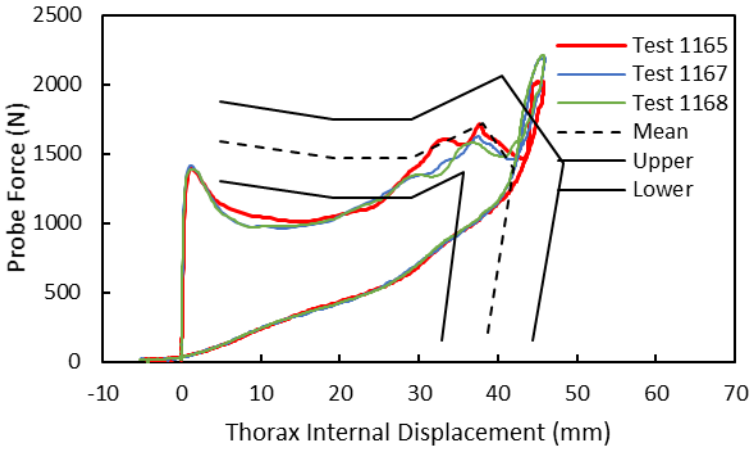

Figure 39. Force vs internal displacement of upper thorax impact test

For BioRank score calculation of the force vs displacement data, the calculation can only be carried up to the lower of the peak value of test data and the corridor mean displacement. The unloading portion was not included because it cannot be calculated numerically.

5.2 Lower Thorax Oblique Impact

5.2.1 Methods

5.2.1.1 Materials

1. Fully assembled THOR-05F dummy with internal 3D IR-TRACC units and abdominal pressure sensors.
2. Impactor with a mass of 14 kg, which includes the shaft of the pneumatic ram, six-axis load cell and all other hardware attached. The impacting end comprised of a solid aluminum disk covered with two pieces of 9.5mm thick Rubatex foam.
3. Thin Teflon® sheet for test bed

5.2.1.2 Instrumentation

1. The velocity was measured using a light trap.
2. An accelerometer for measuring the impactor acceleration was mounted to the non-impacting surface of the circular impactor. This also allowed for redundant measurement of impactor velocity.
3. Dual-axis tilt sensors at T12 and pelvis were used to measure initial angles about the “X” and “Y” axes and keep the values consistent across the three tests.
4. Contact switch was attached to metal tapes on the impactor surface and chest jacket to trigger the event and this corresponded to time zero for all data including sensors and high-speed cameras.
5. One 59-channel chest band was used to obtain the thoracic deformation histories during impact loading.
6. One six-axis load cell (from HIII 3yo ATD lumbar spine) was used to measure impact force.

5.2.1.3 Test Procedure

1. The dummy was inspected for any damages to the ribcage or chest jacket. No damages were identified through visual inspection.
2. The test was conducted at 70F.
3. The dummy was seated upright on a height adjustable table without any back support. The lower extremities were stretched horizontally.
4. The center of the impactor was aligned with the sixth rib anteriorly by adjusting the height of the table.

5. The dummy wore long underwear pants to mimic real world interaction with the seated surface.
6. The dummy was seated on a Teflon sheet facing the impactor.
7. Using laser levels in the sagittal and coronal planes, the dummy was rotated about its spine by an angle of 15 degrees from left to right. Caution was used to ensure that the 0 degree mark was in line with the posterior most point on the base aluminum neck plate when viewed from above.
8. The 59-channel chest band was wrapped around the lower thorax at the level of impact.
9. The arms were positioned so that they do not interfere with the impactor. Wooden arm supports were used to help support the arms and ensured that they did not interfere with the test.
10. The pelvis was positioned so that pelvis tilt sensor read approximately 6° about the Y-axis and 0° laterally about the X-axis. The test setup parameters are shown in Table 28.
11. The lower thorax was positioned so that the T12 tilt sensor (lower thorax) read approximately 0° about the Y-axis and 0° laterally about the X-axis.
12. The dummy was impacted at 4.3 m/s. Actual impact velocities achieved are given in Table 29.

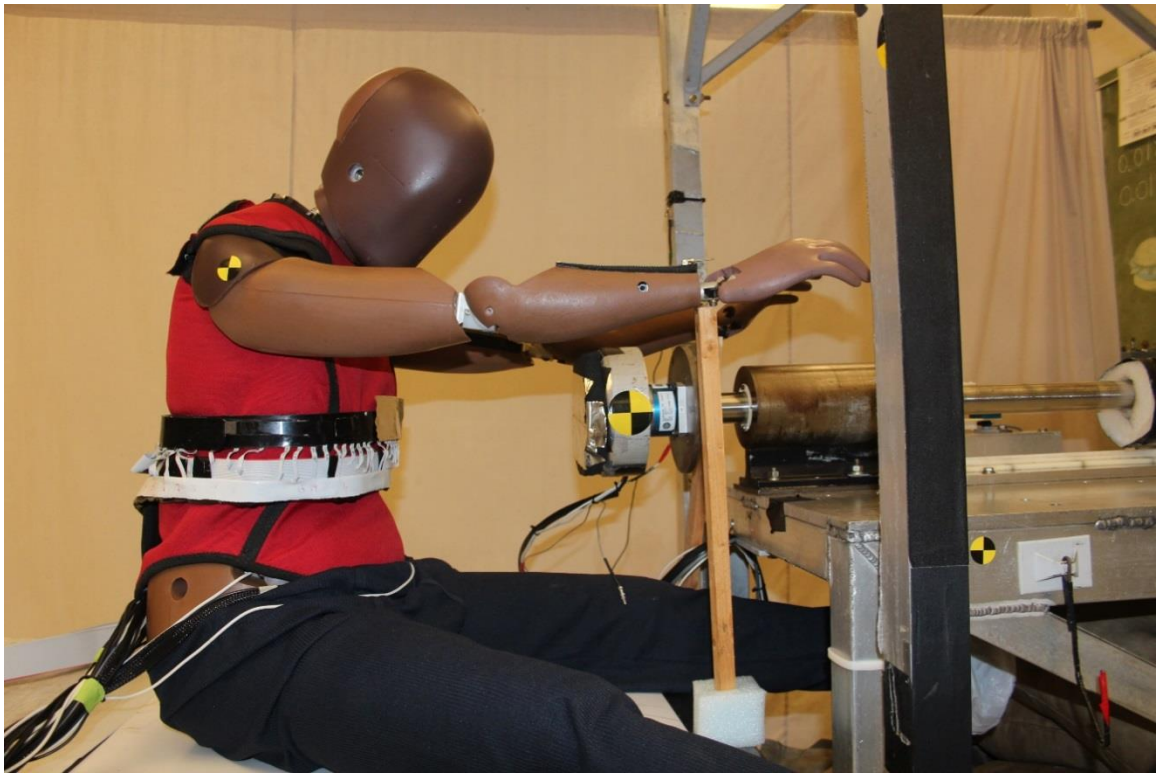

Figure 40. Initial setup for lower thorax impact test

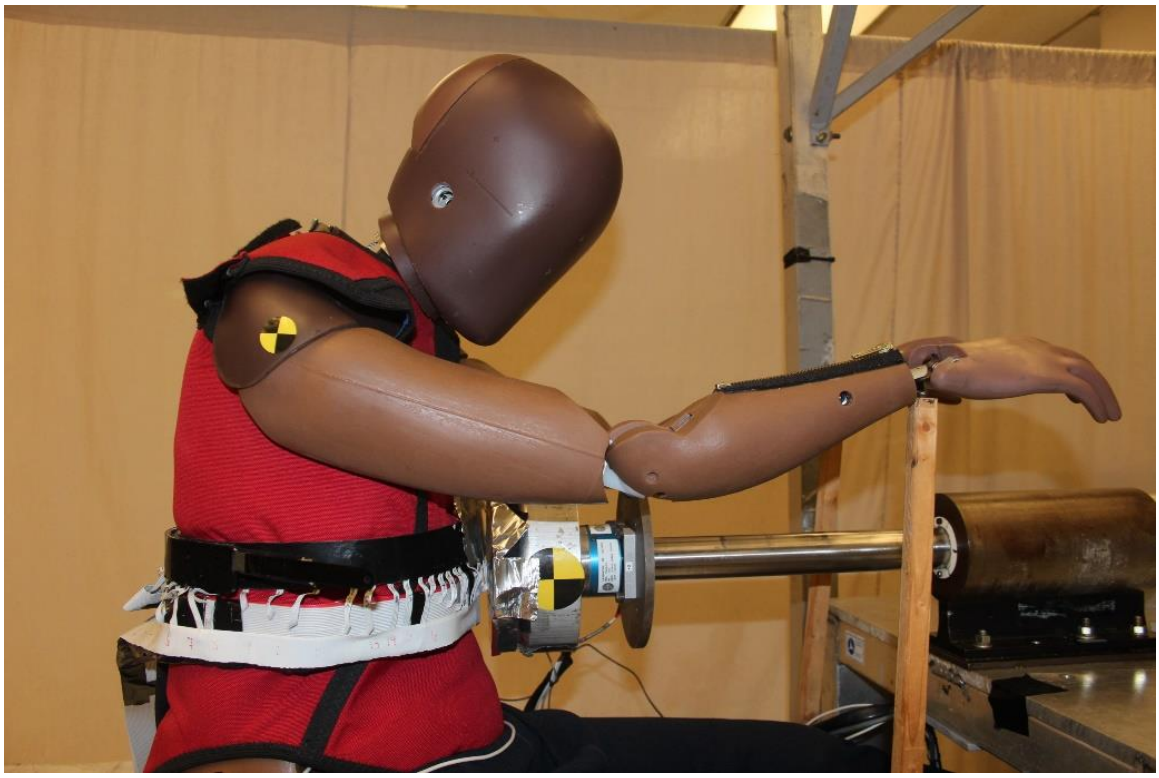

Figure 41. Impactor alignment with lower thorax; chest band wrapped around thorax

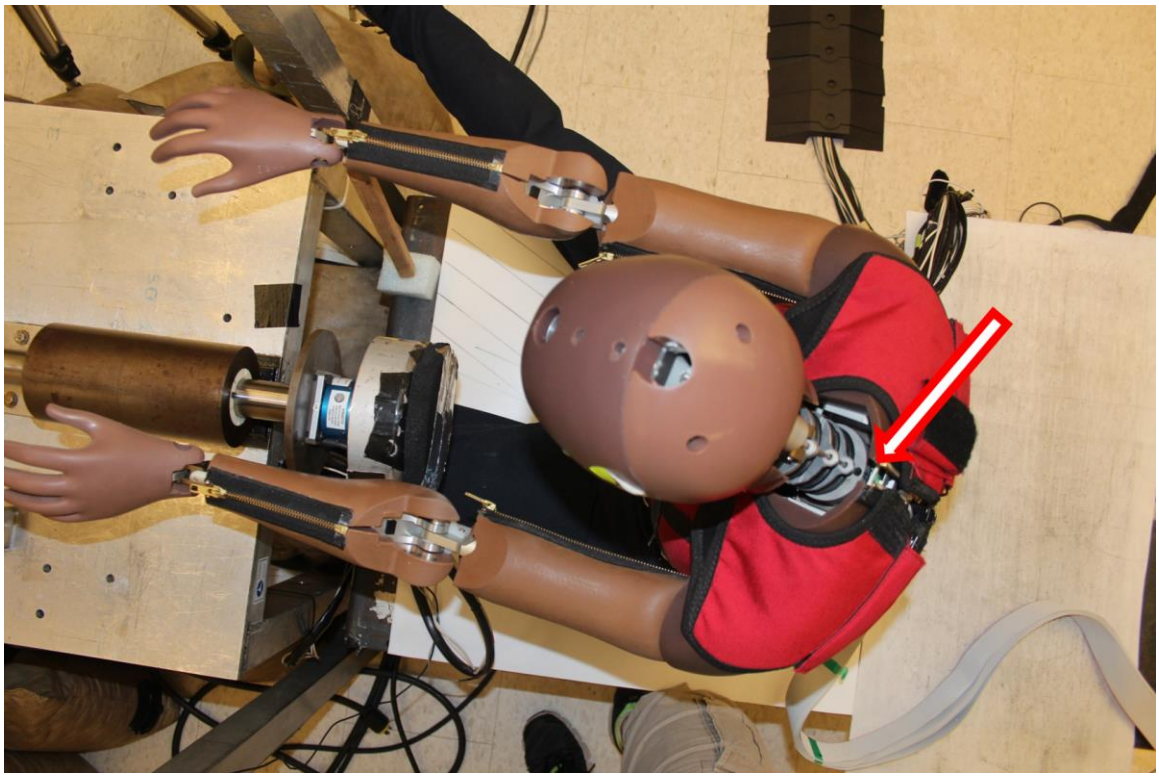

Figure 42. Dummy rotated 15 degrees to the right; 0 degree mark was in line with the posterior most point on the base aluminum neck plate when viewed from above

Table 28. Lower thorax impact setup parameters

Parameter	Setting	
Neck Pitch Change Setting	"Neutral"	
LTS Pitch Change Setting	"Slouched"	
Lower Thorax (T12) Tilt Sensor Reading(s):	X 0.0°	Y 0.0°
Pelvis Tilt Sensor Reading(s):	X 0.0°	Y 6.0°
Teflon® Sheeting on Test Bed?	Yes	
Dummy Clothing?	Jacket + Long underwear	
Wait Time Between Tests	30 minutes	

Table 29. Impact velocities achieved in the lower thorax oblique impact tests

Test ID	Trial3	Trial4	Trial5
Impact velocity	4.27 m/s	4.24 m/s	4.31 m/s

5.2.1.4 Data Processing

1. Data was collected at 20000 Hz using a TDAS system. Video was recorded at 1000 frames per second.
2. Time zero (T_0) was defined when the impactor contacted the dummy using contact switch between the impactor and dummy chest jacket.
3. The impactor load cell force was filtered with a Channel Filter Class (CFC) 600 and compensated for the inertia of the mass of the ram between the load cell and the dummy.
4. Chest band data were processed using CrashStar version 2.5 [NHTSA 2010] to produce contours of the chest band shape at each point in time. Chest deflection at impact site was determined as the distance calculated between the gage corresponding to spine and a gage at the impact line.

5.2.2 Results

The time zero was defined as the contact time with the contact switch between probe and the dummy. The maximum thorax deflection was measured with chestband device. The shape of the chestband was reconstructed with the strain measurements of the chestband. Only the left side was tested assuming the symmetrical design would yield similar responses between the left and right sides. The time history of the displacement of the highest displacement point are shown in

Figure 44. The responses of the probe force and internal displacement are shown in Figure 43 through Figure 45.

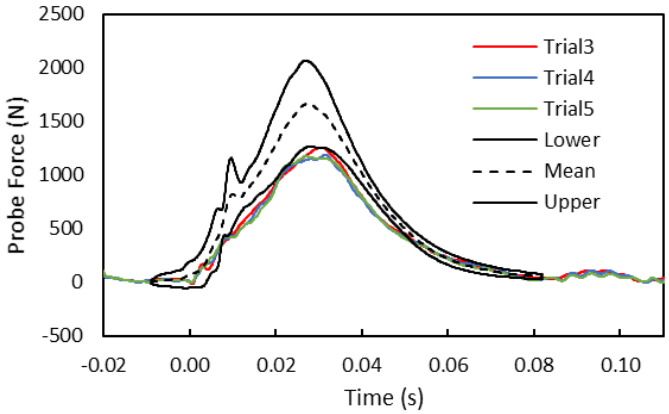

Figure 43. Probe force of lower thorax oblique impact test

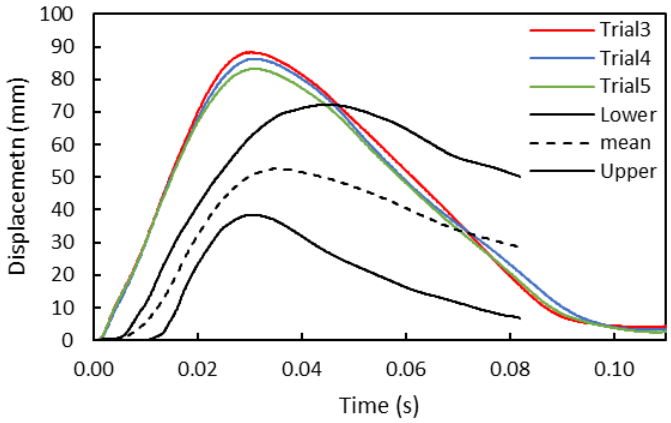

Figure 44. External displacement of lower thorax oblique impact test

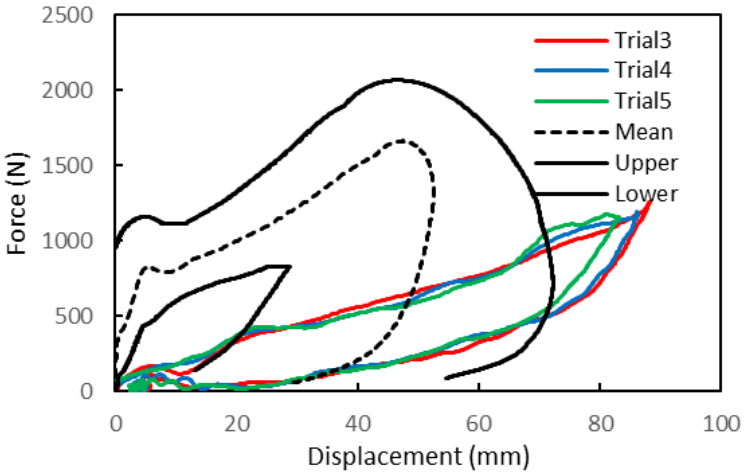

Figure 45. Force vs external deflection of oblique lower thorax impact test

5.3 Thorax Biofidelity Summary

The thorax BioRank scores are summarized in Table 30. Thorax overall BioRank is 1.42, corresponding to “good” biofidelity. The upper thorax and oblique lower thorax impact test BioRank scores are 1.40 and 1.43 respectively, both corresponding to “good” biofidelity.

Table 30. Thorax biofidelity summary

	SM	*P*	*RMS*
Thorax Upper			**1.40**
Force vs internal deflection	1.19	NA	1.19
Force vs external deflection	1.86	NA	1.86
Force	1.29	0.43	1.36
External deflection	1.16	0.27	1.19
Oblique Thorax			**1.43**
Force	1.21	0.11	1.21
External deflection (chestband)	1.14	0.31	1.18
Force vs external deflection	1.90	NA	1.90
Thorax Overall			**1.42**

6 Shoulder

The shoulder biofidelity test conditions consisted of quasi-static pulls to the arms, with three arm positions: 90 degrees (arm horizontal), 135 degrees (45 degrees from horizontal) and 170 degrees (80 degrees from horizontal), see Figure 46. The ATD used for all tests was serial no. ED2634.

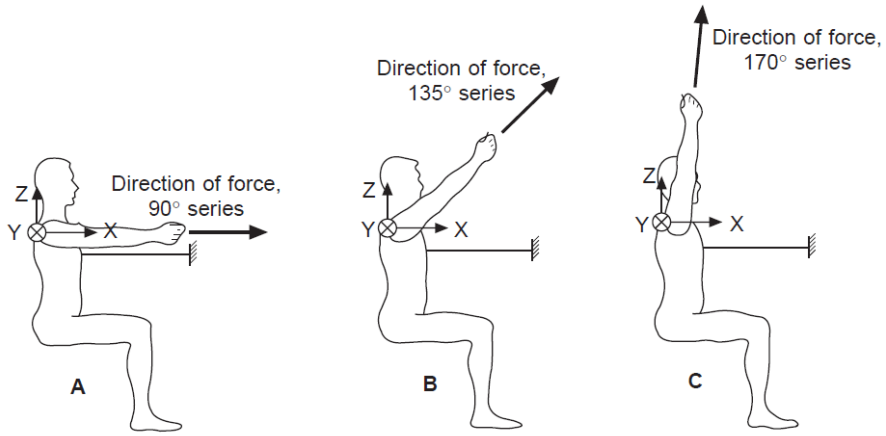

Figure 46. Direction of force and coordinate systems for 90°, 135° and 170° shoulder test

6.1.1 Methods

6.1.1.1 Materials

1. Fully assembled THOR-05F dummy.
2. The test apparatus constructed of square steel columns with cross-beams to which pulleys were fastened. A steel cable was guided through seven pulleys and attached to two arm brackets on both ends with the middle of the cable guided to the back of the apparatus where the load was applied. A standard car seat was attached to the frame with the top-surface of the cushion parallel to the floor.

6.1.1.2 Instrumentation

1. No dummy instrumentation was used in this test series.
2. Two cameras positioned perpendicularly to the dummy: one from above and another from the right-hand side.

6.1.1.3 Test Procedure

1. The dummy was seated on the car seat. The dummy was constrained at mid sternum to the fixture using an adjustable metal plate that was padded. The chest jacket was removed to allow full view of the shoulder joint from top and side.
2. Before applying load or fastening the dummy to the pulling cable, a reference image was acquired, which was referred to as the neutral position. This was a relaxed position with the thorax perpendicular to the lower extremities and without any load on the arms.
3. Then, the elbow of each arm was attached to the Plexiglas arm bracket using an elastic Velcro, maintaining a 30-degree flexion angle about the elbow joint. It was ensured that the cable was in line with the humerus at the desired angles with respect to +Z axis per SAE-J211. Three shoulder test conditions were arm position in 90° (arm horizontal), 135° (45° from horizontal) and 170° (80° from horizontal).
4. For each arm position, both arms were simultaneously pulled at 50N increments, up to 400N (200N per arm). A plastic bucket was hung at the back of the test apparatus at the half-way point on the guided cable (center of the cable attachment points on the arm brackets). Each load increment was applied by adding a

pre-filled sand bag of 5.1kg. The cameras were triggered manually after the dummy was stabilized and stationary, which was approximately 3-5s.

5. The displacement in x, y and z directions were measured using displacements of photo markers with the images recorded for each loading point. On the acromion, the photo marker was positioned as near the shoulder joint as possible, both at the top and right side of the shoulder.
6. An extension bracket was attached on T1 since it was not directly in view of either the top or lateral cameras. This allowed to take out the effects of spinal motion from the acromion displacement measurements.
7. The test conditions are summarized in Table 31.
8. All tests were conducted at 70F.

Table 31. Shoulder test conditions

Test Condition	Arm in 90° position	Arm in 135° position	Arm in 170° position
Input Loads	0 to 400N at 50N increments	0 to 400N at 50N increments	0 to 400N at 50N increments

6.1.1.4 Data Processing

1. The lateral and top view image data were used to calculate the motion of the acromion joint relative to the T1 using TEMA Motion software (Image Systems AB, Linköping, Sweden).
2. Images were scaled using a static coordinate system with using known distances between two separate photo markers located on the seat to define the size of each pixel.
3. Displacement of the shoulder joint between each loading condition was determined by tracking the displacement of the acromion photo marker with respect to a photo marker on the T1 extension bracket.
4. When calculating the range of motion of the shoulder, the neutral position was used as the origin of coordinates. The next point from the origin for each curve was the dummy arms attached to the Plexiglas bracket with the cable, but without load added at the back. The following points for each curve corresponded to an increase of 25N load per arm for each point.
5. The photo marker on the right acromion was used to calculate the shoulder range-of-motion in a xyz coordinate system. The x-axis was directed from posterior to anterior, the y-axis was directed from the right of the body to the left and the z-axis was directed from inferior to superior. The lateral view was used to analyze distance between photo markers in x and z components while the top view defined x and y components
6. Finally, in order to compare the motion difference with the volunteer-based biofidelity corridors, the initial data point from the dummy tests were aligned with the corridor mean initial point.

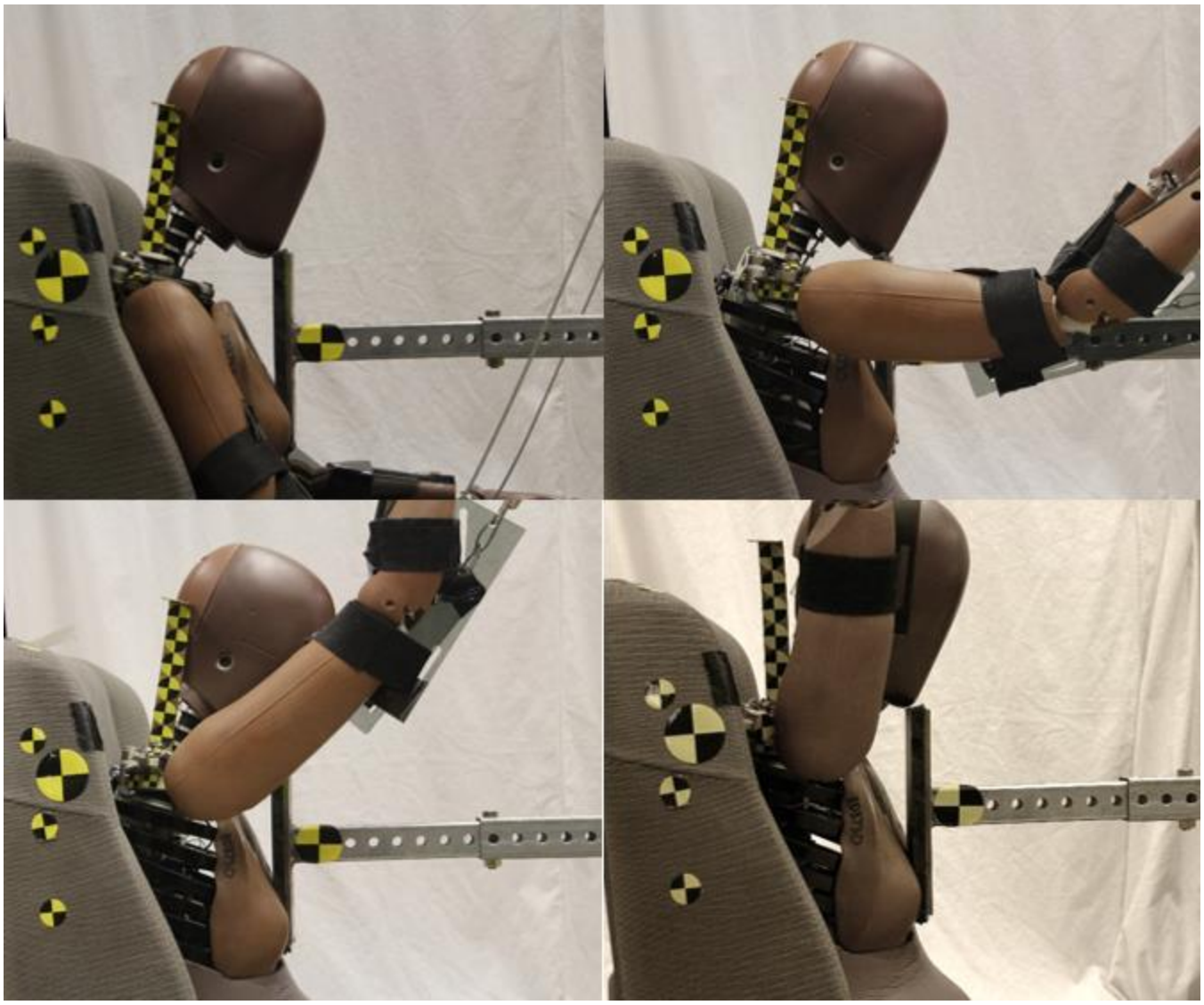

Figure 47. Initial setup for shoulder range of motion testing: neutral arm position (top left), 90° (top right), 135° (bottom left) and 170° (bottom right)

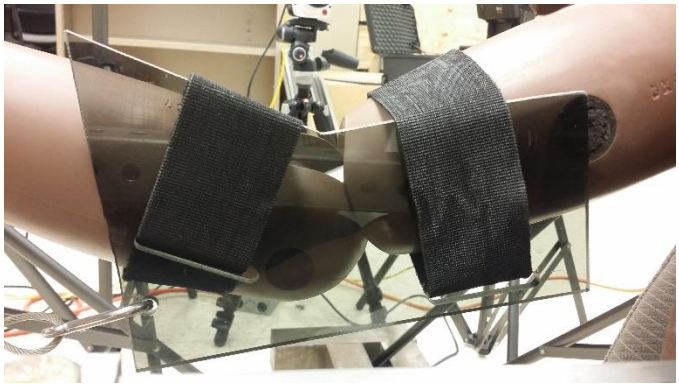

Figure 48. Plexiglas arm bracket strapped to the elbow using Velcro

6.1.2 Results

The shoulder biofidelity responses are shown in Figure 49 through Figure 57.

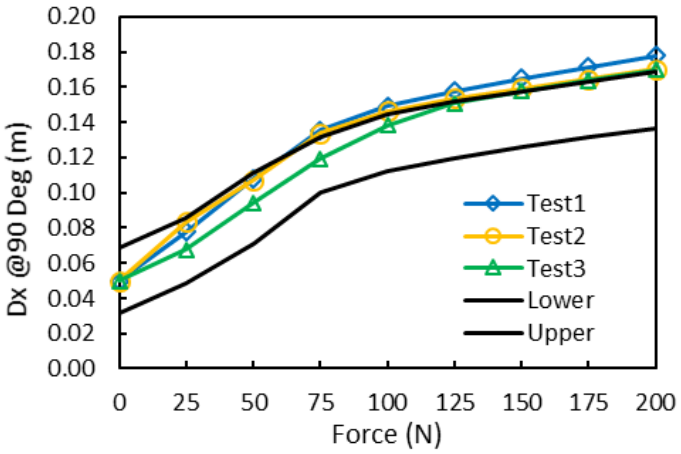

Figure 49. Shoulder displacement (X-direction) with arm in 90-degree position

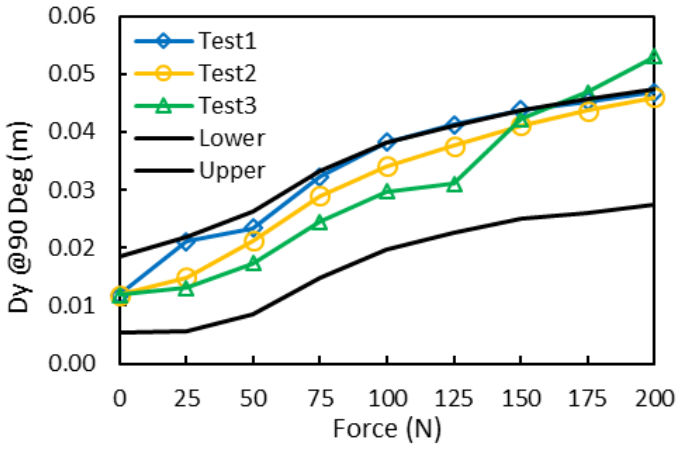

Figure 50. Shoulder displacement (Y-direction) with arm in 90-degree position

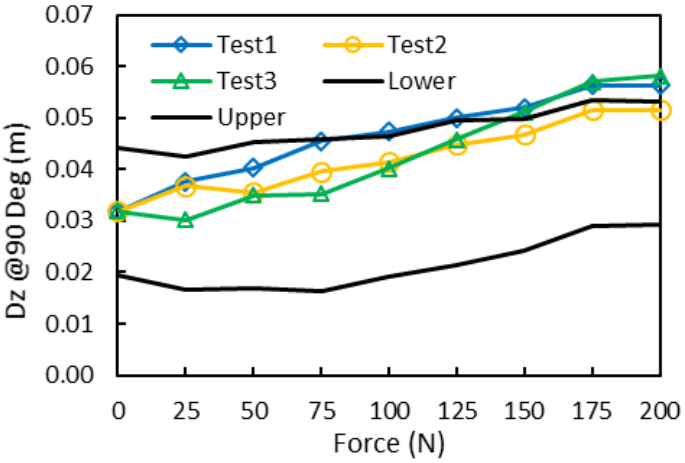

Figure 51. Shoulder displacement (Z-direction) with arm in 90-degree position

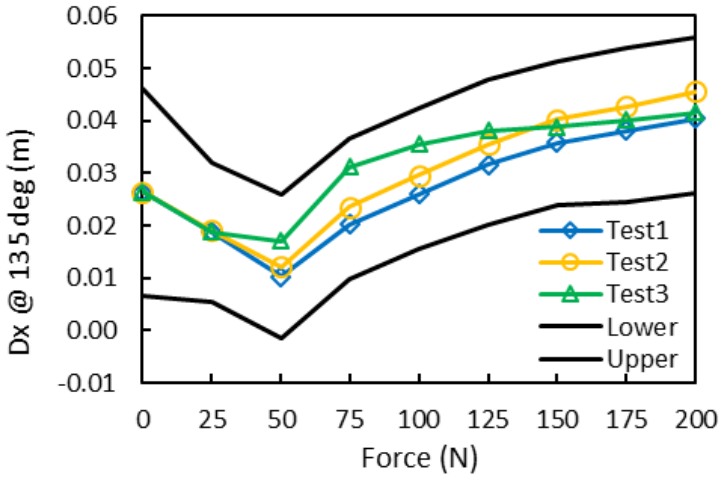

Figure 52. Shoulder displacement (X-direction) with arm in 135-degree position

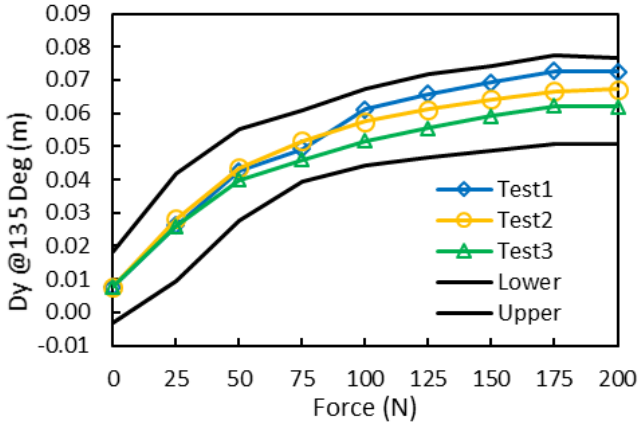

Figure 53. Shoulder displacement (Y-direction) with arm in 135-degree position

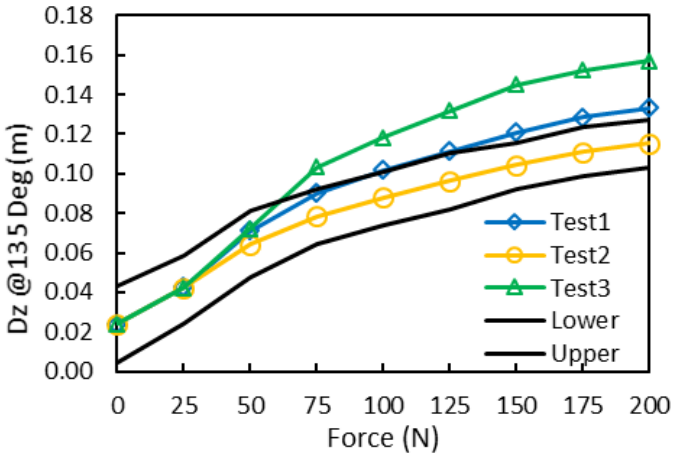

Figure 54. Shoulder displacement (Z-direction) with arm in 135-degree position

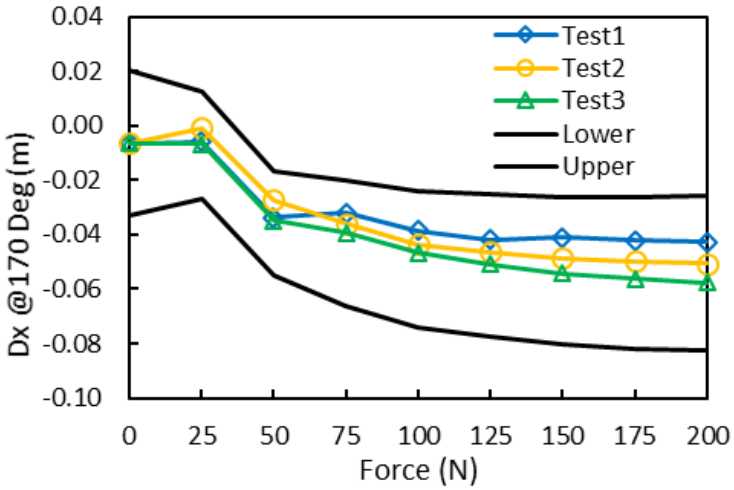

Figure 55. Shoulder displacement (X-direction) with arm in 170-degree position

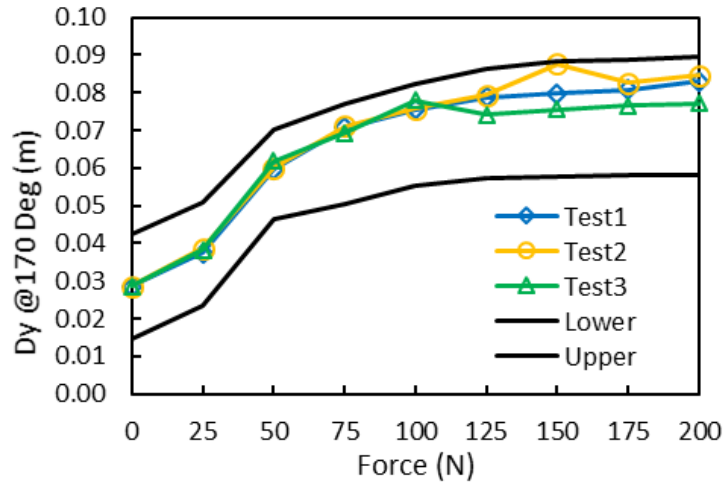

Figure 56. Shoulder displacement (Y-direction) with arm in 170-degree position

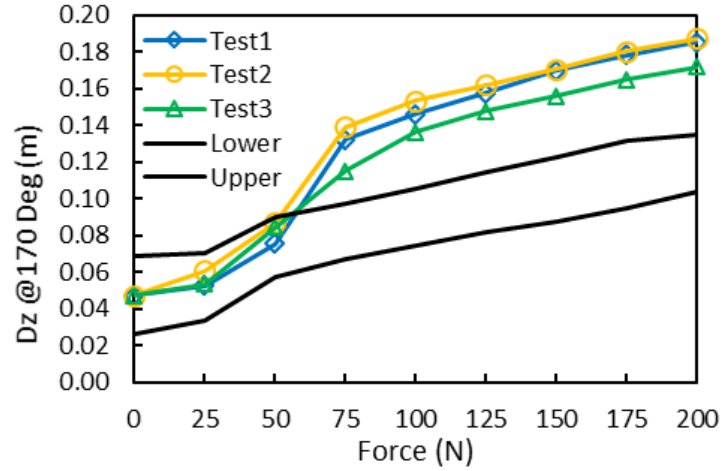

Figure 57. Shoulder displacement (Z-direction) with arm in 170-degree position

6.2 Shoulder Biofidelity Summary

The BioRank scores are summarized in Table 32. The overall shoulder BioRank score is 0.81, corresponding to "excellent" biofidelity. The 90° and 145° degree positions BioRank scores are 0.81 and 0.48 respectively, corresponding to "excellent" biofidelity and the 170° arm position BioRank score is 1.14, corresponding to "good" biofidelity.

Table 32. Shoulder biofidelity summary

	Dx	*Dy*	*Dz*	*Test Condition*
90° Arm Position	0.93	0.73	0.77	0.81
145° Arm Position	0.19	0.27	0.98	0.48
170° Arm Position	0.22	0.42	2.77	1.14
Shoulder Overall				0.81

7 Abdomen

The tests used to evaluate the response of the THOR-05F abdomen were the lower abdomen rigid bar test, upper abdomen steering rim test and belt pull test.

Table 33. Summary of the abdomen test conditions

Test Condition	Input	ATD Identifier
Lower Abdomen	6.1 m/s, 16.0 mass 25 mm diameter x 30 cm long rigid bar Center aligns with L3 level, torso upright	Serial No. ED7441 Abdomen: EE7298
Upper Abdomen	6.7 m/s, 9.0 kg steering wheel, 20° from vertical Leading edge aligns with L2 level, torso upright	Serial No. ED7441 Abdomen: EE7298
Abdomen Belt Pull	Fixed back, approximately 4.5 m/s peak belt loading speed	Serial No. ED7441

7.1 Lower Abdomen Impact

7.1.1 Methods

7.1.1.1 Materials

1. Fully assembled THOR-05F dummy with internal 3D IR-TRACC units and pressure sensors.
2. Impact probe with a mass of 15.992 kg, which includes all attached hardware and 1/3 of the weight of the suspension cables. The impacting end of the probe is a horizontally-oriented rigid bar 25 mm diameter and 300 mm long cylindrical bar (Figure 58).
3. Targets for external displacement calculation using high-speed cameras.

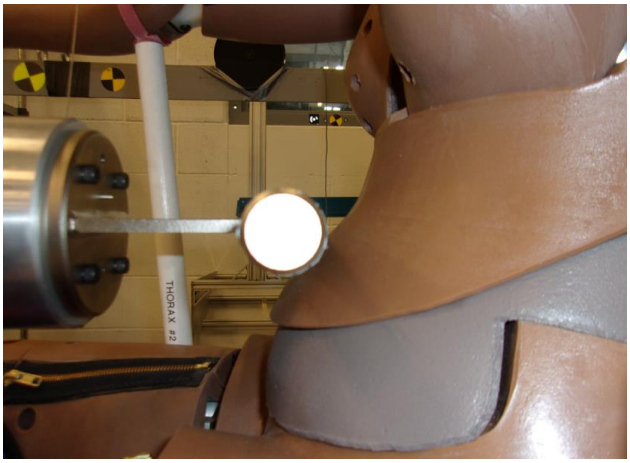

Figure 58. Lower abdomen cylindrical bar face

7.1.1.2 Instrumentation

1. Instrumentation to measure impact velocity.
2. Accelerometer for measuring the impactor acceleration, mounted to the probe with its sensitive axis in line with the longitudinal centerline of the test probe.
3. A dual-axis tilt sensor at T12 (lower thoracic spine or LTS) to measure initial angles about the "X" and "Y" axes.
4. A dual-axis tilt sensor in the pelvis to measure initial angles about the "X" and "Y" axes.
5. Contact switch for syncing external deflection with probe force.
6. Method for measuring external abdominal displacement (High-speed cameras)
7. Targets on impact probe, dummy and test fixture for external displacement calculations. Target must be attached to the local body segment being impacted.

7.1.1.3 Test Procedure

1. The abdomen foam and the outer neoprene suit were inspected for wear, tears, or other damage.
2. Dummy was soaked in a controlled environment at a temperature between 20.6° to 22.2°C (69° to 72°F) and a relative humidity from 10 to 70% for a period of at least 4 hours prior to testing. The test environment had the same temperature and humidity as the soak environment.
3. The neck pitch change joint was kept in the neutral position.
4. The lower thoracic spine (LTS) pitch change joint was set to the slouched posture position.
5. Joints were set to 1-2g setting.
6. The dummy was seated on a steel, horizontal surface (± 0.5°) that was flat, smooth, rigid, clean, and dry with no back support.
7. All limbs were extended horizontally and forward to the midsagittal plane (median plane) with the midsagittal plane vertical within ± 1°. Arms were positioned so they did not interfere with the impact probe or suspension cables. Arm supports were used to help support the dummy.
8. The crotch strap portion of the jacket was placed under the pelvis so that later jacket installation did not affect positioning.
9. Pelvis was positioned so that the pelvis tilt sensor read approximately 8° (rearward tilt about the Y-axis) and 0° laterally (about the X-axis). The test setup parameters are shown in Table 35.
10. Lower thorax was positioned so that the T12 tilt sensor (lower thorax) read approximately 0° about the Y-axis and 0° laterally about the X-axis (Figure 59).

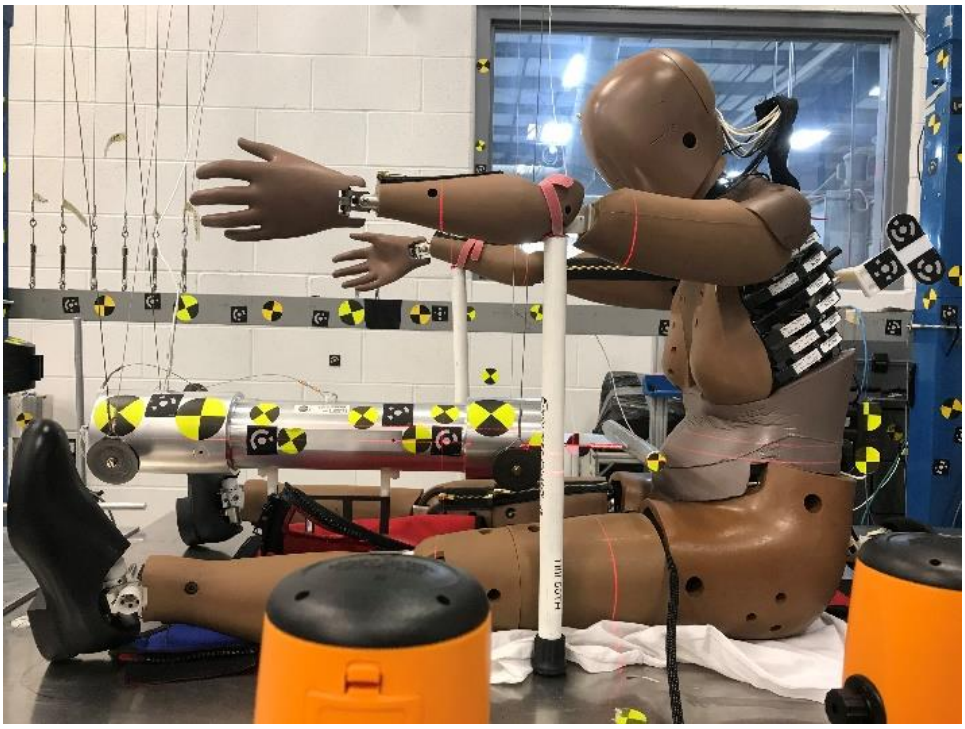

Figure 59. Initial setup for lower abdomen impact test

11. The vertical centerline of the probe was aligned with the midsagittal plane of the ATD (Figure 60). The midsagittal plane was visualized using the center of the hole for the front neck cable, and the belly button landmark.

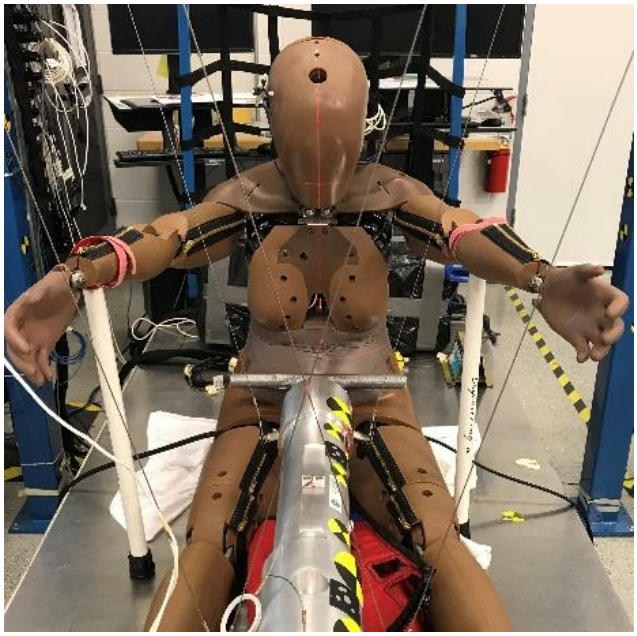

Figure 60. Vertical alignment

12. The table height was adjusted so the center of the rigid bar was 20.7 mm below the umbilicus.
13. The jacket was reattached once the dummy was in position by zipping up the back and shoulders. (the cloth under the dummy seen in Figure 60 was removed prior to testing).

14. The dummy was positioned so the abdomen was just barely touching the impact probe when the probe was at rest. ***NOTE:*** *Test probe centerline was horizontal (± 0.5°) at impact.*
15. Cloths under dummy used in positioning were removed.
16. At least 20 milliseconds of pre-time zero data and 100 milliseconds of post-time zero data was recorded.
17. The motion of the impactor was constrained so that there was no significant lateral, vertical, or rotational movement.
18. At least 30 minutes had passed since the last lower thorax or abdomen test.
19. The probe was raised ~75" above the resting position to generate an impact velocity of 6.1 m/s. Actual impact velocities achieved are shown in Table 34.

Table 34. Impact velocities achieved in the lower abdomen impact tests

Test ID	607	608	609
Impact velocity	6.08 m/s	6.07 m/s	6.10 m/s

Table 35. Lower abdomen impact setup parameters

Parameter	**Setting**	
Neck Pitch Change Setting	"Neutral"	
LTS Pitch Change Setting	"Slouched"	
Lower Thorax (T12) Tilt Sensor Reading(s):	X 0.7° 0.7° 0.2°	Y 0.4° 0.4° 0.4°
Pelvis Tilt Sensor Reading(s):	X 0.9° 0.9° 0.0°	Y 6.8° 6.8° 6.8°
Teflon® Sheeting on Test Bed?	No	
Dummy Clothing?	Jacket	
Wait Time Between Tests	30 minutes	

7.1.1.4 Data Processing

1. The polarity conventions and data acquisition system conformed to the latest requirements of SAE Recommended Practice J211.
2. Data channel offset was removed; per SAE J211 Section 8.4.3, the normalized value of a stable pre-test section of data was set to the *proper* initial value for the transducer.
3. Time zero (T_0) was defined when the probe contacted the dummy (for BioRank evaluation) or when the accelerometer with a CFC1000 response mounted on the probe rose through the 1g level.
4. Channels were filtered based on the CFC filter classes listed in Table 36.
5. The time history of the Probe Force was calculated using the Probe Acceleration at each time step:

$$Force_{Probe}(N) = Acceleration_{Probe}(m/s^2) * Mass_{Probe}(kg)$$

6. The external X-axis deflection was calculated from the high-speed video system.

Table 36. Lower abdomen test data channels

Item #	Channel Description	Filter Class	Comments
1	Contact Switch	N/A	For BioRank
2	Pendulum Acceleration	CFC-600	
3	Lower Right Abdomen Pressure Sensor	CFC-600	
4	Lower Left Abdomen Pressure Sensor	CFC-600	
5	Probe Force	N/A	Calculated
6	Abdomen X-Axis Deflection (External using High-speed Camera)	N/A	External Deflection

7.1.2 Results

For BioRank evaluation, the time zero was defined as contact time between the probe and the dummy with a contact switch. The lower abdomen rigid bar impact test results are shown in Figure 61 through Figure 63.

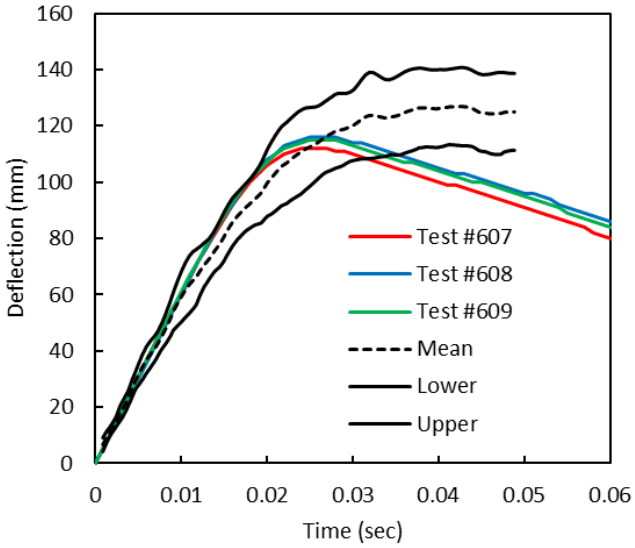

Figure 61. Deflection of lower abdomen rigid bar impact test

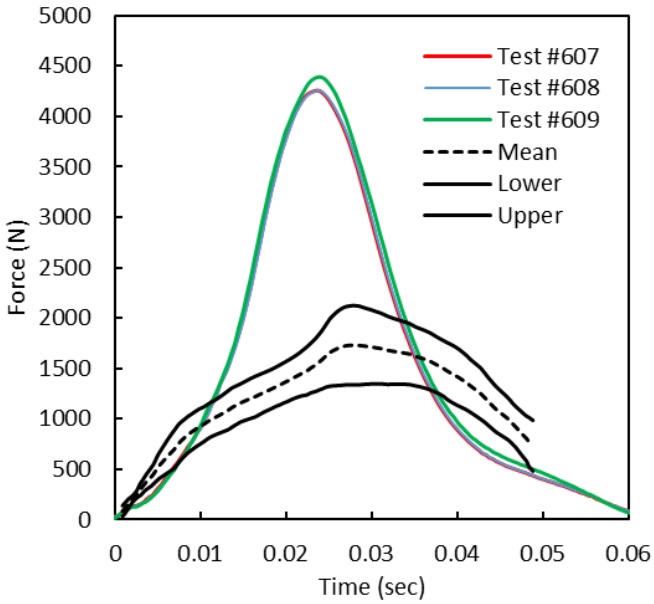

Figure 62. Probe force of lower abdomen rigid bar test

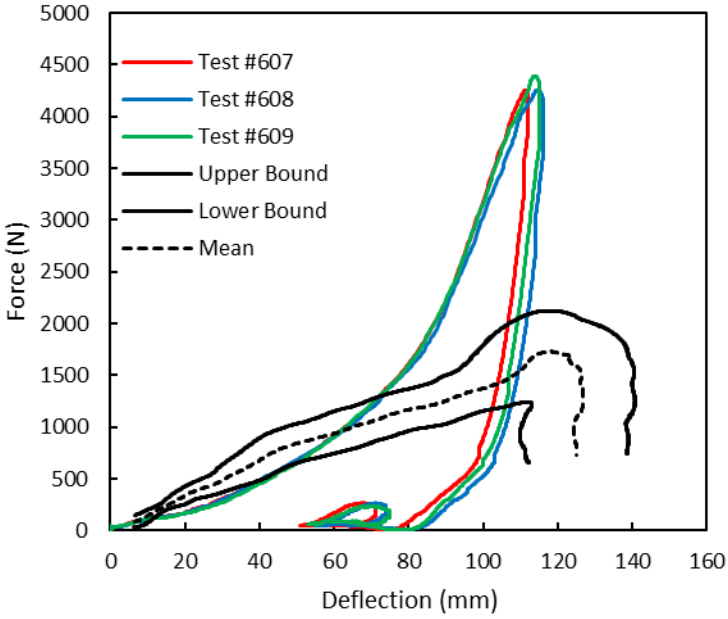

Figure 63. Force vs deflection of the lower abdomen rigid bar test

7.2 Upper Abdomen Impact

7.2.1 Methods

7.2.1.1 Materials used

1. Fully assembled THOR-05F dummy with left and right internal 3D IR-TRACC units in the upper and lower thorax (the lower ribs are engaged during test) and left and right abdomen pressure sensors.
2. Impact pendulum with a mass of 9.00 kg, which includes all attached hardware and 1/3 of the weight of the suspension cables. The impacting end of the probe is a rigid steering wheel shaped impact

face, mounted at an angle of 20° to the vertical axis. A sketch of the steering wheel geometry is shown in Figure 64.

3. Thin Teflon® sheet (62 cm x 122 cm x 0.2 cm) for test bed
4. Dummy clothing including suit and long underwear
5. Targets for external displacement calculation using high-speed cameras.

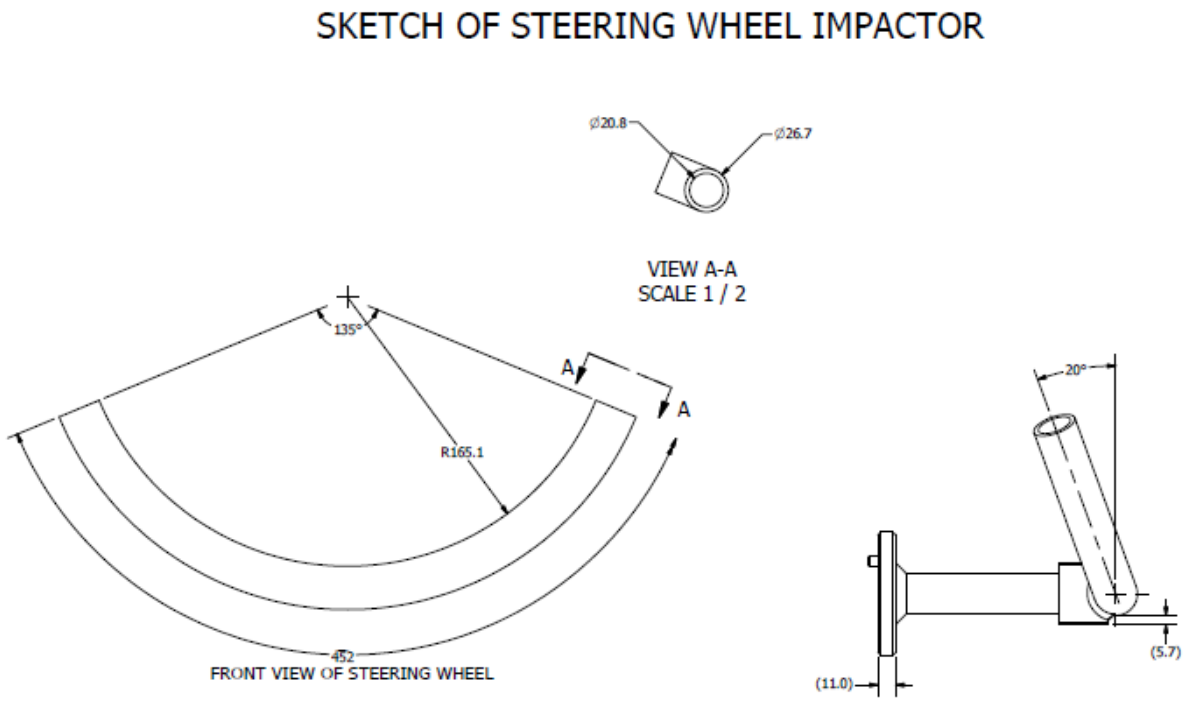

Figure 64. Dimensions and geometry of steering wheel impactor

7.2.1.2 Instrumentation

1. Impact velocity measuring instrumentation consists of a light trap and evenly spaced mechanical vanes that can generate square electrical pulse for velocity calculation.
2. Accelerometer for measuring the impactor acceleration, mounted to the probe with its sensitive axis in line with the longitudinal centerline of the test probe.
3. A dual-axis tilt sensor at T12 (lower thoracic spine or LTS) to measure initial angles about the “X” and “Y” axes.
4. A dual-axis tilt sensor in the pelvis to measure initial angles about the “X” and “Y” axes.
5. Contact switch for synchronizing external deflection with probe force.
6. Method for measuring external abdominal displacement (high-speed cameras).
7. Targets on impact probe, dummy and test fixture for external displacement calculations. Target must be attached to the local body segment being impacted.

7.2.1.3 Test Procedure

1. The abdomen foam and the outer neoprene suit was inspected for wear, tears, or other damage.

2. Dummy was soaked in a controlled environment at a temperature between 20.6° to 22.2°C (69° to 72°F) and a relative humidity from 10 to 70% for a period of at least 4 hours prior to testing. The test environment had the same temperature and humidity as the soak environment.
3. The neck pitch change joint was set to the neutral position.
4. The lower thoracic spine (LTS) pitch change joint was set to the slouched position.
5. Joints were set to 1-2g setting.
6. The dummy was dressed in long underwear.
7. The dummy was seated atop the thin Teflon® sheet on a horizontal surface (± 0.5°) with no back support.
8. All limbs were extended horizontally and forward to the midsagittal plane. Arms were positioned so they did not interfere with the impact probe or suspension cables. The midsagittal plane was vertical within ± 1.0 degree (Figure 65). Arm supports were used to help support the dummy.
9. The crotch strap portion of the jacket was placed under the pelvis so that later jacket installation did not affect positioning.
10. The pelvis was positioned so that the pelvis tilt sensor read approximately 8° (rearward tilt about the Y-axis) and 0° laterally (about the X-axis). The test setup parameters are shown in Table 37.
11. The lower thorax was positioned so that the T12 tilt sensor (lower thorax) read approximately 0° about the Y-axis and 0° laterally about the X-axis.
12. The table height or impactor height was adjusted so that the bottom of the steering wheel impact face was 8mm below the umbilicus (Figure 66).

Figure 65. Setup of upper abdomen test

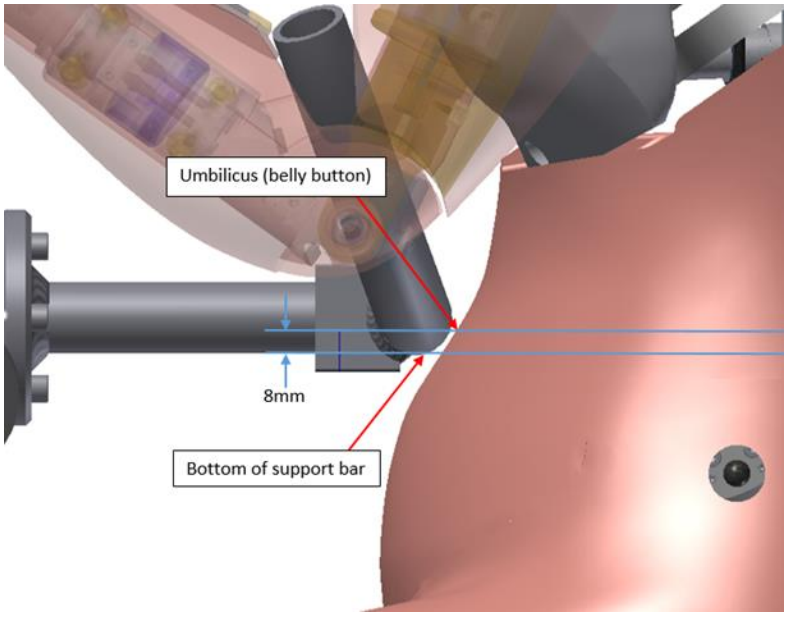

Figure 66. Upper abdomen impact point

13. The jacket was reattached once the dummy was in position by zipping up the back and shoulders.
14. The dummy was positioned so the abdomen was just barely touching the impact probe when the probe was at rest. ***NOTE:*** *Test probe centerline was horizontal (± 0.5°) at impact.*
15. At least 20 milliseconds of pre-time zero data and 100 milliseconds of post-time zero data was recorded.
16. The motion of the impactor was constrained so that there was no significant lateral, vertical, or rotational movement.
17. At least 30 minutes had passed since the last upper thorax, lower thorax, or abdomen test.
18. The probe was raised ~90" above the resting position to generate an impact velocity of 6.7 m/s. Actual impact velocity achieved is shown in Table 38.

Table 37. Upper abdomen impact setup parameters

Parameter	Setting	
Neck Pitch Change Setting	"Neutral"	
LTS Pitch Change Setting	"Slouched"	
LTS(T12) Tilt Sensor Reading(s):	X -0.1° -0.8° 0.0°	Y -0.2° 0.0° 1.0°
Pelvis Tilt Sensor Readings(s):	X -0.4° -0.6° -0.5°	Y 8.3° 9.2° 8.5°
Teflon® Sheeting on Test Bed?	Yes	
Dummy Clothing?	Jacket + Long underwear	
Wait Time Between Tests	30 minutes	

Table 38. Impact velocities achieved in the upper abdomen impact tests

Test ID	603	604	606
Impact velocity	6.62 m/s	6.71 m/s	6.70 m/s

7.2.1.4 Data Processing

1. The polarity conventions and data acquisition system conformed to the latest requirements of SAE Recommended Practice J211.
2. Data channel offset was removed; per SAE J211 Section 8.4.3, the normalized value of a stable pre-test section of data was set to the proper initial value for the transducer.
3. Time zero (T_0) was defined when the probe contacted the dummy (for BioRank evaluation).
4. The time history of the Probe Force was calculated:

$$Force_{Probe}(N) = Acceleration_{Probe}(m/s^2) * Mass_{Probe}(kg)$$

5. The external X-axis deflection was calculated from the high-speed video system.

Table 39. Upper abdomen test data channels

Item #	Channel Description	Filter Class	Comments
1	Contact Switch	N/A	For BioRank
2	Pendulum Acceleration	CFC-600	
3	Probe Force	N/A	Calculated
4	Abdomen X-Axis Deflection (External using High-speed Camera)	N/A	External Deflection

7.2.2 Results

For BioRank evaluation, the time zero was defined as the contact time between the probe and the abdomen with contact switch. The upper abdomen steering wheel impact test responses are shown in Figure 67 through Figure 69.

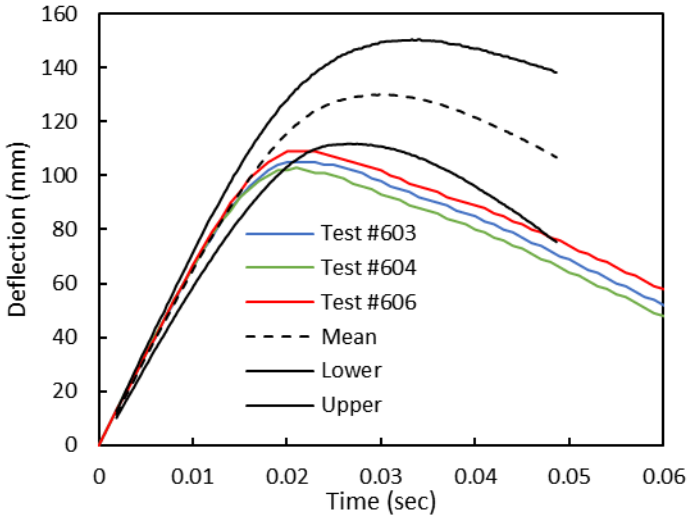

Figure 67. Deflection of the upper abdomen steering wheel impact test

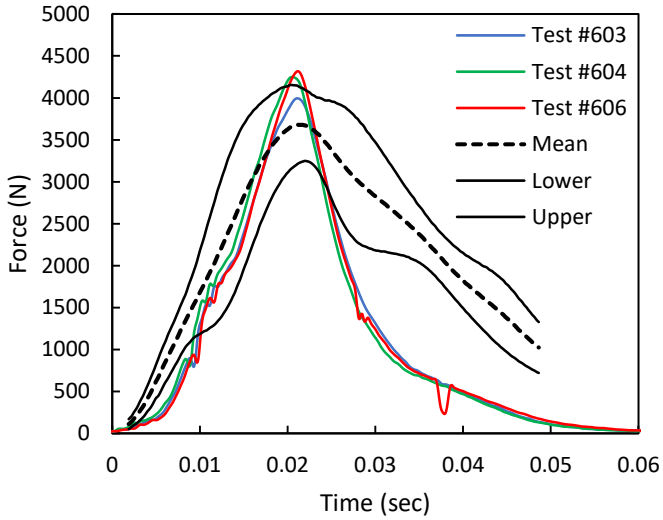

Figure 68. Probe force of the upper abdomen steering wheel impact test

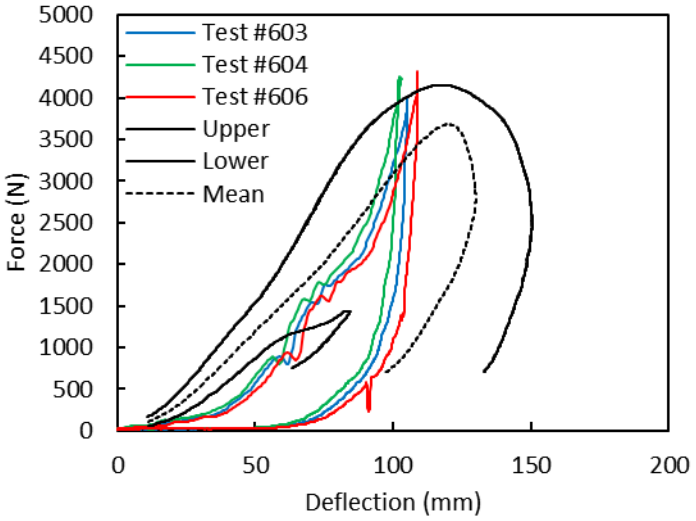

Figure 69. Force vs deflection of the upper abdomen steering wheel impact test

7.3 Abdomen Belt Pull

7.3.1 Methods

7.3.1.1 Test Setup

The seatbelt loading device described in Ramachandra et al (2016) was modified to accommodate a back support and used to test the THOR-05F ATD to mimic the targeted test setup as described in Lee et al. (2019). The device used a pneumatic piston to pull a seatbelt into the abdomen of the ATD in a controlled manner.

7.3.1.2 Instrumentation

A linear displacement potentiometer (Penny Giles, UK, Model #SLS190) mounted between the moving ram and its stationary frame measured ram displacement. A string potentiometer (Celesco, CA, Model #PT101) attached to the seatbelt webbing in front of the ATD at the level of the umbilicus measured displacement of the belt with respect to the table. This measurement was also used as the abdomen penetration.

Seatbelt load cells (Denton, Model #5755) were affixed to the belt on the left and right sides of the ATD to measure belt forces. Belt force was calculated as the sum of forces obtained from the two seatbelt load cells. A load cell and a linear accelerometer (Endevco, CA, Model #7264c) was also attached behind the ram as a redundant measure to obtain inertially compensated loading data in case the belt load cells failed. Data was collected using a TDAS G5 32-channel data acquisition system (DTS, Seal Beach, CA).

Figure 70 shows the pre-test position of the THOR-05F along with the external instrumentation used. The lumbar spine was positioned to be upright without any slouched and the lower thoracic spine was adjusted such that the T12 tilt sensor read 0 about the Y-axis and 0 ± 1° laterally about the X-axis. This allowed to minimize spinal flexion/extension during impact providing a true abdominal response.

Prior to impact, the arms were lifted to shoulder level to ensure that they would not interfere with the movement of the ATD. The legs splayed slightly outward in a natural seated position. The seatbelt was positioned to wrap around the anterior and lateral aspects of the ATD abdomen at the mid-abdomen level. Anteriorly, this position corresponded to the belly-button mark on the one-piece abdomen visible when the jacket was removed. The initial belt tension was adjusted so that each belt load cell measured 15-20 N, to ensure repeatable initial position of the belt with respect to each ATD and remove any slack.

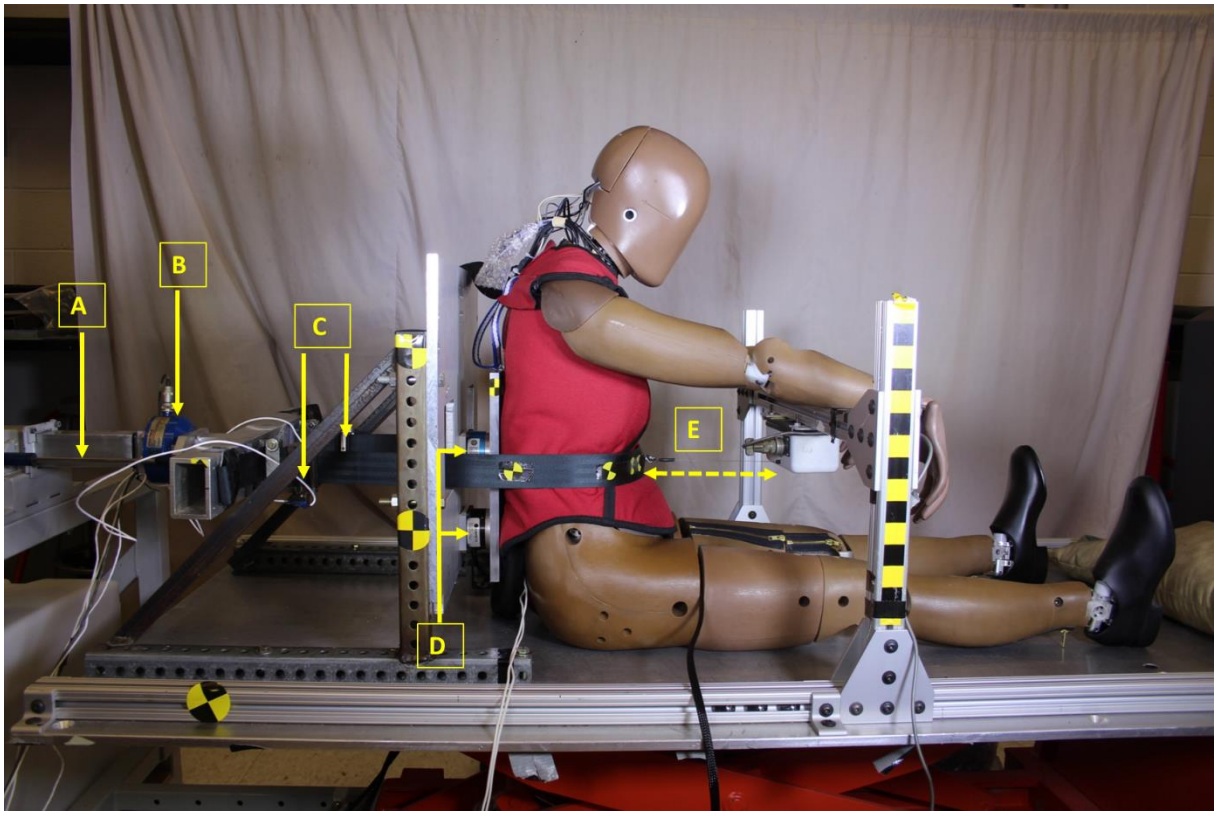

Figure 70. Pre-test positioning of THOR-05F on the seatbelt test device (A: Linear potentiometer on ram; B: Force transducer on ram; C: Seatbelt load cells; D: Load cells attached to lumbar back plate; and E: String potentiometer attached to seatbelt).

For all the trials, the chest jacket was used for accurate ATD representation and to take into account the influence of outer flesh/skin on the abdominal response. All tests were conducted using an accumulator pressure of 620 kPa. The penetration was limited to approximately 27% of seated abdominal depth.

Data were acquired at a sampling frequency of 20,000 Hz and in the laboratory coordinate system (LCS), with the positive x-axis directed from posterior to anterior, positive y-axis directed from left to right, and positive z-axis directed from superior to inferior, per standard SAE-J211.

7.3.2 Results

The current abdomen belt test was unable to match the target input loading (Figure 71). However, given similarity in overall loading rates, the force vs. deflection response was evaluated against the corridor (

Figure 72.). To determine the time zero for BioRank evaluation, the test data was aligned with the first force corridor value, the time coincident with the corridor time zero is defined as the time zero.

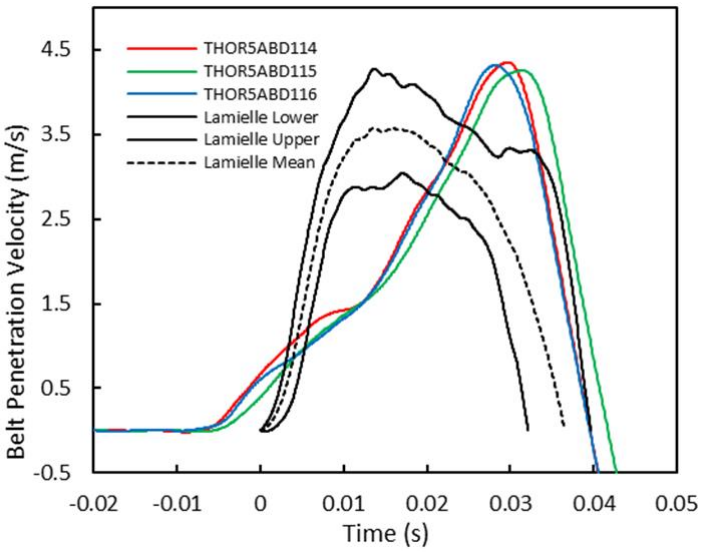

Figure 71. Belt penetration velocity achieved in THOR-05F test, compared with target corridor.

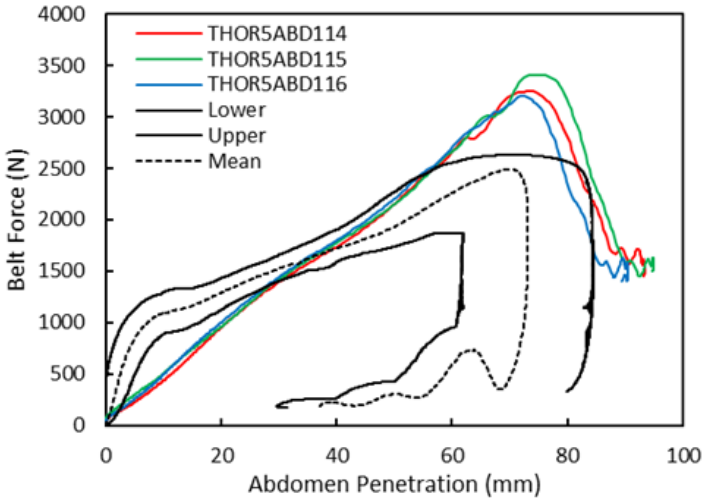

Figure 72. Force vs. belt penetration of the abdomen belt test with fixed seatback

7.4 Abdomen Biofidelity Summary

The abdomen BioRank scores are summarized in

Table 40. The overall abdomen BioRank score is 2.04, corresponding to “marginal” biofidelity. The upper abdomen BioRank is 1.33, corresponding to “good” biofidelity, while the lower abdomen impact test BioRank is 3.33, corresponding to “poor” biofidelity. The belt test BioRank is 1.46, corresponding to “good” biofidelity.

Table 40. Abdomen biofidelity summary

	SM	*P*	*RMS*
Upper Abdomen			**1.30**
Force	1.92	0.42	1.97
External deflection	1.31	0.21	1.32
Force vs External deflection	0.62	N/A	0.62
Lower Abdomen			**3.32**
Force	4.88	0.76	4.94
External deflection	1.18	0.20	1.20
Force vs External deflection	3.81	N/A	3.81
Abdomen Belt Test			**1.46**
Force vs Deflection	1.46	N/A	1.46
Abdomen Overall			**2.03**

8 Lumbar Spine

There was not a biofidelity requirement for the lumbar spine. The test was therefore intended to compare the results to a scaled result from THOR-50M lumbar spine. The test performed was a flexion test in which the bottom part of the lumbar was rigidly attached to the bottom of the head-neck pendulum, and the pendulum was decelerated from the specified velocity during contact with Hexcel® aluminum honeycomb (or equivalent). The ATD used for these tests was serial no. ED2634.

8.1.1 Methods

8.1.1.1 Materials

1. THOR-05F ATD assembly from base of lumbar to top of upper thorax, including thorax and abdominal foam inserts.
2. Head-neck pendulum (as defined in CFR Title 49, §572.33(c)3). Modifications to the mounting plate referenced in §572.33(c)3 may be necessary to match the hole pattern of the THOR-05F lumbar base. A drawing for such is shown in Figure 74.

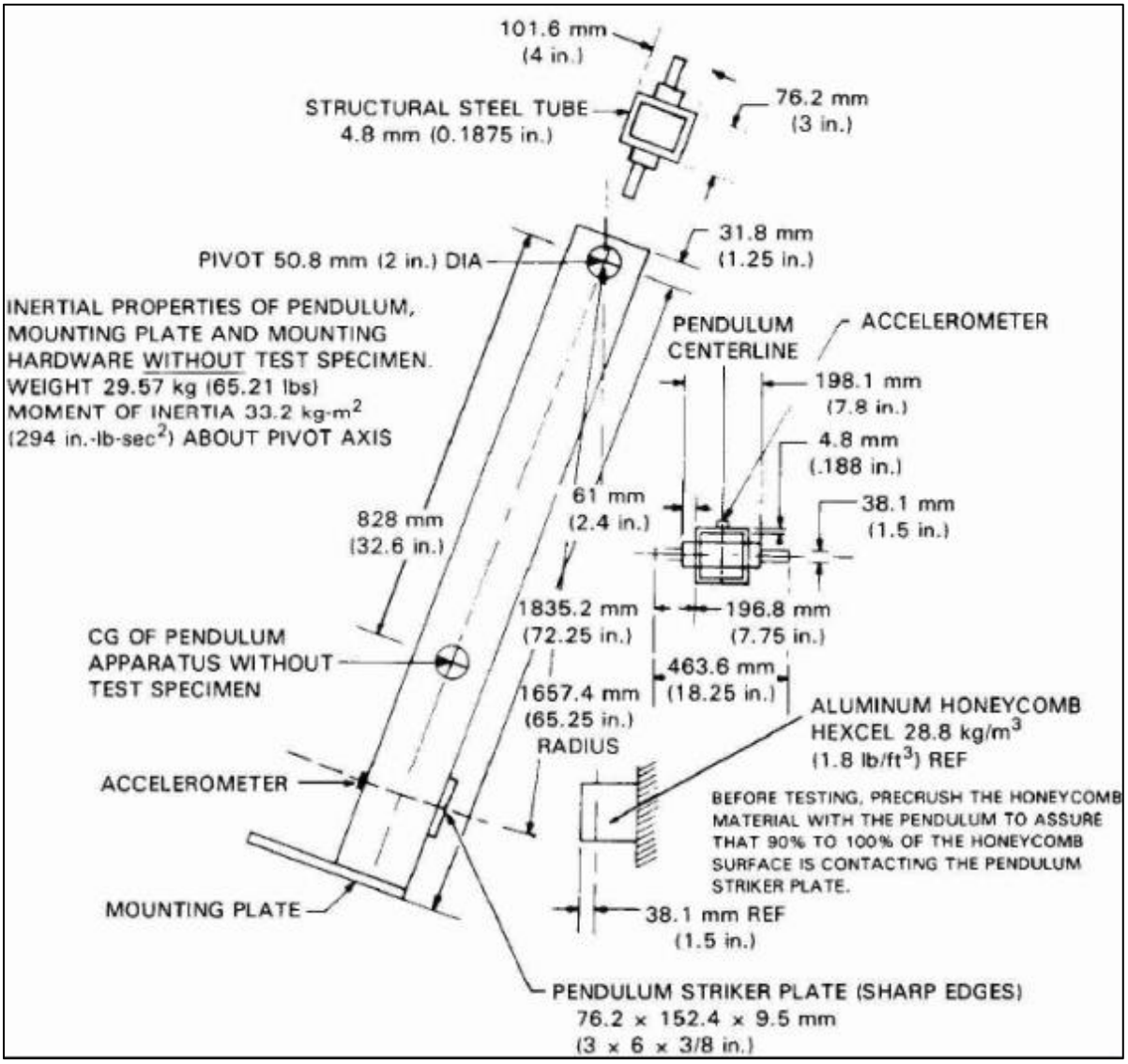

Figure 73. Neck Pendulum Apparatus (CFR Title 49, §572.33(c)3, Figure 22)

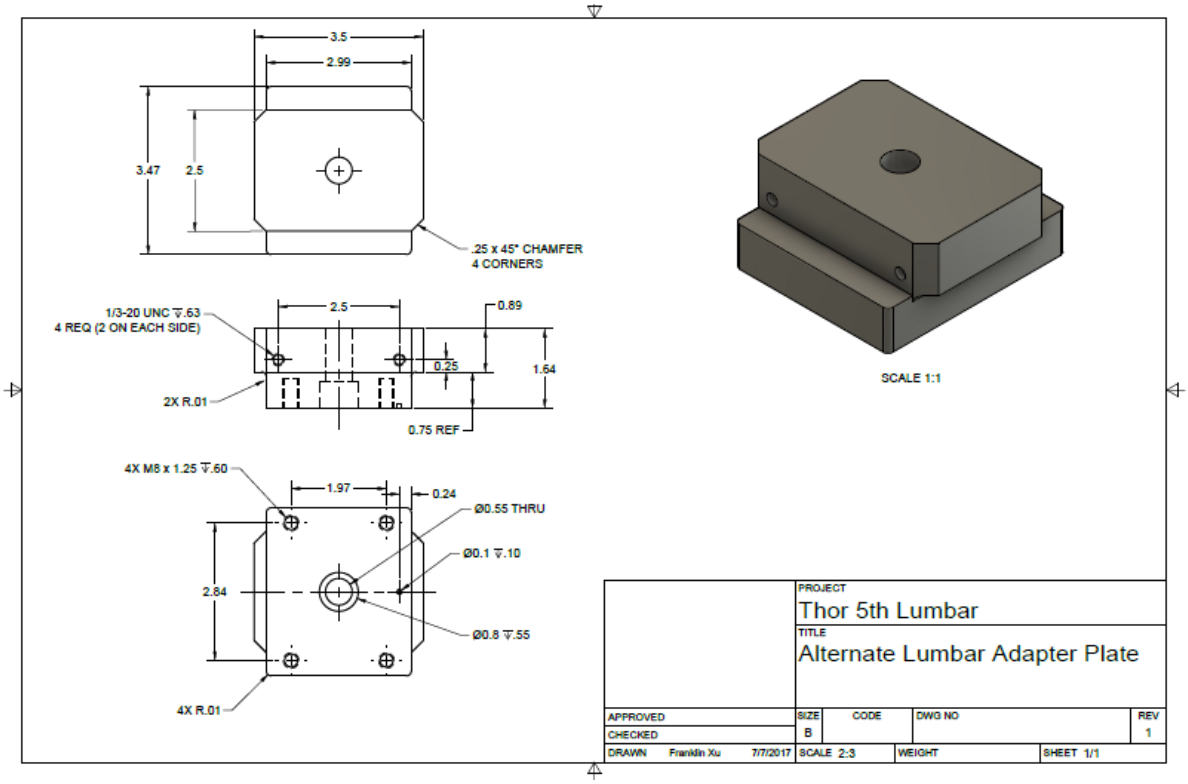

Figure 74. Adapter Plate Weldment

3. Head and neck structural replacements; a rigid bar and mass weighing 2.51 ± 0.1 kg. Drawings for each piece are shown in Figure 75 and Figure 76.

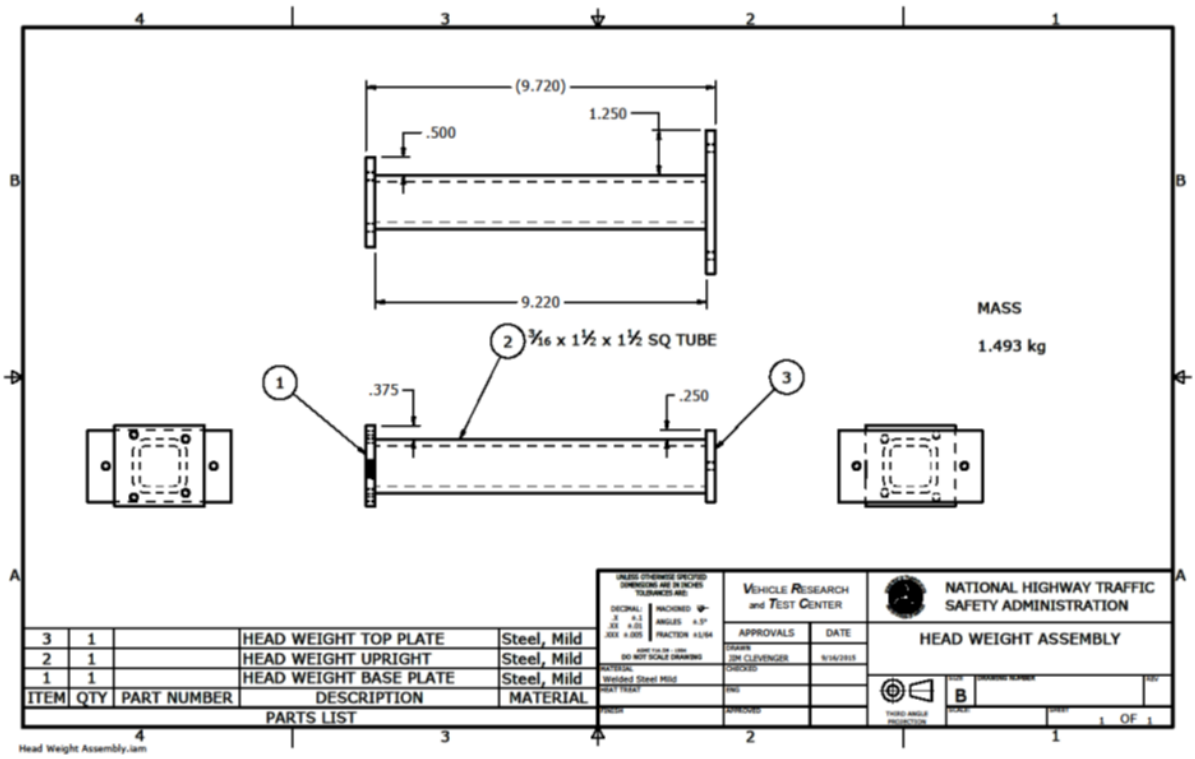

Figure 75. Rigid Bar Neck Structural Replacement

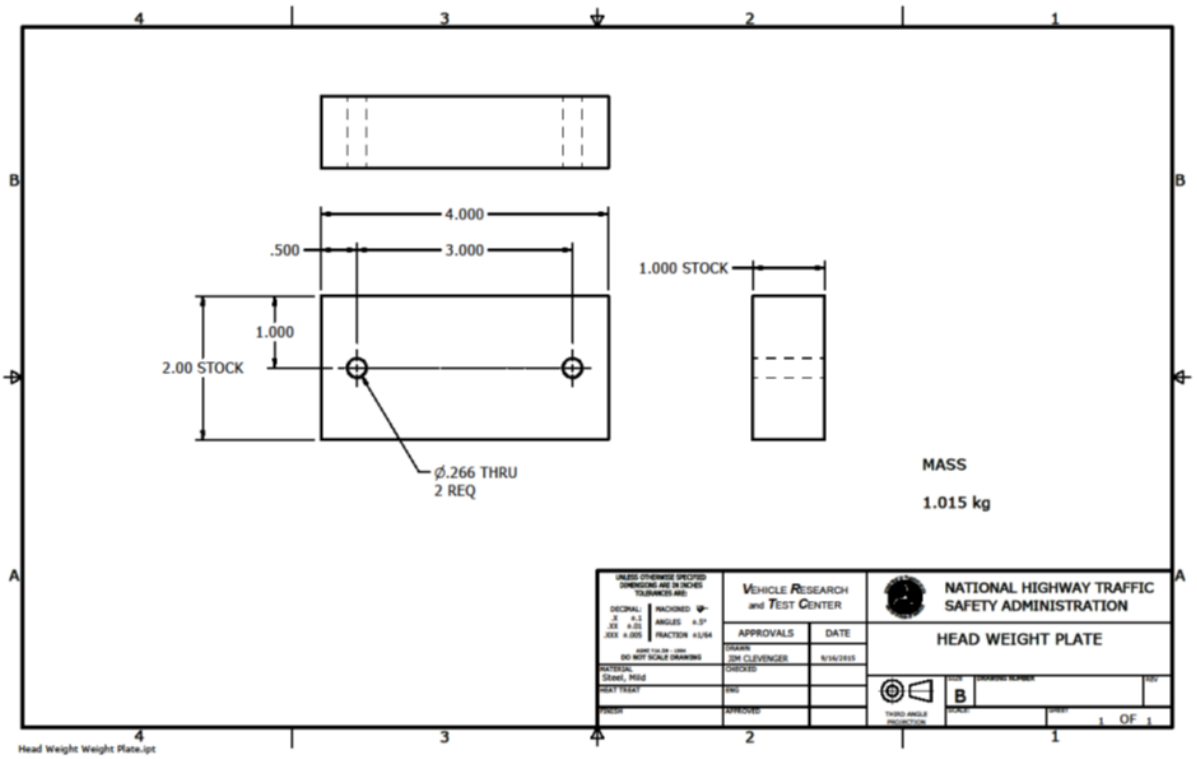

Figure 76. Head and Neck Mass Structural Replacement

4. 152.44 mm (6”) deep aluminum honeycomb used for decelerating the pendulum. Note that Length and width of the honeycomb are specific to each lab’s pendulum setup in order to obtain the specified pulse as detailed in Table 41, so honeycomb sizes may vary between labs. Alternate deceleration methods may be used provided that the deceleration pulse requirements are met.

Table 41. Pendulum Pulse for Lumbar Flexion Test

Parameter	Units	Specifications	
		Min.	Max.
Pendulum velocity at 5 ms after T0	m/s	0.363	0.441
Pendulum velocity at 15 ms after T0	m/s	1.162	1.331
Pendulum velocity at 25 ms after T0	m/s	1.743	2.005

8.1.1.2 Instrumentation

1. Accelerometer and Angular Rate Sensor on pendulum arm
   a. Mount the ARS to a surface on the pendulum arm that is perpendicular to the plane of motion on the pendulum’s longitudinal axis, such that the rotational velocity about the global Y-axis is recorded (Figure 77). Set the polarity of the pendulum ARS such that the rotation of the pendulum towards the honeycomb decelerator results in a positive angular velocity before impact.

Figure 77. Pendulum ARS Mounted about the Y-axis

2. T12 Y-Axis Angular Rate Sensor
3. Thoracic Spine Load Cell (Humanetics Model IH-11460J-09-PR-W253)
   a. Y-Axis Moment

8.1.1.3 Pre-Test Setup Procedure

1. Before the lumbar test was performed, the spine pitch and neck pitch were properly adjusted and

locked in place by ensuring the teeth were engaged and the hex bolt was tight.

2. The lower spine pitch change joint was set in “Slouched” Position (Figure 78).

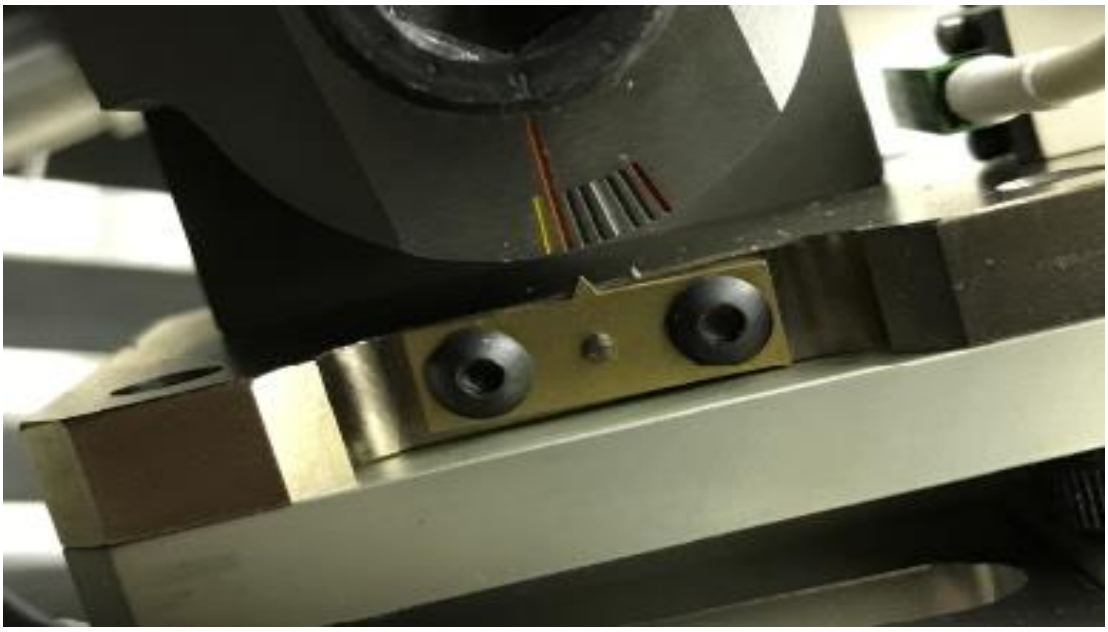

Figure 78. Lower Spine Pitch Change Joint in “Slouched” Position

3. The neck pitch change joint was set in “Neutral” Position (Figure 79).

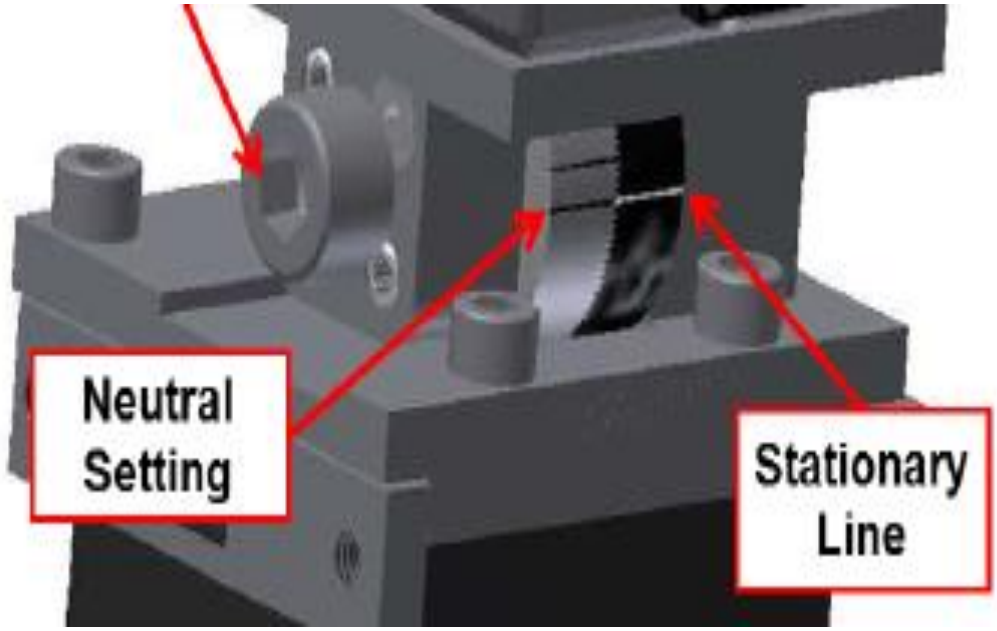

Figure 79. Neck Pitch Change Joint in “Neutral” Position

4. The pelvis and lower legs were removed at the base of the lumbar (Figure 80)

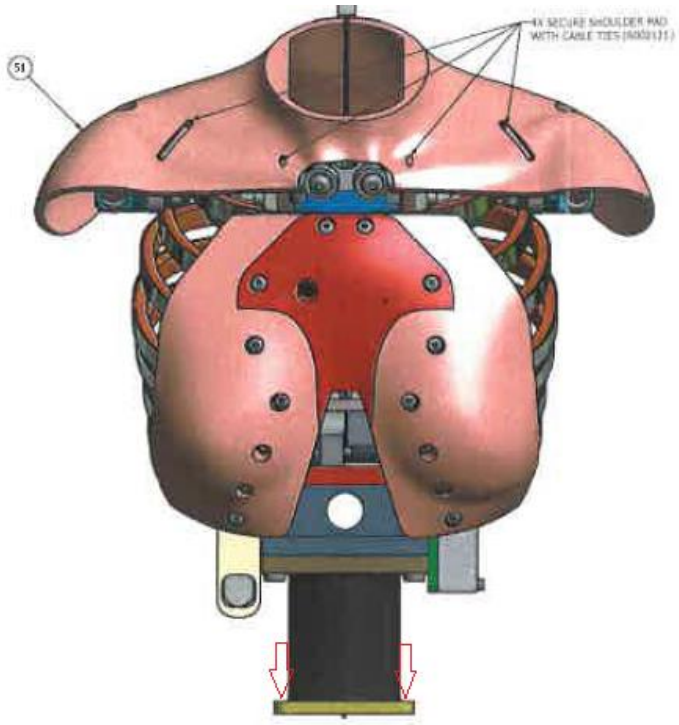

Figure 80. Pelvis and Lower Legs Removed at Base of Lumbar

5. Remove the two M8 x 1.25 x 16 LG. BHCS SS clavicle bolts (Figure 81)

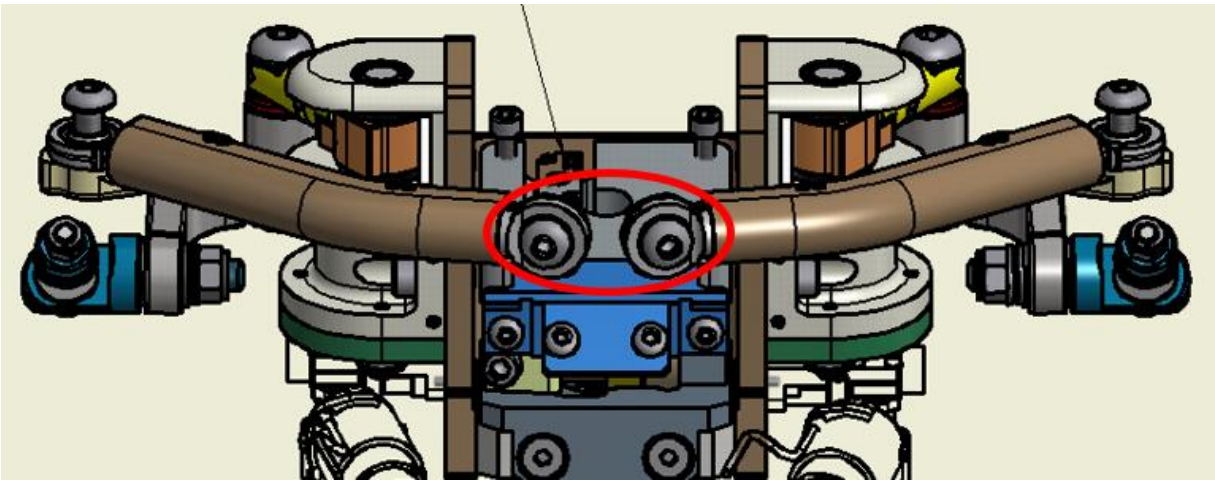

Figure 81. M8 x 1.25 x 16 LG. BHCS SS Bolts to Clavicles

6. Four M6 x 1 x 16 LG. SHCS bolts were removed from shoulders (Figure 82)

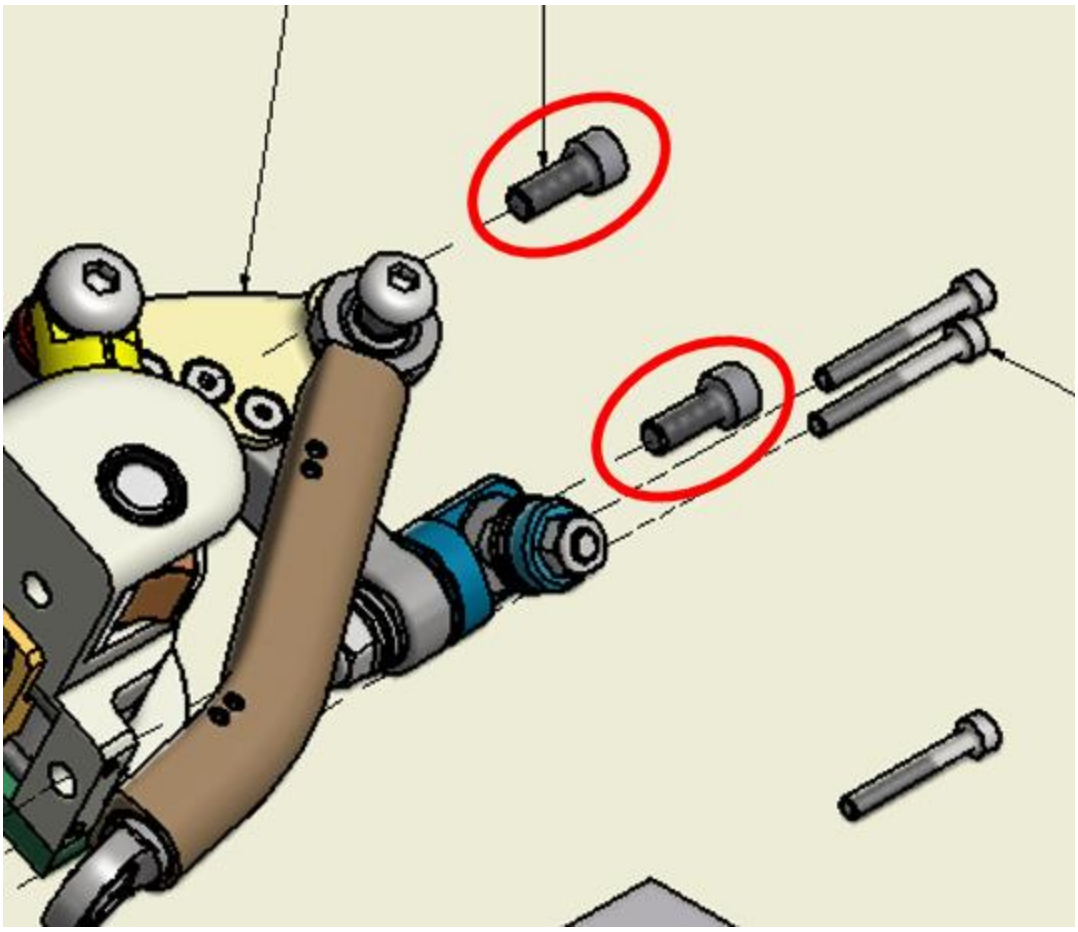

Figure 82. M6 x 1 x 16 LG. SHCS Bolts to Shoulders

7. The head and neck were replaced with the head and neck rigid bar and mass (Figure 83)

Figure 83. Mounted Head and Neck Structural Replacements

Figure 84. Mounted Final Assembly

8.1.1.4 Test Procedure

1. The upper thorax assembly, lumbar, and inserts were inspected for wears, tears, or other damage and for any debonding between the metal plates and rubber of the lumbar spine. The lower thorax insert and abdominal insert foams were inspected for any deformation or evidence of permanent set.
2. The upper thorax assembly, lumbar, and inserts were soaked in a controlled environment with a

temperature of 20.6 to 22.2°C (69 to 72°F) and a relative humidity from 10 to 70% for at least 4 hours prior to a test. The test environment had the same temperature and humidity requirements as the soak environment.

3. The appropriate 152.4 mm (6") aluminum honeycomb (or equivalent) was installed, to meet the pendulum pulse specified in Table 41 for an impact velocity of 2.00 ± 0.05 m/s. The contact area of the aluminum honeycomb engaged the inspector plate on the pendulum upon impact. An 8 x 2 - 3 piece of honeycomb was used to meet the specified pulse.
4. The "as measured (AM)" channels listed in Table 42 were recorded in accordance with SAE-J211. The time of first contact between the striker and the honeycomb (or equivalent deceleration device) was determined using a contact strip. At least 400 milliseconds of data were recorded before contact.
5. At least 30 minutes had passed since the last test involving the lumbar.
6. The pendulum was released from a height to generate a 2.00 ± 0.05 m/s velocity at impact.

8.1.1.5 Data Processing

1. Time zero (T0) was defined as the time when the striker contacted the honeycomb.
2. Data channel offset removed per SAE J211 Section 8.4.3
3. Channels were filtered based on the CFC filter classes listed in Table 42.
4. Pendulum velocity was calculated using the pendulum accelerometer.

$$Pendulum\ X\ velocity = \int_{t_0}^{t_f} (Pendulum\ Accel_x) dt$$

$$where\ t_0\ and\ t_f\ are\ the\ first\ and\ last\ time\ points, respectively, for\ data\ collection.$$

5. Lumbar flexion angle was calculated using pendulum angular rate sensor and lumbar spine angular rate sensor.

$$Pendulum\ angle\ Y = \int_{t_0}^{t_f} (Pendulum\ ARS_y) dt$$

$$Lumbar\ spine\ angle\ Y = \int_{t_0}^{t_f} (T12\ ARS_y) dt$$

$$Lumbar\ spine\ flexion\ angle\ Y = Lumbar\ spine\ angle\ Y - Pendulum\ angle\ Y$$

Table 42. Required Measurement Channels for the Lumbar Flexion Test

Channel Description	CFC	ISO-MME Code	AXIS	DASTAT	SENATT	SENTYP	YUNITS
Pendulum Accelerometer	180	T0SENSMI0000ACXD	X	AM	PEND	AC	G'S
Pendulum Angular Rate Sensor	180	T0SENSMI0000AVXD	Y	AM	PEND	AV	DPS
T12 Angular Rate Sensor	180	THSP1200THAVYA	Y	AM	SPNM	AV	DPS
Thoracic Spine Moment	180	THSP1200THMOYA	Y	AM	SPNM	MO	NWM

8.1.2 Results

The response of the lumbar is shown in Figure 85. The THOR-05F lumbar response did not meet the target specification (shown as a black box in Figure 85).

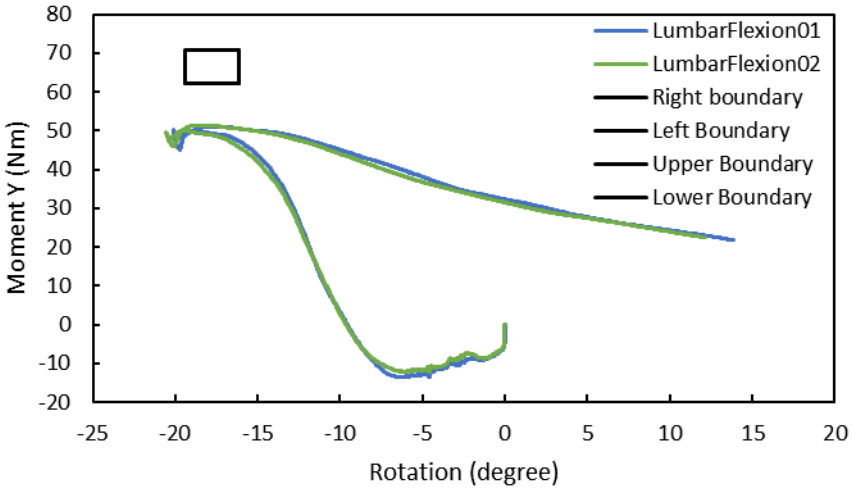

Figure 85. Moment Y vs rotation of the lumbar pendulum impact test

Uriot et al. (2015) conducted static lumbar stiffness tests on nine PMHS and THOR-50M. The lumbar stiffness (i.e. slope of response) of the PMHS ranged from approximately 1 Nm/degree to 4 Nm/degree with a mean 2.5 Nm/degree. The stiffness of actual THOR-05F response in the dynamic test was approximately 2.8 Nm/degree from the test data, which is within the range of the available PMHS data. Given that THOR-50M lumbar was stiffer than that in PMHS, the THOR-05F lumbar stiffness target is also expected to be stiffer than human. Therefore, it was decided not to make any additional design changes to this softer-than-target lumbar.

The BioRank score was not calculated because there was no appropriate biofidelity corridor for such calculation.

9 Knee-Thigh-Hip

The knee-thigh-hip complex biofidelity test consists of femur impact test with the whole body at 3.5 m/s, isolated lower extremity impact test at 1.2 m/s, and knee slider impact test at 2.15 m/s.

Table 43. Summary of the KTH biofidelity test conditions

Test Condition	Input	ATD Identifier
KTH full body	3.5 m/s, 255 kg impactor mass	Serial No. ED7441
KTH Isolated	1.2 m/s, 250 kg platform mass impact to static guided ram 9.5 mm diameter Hexcel and 13 floatation foam between the ram and loading platform. Deflection zeroed at 100 N	Serial No. ED7441
Knee Slider	2.15 m/s, 7.26 kg mass, including 1/3 of the suspension cable, 76.2 mm face diameter with 0.5 mm edge radius	Serial No. ED7441 Knee slider: EE2949 and EC2848

9.1 Knee-Thigh-Hip Full Body Impact

9.1.1 Methods

9.1.1.1 Materials

1. Fully assembled THOR-05F dummy with pelvis and femur instrumentation.
2. Impactor with a mass of 255 kg, which includes the cart carrying the mass, two uniaxial load cells and all other hardware attached. The impacting end comprised of a solid aluminum plate covered with two pieces of 25mm thick Sorbothane [Sorbothane Inc., Kent OH] padding.
3. Symmetric loading was applied to the left and right knees of the dummy.
4. Thin Teflon® sheet for test bed

9.1.1.2 Instrumentation

1. The velocity was measured using a light trap with the metal piece of 1” width.
2. An accelerometer for measuring the impactor acceleration was mounted to the 255kg impacting cart. This also allowed for redundant measurement of impactor velocity.
3. Two accelerometers were attached to the non-impacting surface of the knee plates, one on each plate.
4. Two uniaxial load cells were attached to the knee impact plates, one on each plate, to measure the impact forces on each knee.
5. Acetabulum forces were measured using load cells in the left and right acetabulum load cells in the dummy.
6. Contact switch was attached to metal tapes on the left impactor surface and left knee to trigger the event and this corresponded to time zero for all data including sensors and high-speed cameras.

9.1.1.3 Test Procedure

1. The dummy was inspected for any damages to the thorax, pelvis or lower extremities. No damages were identified through visual inspection.
2. The dummy wore long underwear pants to mimic real world interaction with the seated surface.
3. The dummy was seated upright on a flat, rigid surface covered with a thin layer of Teflon sheet. The pelvis was positioned so that pelvis tilt sensor read approximately 6° about the Y-axis and 0° laterally about the X-axis. The lower thorax was positioned so that the T12 tilt sensor read approximately 0° about the Y-axis and 0° laterally about the X-axis.
4. The torso was unsupported and the arms were placed to the sides such that they did not interfere with the impactor or dummy movement. The lower leg was placed at an angle of 90 degrees relative to the femur. The feet were lightly supported on the platform.
5. The dummy was positioned fore-aft such that only pelvis was in contact with the Teflon by placing the posterior aspect of knee 15mm in front of the seat. This allowed for a free rearward movement of the dummy upon impact.
6. A 255kg cart was designed as a mini-sled to travel at the desired velocity when struck with a pendulum mass. The knee impactor plates were attached to the cart. The rails of the mini-sled were cleaned and lubricated prior to the test to remove frictional effects.
7. Two pads including a 25mm thick 50-durometer Sorbothane [Sorbothane Inc., Kent OH] over a 25mm thick 70-durometer Sorbothane were placed over the impacting plate of each knee. The center of the impactor plates was aligned with center of the knee.
8. The dummy knees were struck at the same and symmetrically using the 255kg impactor.
9. The test was conducted at 70F.
10. The dummy was impacted at a target speed of 3.5 m/s. The actual velocities achieved are shown in Table 44.

Table 44. Velocities achieved in full body KTH tests

Test ID	KTHFB23	KTHFB24	KTHFB25
Impact velocity	3.27 m/s	3.58 m/s	3.55 m/s

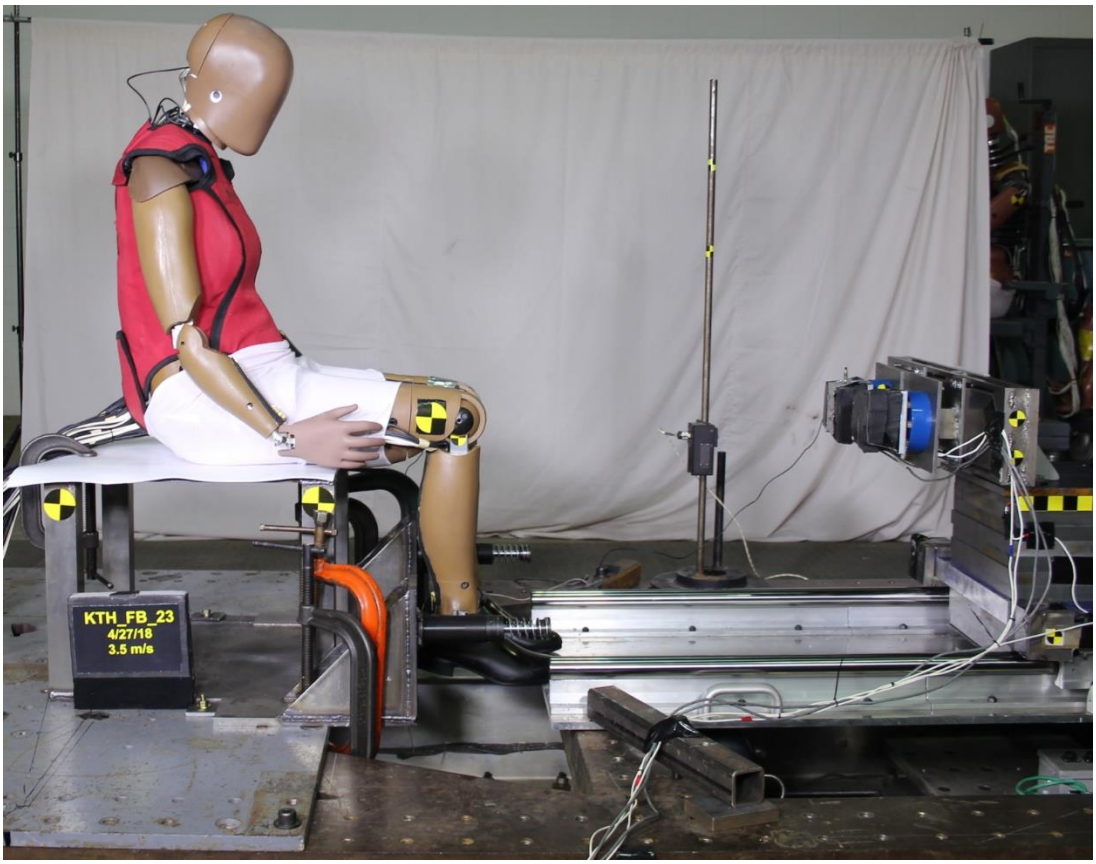

Figure 86. Initial setup for whole body KTH impact test

Figure 87. Front oblique view of pre-test dummy position

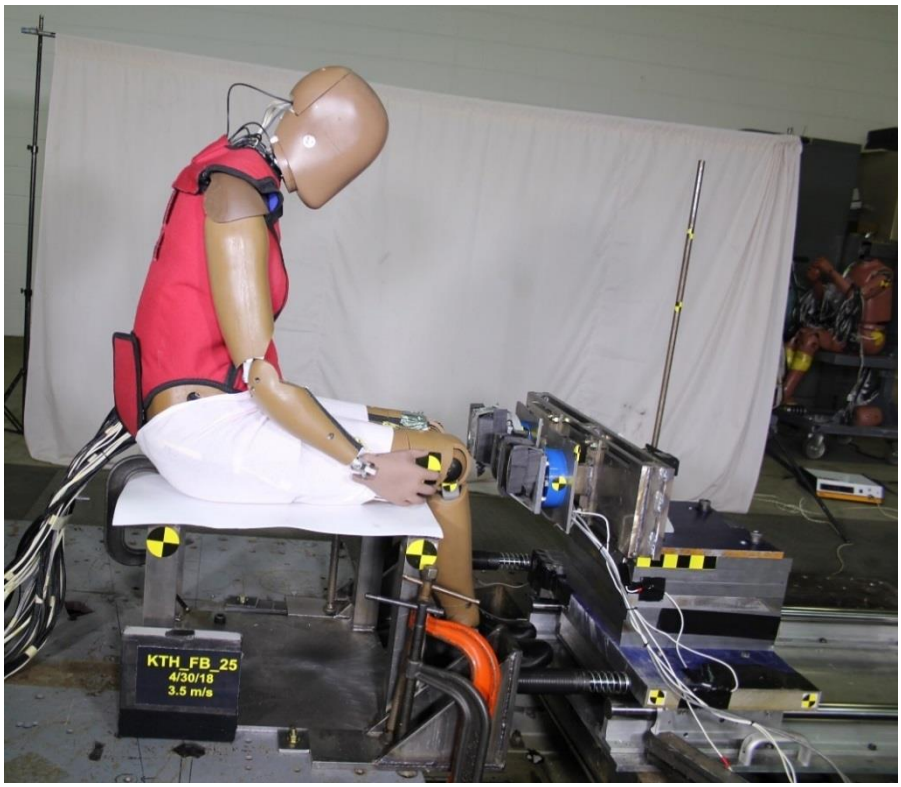

Figure 88. Final position of the dummy after impact

9.1.1.4 Data Processing

1. Data was collected at 20000 Hz using a TDAS system.
2. Video was recorded at 1000 frames per second.
3. Time zero (T_0) was defined when the impactor contacted the dummy using contact switch.

9.1.2 Results

Preliminary tests using an impact speed of 4.9 m/s were unsuccessful due to major sled damage after each test. Subsequent tests at the 3.5 m/s impact speed were successful though minor repairs were necessary after each test. The responses are shown in Figure 89 through Figure 91.

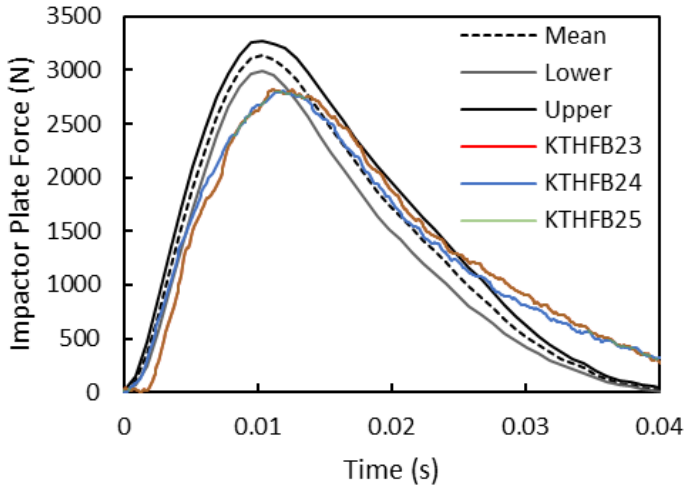

Figure 89. Impactor force of the KTH full body test.

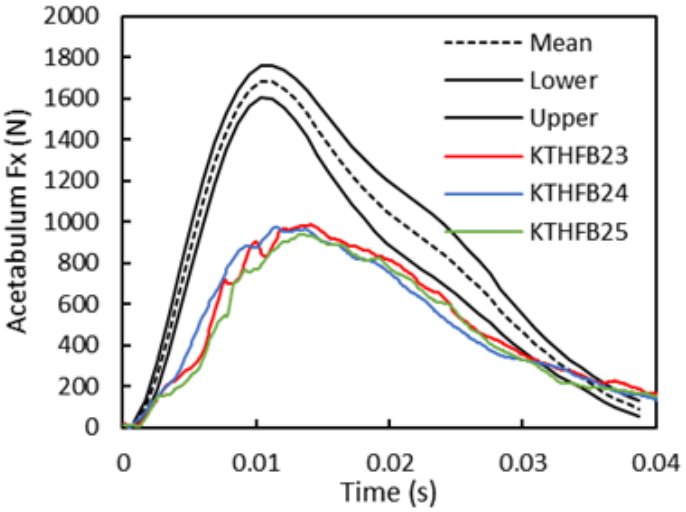

Figure 90. Acetabulum force Fx of KTH full body impact

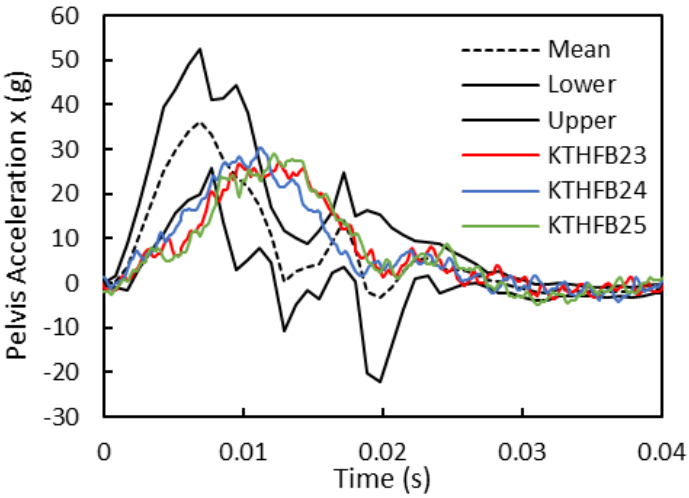

Figure 91. Pelvis acceleration x of KTH full body impact test.

9.2 Knee-Thigh-Hip Isolated Impact

9.2.1 Methods

9.2.1.1 Materials

1. THOR-05F dummy iliac wing and left lower extremity with pelvis and femur instrumentation.
2. Impactor with a mass of 250 kg, which includes the cart carrying the mass and all other hardware attached. The impacting end comprised of a solid aluminum plate covered with a 3.3 inch honeycomb (Hexcel) with 3/8" cells.
3. Ram connected to the knee as an interface fixture between the impactor and knee-thigh-hip complex.
4. Custom designed pelvic wing support rigidly attached to the base.

9.2.1.2 Instrumentation

1. The velocity was measured using a light trap with the metal piece of 1” width.
2. An accelerometer for measuring the impactor acceleration was mounted to the 250kg impacting cart. This also allowed for redundant measurement of impactor velocity.
3. One accelerometer attached to the non-impacting surface of the ram flange.
4. One six axis load cell attached to the ram behind a molded knee interface to measure forces on the knee.
5. Femur forces were measured using load cell in the femur of the dummy leg.
6. A uniaxial load cell was attached to the iliac wing support to measure the reaction load.
7. Contact switch was attached to metal tapes on the Hexcel on impactor surface and the blue floatation foam attached to the ram flange. The contact triggered the event and this corresponded to time zero for all data including sensors and high-speed cameras.

9.2.1.3 Test Procedure

1. The pelvis and left lower extremity of the dummy was inspected for any damages. No damages were identified through visual inspection.
2. The pelvis was rigidly attached to a custom designed iliac wing support using three long attachment pins each on the left and right iliac wing (Figure 93). This allowed for constraining the pelvis from translating or rotation upon impact.
3. The femur was positioned parallel to the ground (in x-axis) and the knee was firmly held using a molded wooden interface. The lower leg was placed at an angle of 90 degrees relative to the femur with the bottom of the feet facing upwards.
4. The ram was connected to the knee of the dummy using an interface fixture consisting of a ram shaft on a platform rigidly attached to the base. The free end of the ram shaft was attached to a flange which was covered using a 1 inch thick blue floatation foam (Figure 94).
5. The 250kg cart was designed as a mini-sled to strike the ram at the desired velocity when struck with a pendulum mass. The rails of the mini sled were cleaned and lubricated prior to the test to remove frictional effects. A 3.3 inch honeycomb (Hexcel) with 3/8" cell, 3000 series aluminum was cut to 5 inch diameter and pre-crushed to 2.5 inch which was attached to the impacting end of the cart (Figure 95).
6. The cart was accelerated to a velocity of approximately 1.2m/s and the rate of loading to the KTH was controlled using the combination of Hexcel and floatation foam at the interface of ram and impactor. Actual achieved velocities are shown in Table 45.
7. The test was conducted at 70F.

Table 45. Resulting velocities of the three isolated KTH tests

Test ID	KTHISO44	KTHISO45	KTHISO46
Impact velocity	1.12 m/s	1.20 m/s	1.19 m/s

9.2.1.4 Data Processing

1. Data was collected at 20000 Hz using a TDAS system.
2. Video was recorded at 1000 frames per second.
3. Time zero (T_0) was defined when the Hexcel on the impactor contacted the blue floatation foam on the ram shaft flange using contact switch.
4. The video data was used to calculate the displacement of the knee relative to the pelvic wing support using TEMA Motion software (Image Systems AB, Linköping, Sweden).
5. The resultant force was calculated from the six-axis load cells on the ram and in the femur.

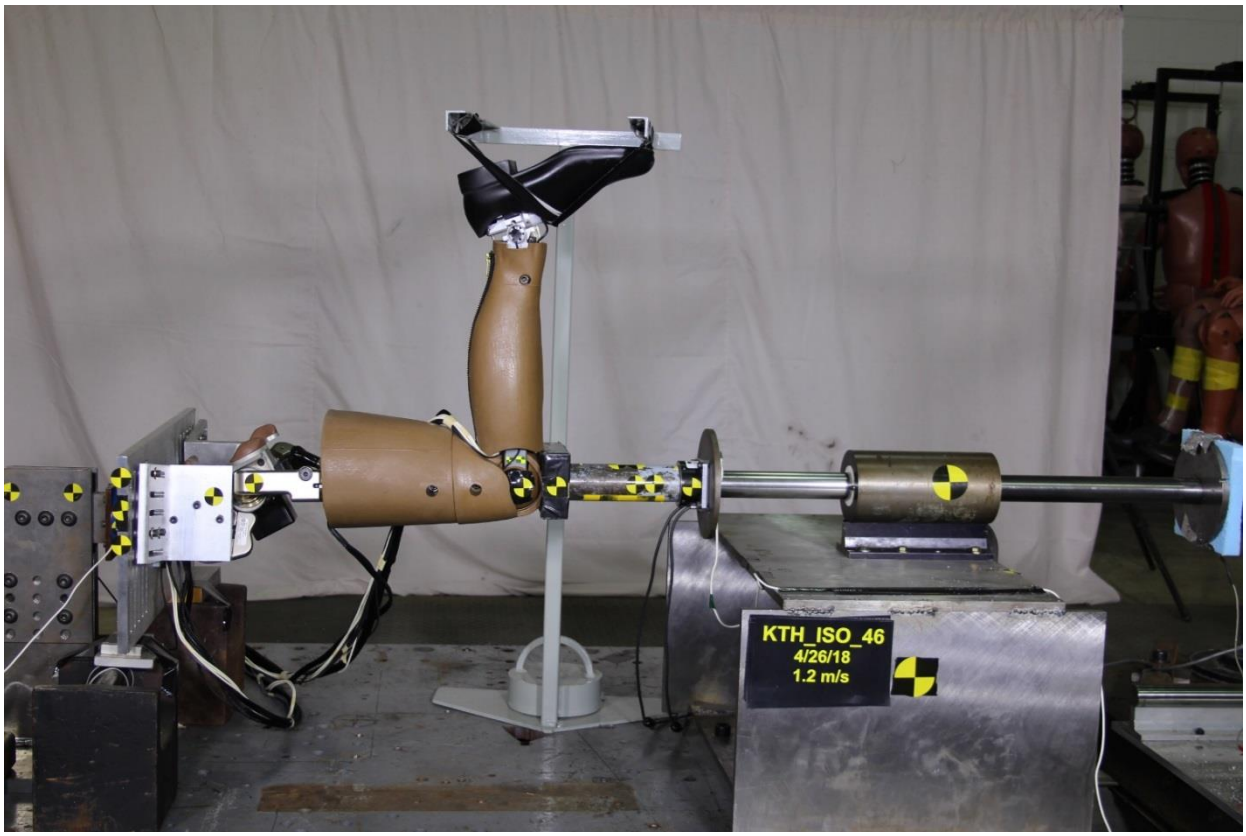

Figure 92. Initial setup for isolated KTH impact test

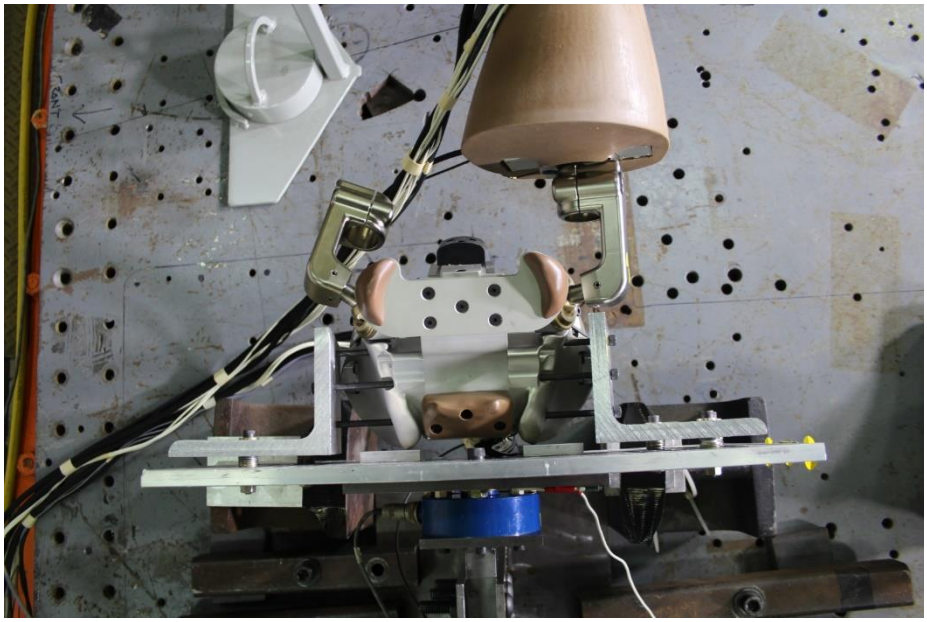

Figure 93. Iliac wing support with pelvis rigidly attached using three pins on each wing

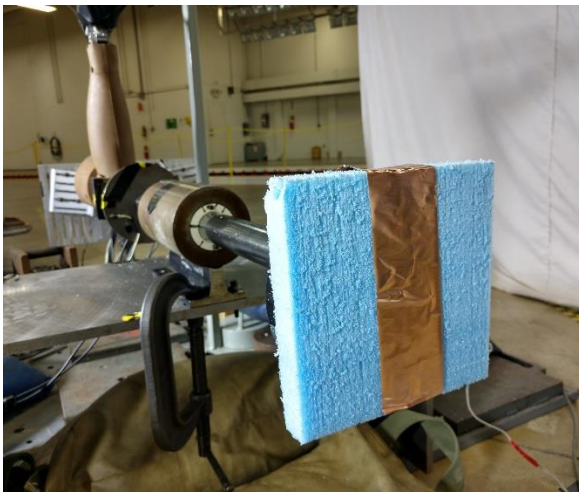

Figure 94. Blue floatation foam affixed on ram shaft flange

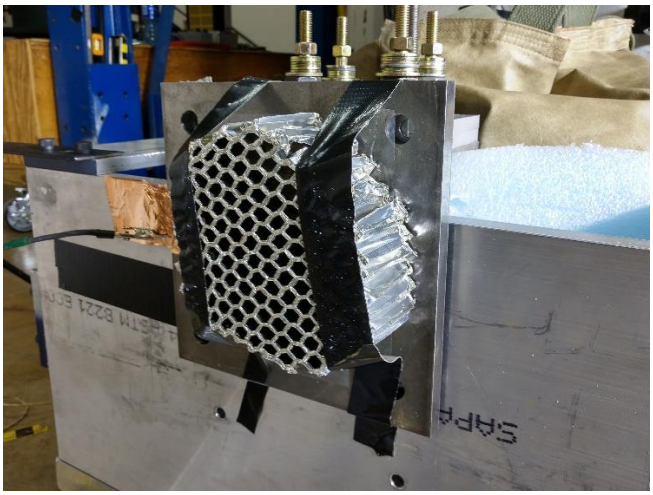

Figure 95. Pre-crushed Hexcel affixed on the impactor

9.2.2 Results

To determine the time zero for BioRank evaluation, the force of the test data was aligned with initial value of the corridor mean (81.9 N), the time coincident with the corridor time zero was the time zero for the test data. The results are shown in Figure 96 through Figure 98.

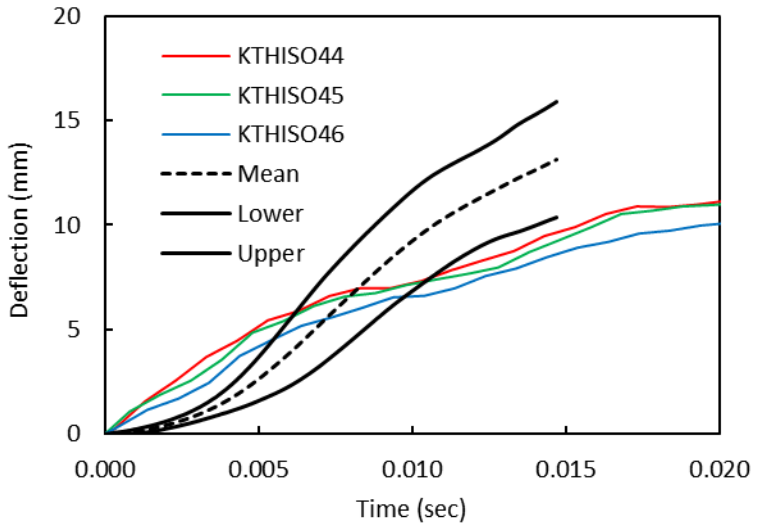

Figure 96. Deflection of the knee-thigh-hip isolated impact test

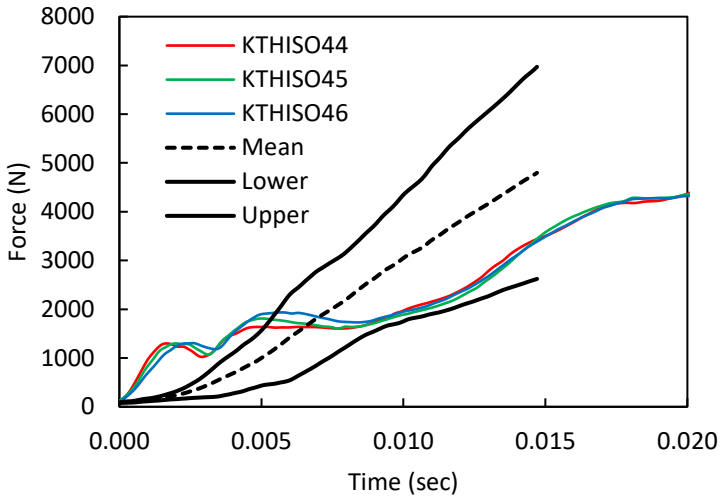

Figure 97. Force of the knee-thigh-hip isolated impact test

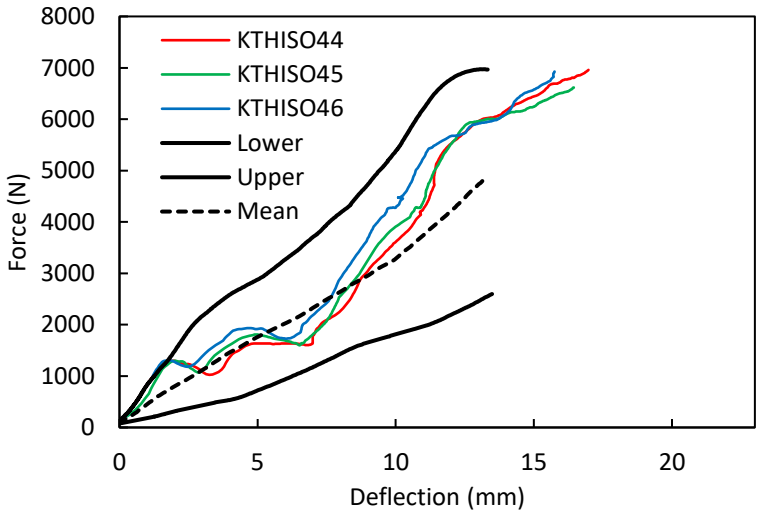

Figure 98. Force vs deflection of the knee-thigh-hip impact test

9.3 Knee Slider Impact

9.3.1 Methods

9.3.1.1 Materials used

1. THOR-05F knee assembly (including knee slider: 474-5300).
   NOTE: *Knee flesh and insert are not required for the test and may be left in place or removed.*
2. Impact fixture with THOR-05F leg adaptor (TH-474-0401)
3. Impact probe with a mass of 7.26 kg, including instrumentation, rigid attachments, and the lower 1/3 of the suspension cable mass. The diameter of the impacting face is 76.2 with an edge radius of 0.5 mm.
4. Load distribution bracket (Figure 99)
5. Torque wrench to torque mounting bolts
6. Mounting hardware (8) W50-61042 Modified BHSS M6 Thread

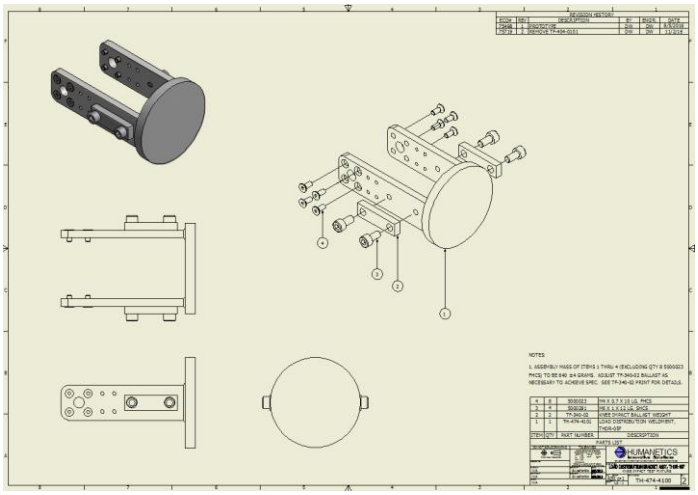

Figure 99. Knee slider distribution bracket

9.3.1.2 Instrumentation

1. Instrumentation to measure impact velocity consists of a light trap and evenly spaced mechanical vanes that can generate square electrical pulses for velocity calculation.
2. Knee potentiometer (150-0121V)
3. Femur load cell (IH-11510J)

9.3.1.3 Test Procedure

1. The knee slider assembly was inspected for damage. The left and right side slider assemblies were inspected to ensure the tracks were clean and free from damage which could affect the operation. The potentiometer string moved freely with the pot s installed.
2. The knee assembly was soaked in a controlled environment at a temperature between 20.6° to 22.2°C (69° to 72°F) and a relative humidity from 10 to 70% for a period of at least 4 hours prior to testing. The test environment had the same temperature and humidity as the soak environment.
3. The THOR-05F femur load cell was installed between the leg adapter and kneecap using the eight modified M6 BHSS and torque to 10.0 N-m (7.37 ft-lbf).
4. The assembly (Figure 100) was mounted to the knee impact test fixture using 3/8-16 SHCS and torque to 40.7 N-m (30 ft-lbf).
5. The inboard/outboard knee slider assembly (474-5380) was oriented such that motion along the knee slider track is horizontal, parallel to the long axis of the femur load cell.
6. The load distribution bracket was installed to the inboard and outboard slider assemblies in the orientation shown in Figure 100 using four M4x0.7 FHCS on each side and torque to 2.5 N-m (2.1 ft-lbf). ***NOTE:*** *The load distribution bracket was installed perpendicular to the orientation of the knee clevis in the fully assembled, seated dummy.*

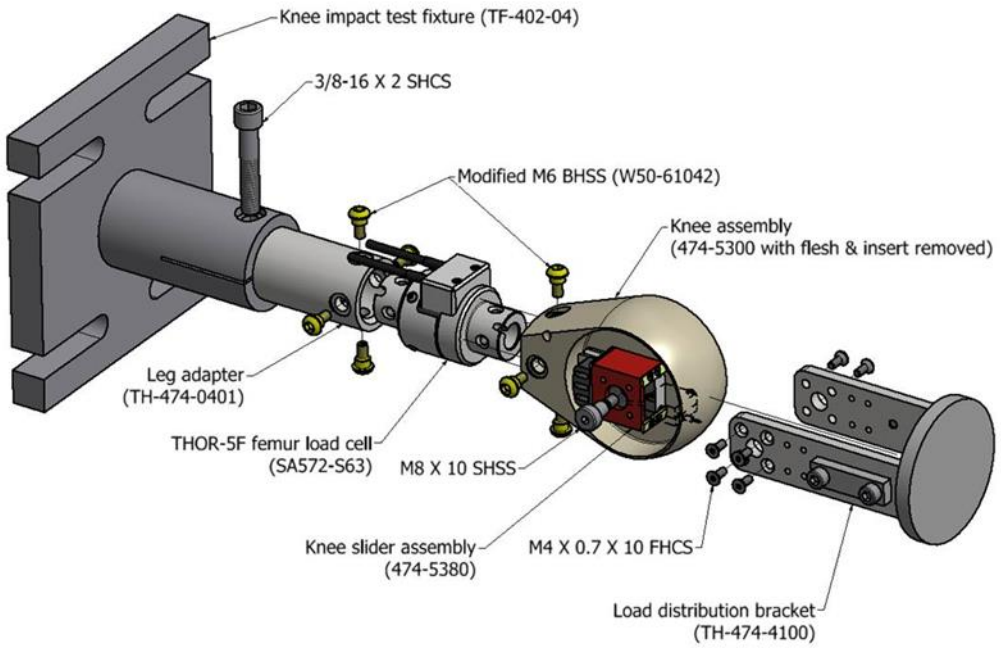

Figure 100. Knee slider impact test fixture

7. Once the load distribution bracket was installed, the torque on the M8 shoulder bolt was set to 5 N-m (3.69 ft-lbf) (Figure 101).

Figure 101. Knee joint bolt torque setting

8. The position of the impact probe was adjusted such that its longitudinal centerline was collinear within 1° with the centerline of the femur load cell. A laser level positioned between the centerline of the knee and the centerline of the probe both laterally (Figure 102) and on the top surface of the probe/knee (Figure 103) was used in this process.

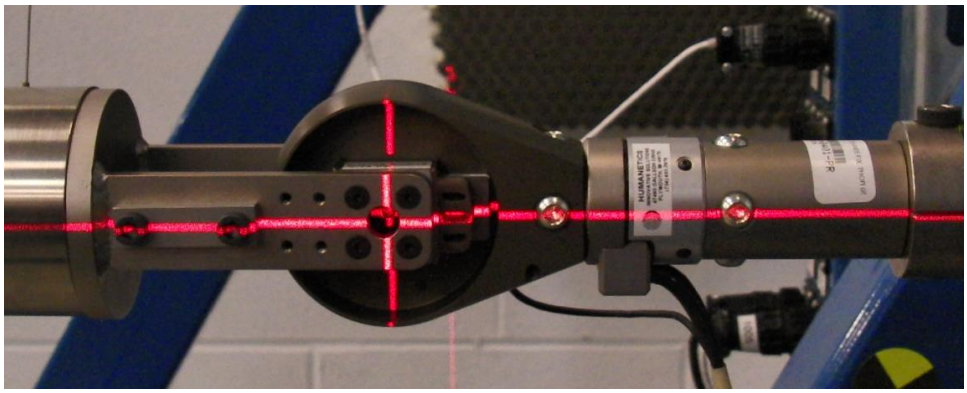

Figure 102. Vertical alignment of impact location

Figure 103. Lateral alignment of impact location

9. After alignment, the impact surfaces of the probe and the load distribution were approximately flush (Figure 104).

Figure 104. Alignment probe and distribution bracket impact surfaces

10. The distribution bracket was positioned so it was just barely touching the impact probe when the probe was at rest. ***NOTE:*** *Test probe centerline was horizontal (± 0.5°) at impact.*
11. At least 20 milliseconds of pre-time zero data and 50 milliseconds of post-time zero data was recorded.

12. The motion of the impactor was constrained so that there was no significant lateral, vertical, or rotational movement.
13. At least 30 minutes had passed since the last knee slider test (including break-in).
14. The probe was raised ~9" above the resting position to generate an impact velocity of 2.15 m/s. Actual velocities achieved are shown in Table 46.
15. Allow one break-in test before evaluating.

Table 46. Resulting velocities of the three knee slider tests

Test ID	537	538	539
Impact velocity	2.18 m/s	2.18 m/s	2.18 m/s

9.3.1.4 Data Processing

1. The polarity conventions and data acquisition system conformed to the latest requirements of SAE Recommended Practice J211.
2. Data channel offset removed from the Femur Load Cell and Potentiometer channels per SAE J211 Section 8.4.3.
3. Time zero (T_0) was defined when the femur load cell with a CFC-1000 response rose through the 40N level.
4. Channels were filtered based on the CFC filter classes listed in Table 47.

Table 47. Knee slider impact data channels

Item #	Channel Description	Filter Class	Comments
1	Knee String Pot	CFC-180	
2	Femur Load Cell, Fz	CFC-180	

9.3.2 Results

The knee slider response is shown in Figure 105.

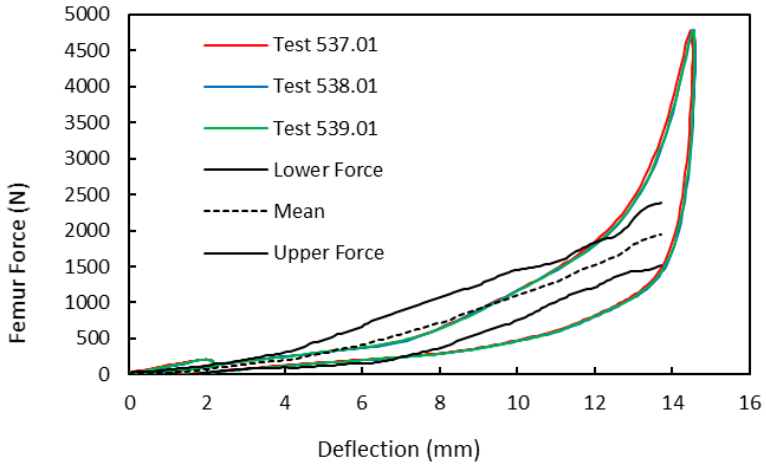

Figure 105. Femur force vs deflection of knee slider impact test at 2.15 m/s

9.4 Knee-Thigh-Hip Biofidelity Summary

The Knee-Thigh-Hip BioRank scores are summarized in Table 48. The knee slider has a BioRank score of 0.97, corresponding to "excellent" biofidelity. The KTH full body BioRank score is 2.19, corresponding to "marginal" biofidelity. The KTH isolated test BioRank score is 0.78, corresponding to "excellent" biofidelity. The knee-thigh-hip overall body region BioRank is 1.31, corresponding to "good" biofidelity.

Table 48. Knee-thigh-hip biofidelity summary

	SM	P	RMS
KTH Full Body (3.5 m/s)			**2.19**
Acetabulum Fx	3.84	0.52	3.88
Impactor Force	1.55	0.67	1.69
Pelvis Acceleration X	0.94	0.35	1.00
KTH Isolated			**0.78**
Force	0.78	0.21	0.81
Deflection	1.26	0.04	1.26
Force vs Deflection	0.29	NA	0.29
Knee Slider			**0.97**
Force vs Deflection	0.97	NA	0.97
KTH Overall BioRank			**1.31**

10 Lower Extremity

The four lower extremity biofidelity test conditions were dorsiflexion dynamic impact, axial heel impact test, and dynamic inversion and eversion tests. In order to evaluate the ATD response against the biofidelity corridor developed from PMHS test, the moment at the ankle joint center needs to be calculated. The moment at the ankle joint center for the dorsiflexion impact test was calculated with the following formula:

$$MANKL = MyTBLL-0.0864*FxTBLL$$

where 0.0864 is the distance in meters between the lower tibia load cell neutral axis and the ankle dorsiflexion pivot centerline (the upper pivot axis in THOR-05F ankle joint design), and TBLL is the **Tib**ia **L**ower **L**oadcell.

The moment at the ankle joint center for eversion and inversion impact test was calculated with the following formula:

$$MANKL = MxTBLL- 0.1014*FyTBLL$$

where 0.1014 is the distance in meters between the lower tibia load cell neutral axis and the ankle inversion/eversion pivot centerline (the lower pivot axis in THOR-05F ankle joint design), and TBLL is the **Tib**ia **L**ower **L**oadcell.

The test conditions are summarized in Table 49.

Table 49. Summary of the lower extremity test conditions

Test Condition	Input	ATD Identifier
Axial Heel Impact	3.1 m/s, 28.4 kg mass	Serial No. ED2634
Dorsiflexion (BOF) Impact	5.0 m/s, 3.0 kg mass Impact point: 110 mm above the ankle joint center, foot was flexed to 15° in plantar flexion from vertical	Right: SHOE #EC7694; ACHILLES #ED0420; DORSI #EE2398 Left: SHOE #ED2427; ACHILLES #EF8660; DORSI #EE9243
Inversion	Impact energy to generate 1000°/s rotational velocity	Serial No. ED2634
Eversion	Impact energy to generate 1000°/s rotational velocity	Serial No. ED2634

10.1.1 Ankle Setup

10.1.1.1 Materials

1. Fully assembled lower leg (474-5500-1/2) without shin guard, knee clevis, and lower leg flesh. Dynamic impactor with a PTFE (Teflon®) impact surface that is a rigid semi-cylinder 63.5 ± 2.5 mm in diameter and 88.9 ± 3.5 mm in length (Figure 106). Effective mass must be 3.00 ± 0.02 kg (6.68 ± 0.04 lbs). Effective mass calculation is defined in Appendix 2.

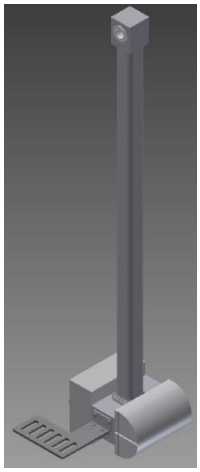

Figure 106. Example of dynamic impactor for THOR-05F ankle and foot tests (not to scale)

2. Rigid fixture for supporting lower leg in ball of foot impact test with the Achilles assembly attached to the leg.
3. Rigid fixture for supporting lower leg in heel of foot impact test.
4. Rigid fixture for supporting lower leg in inversion and eversion impact tests.
5. Inversion/eversion test bracket that consists of a 3.18 mm (1/8”) thick Delrin® pad attached to a 16 mm x 44.5 mm x 152 mm aluminum block as shown in APPENDIX 3.
6. Ankle zeroing bracket (Figure 107) to hold the ankle at 0°about all three axes while taking angle offset measurements for X, Y, Z ankle rotation.
7. Locking bracket (Figure 108) to hold ankle at 0° dorsiflexion for heel of foot testing.
8. Equipment for setting the Achilles cable tension (Figure 109).

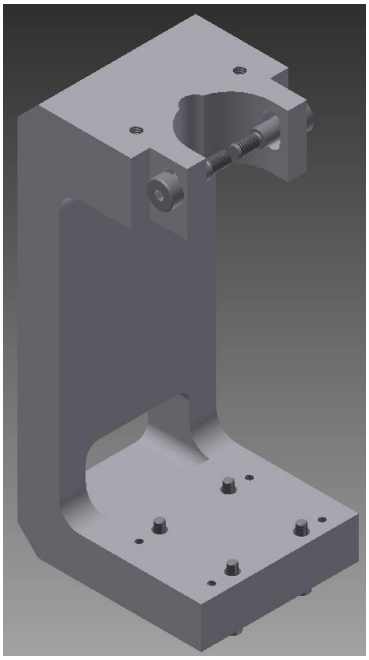

Figure 107. Example of Ankle zeroing Bracket

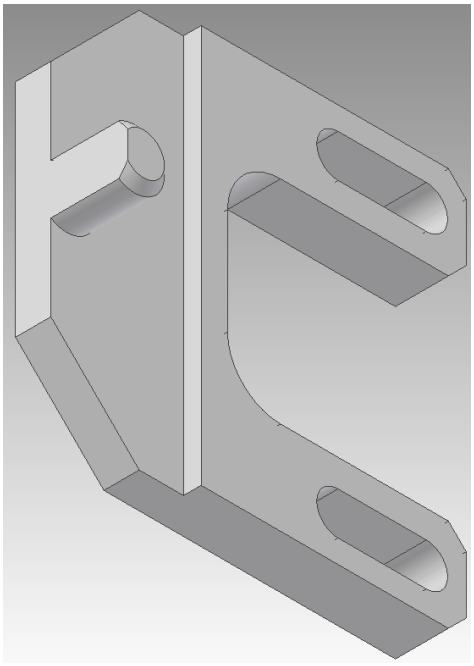

Figure 108. Locking Bracket

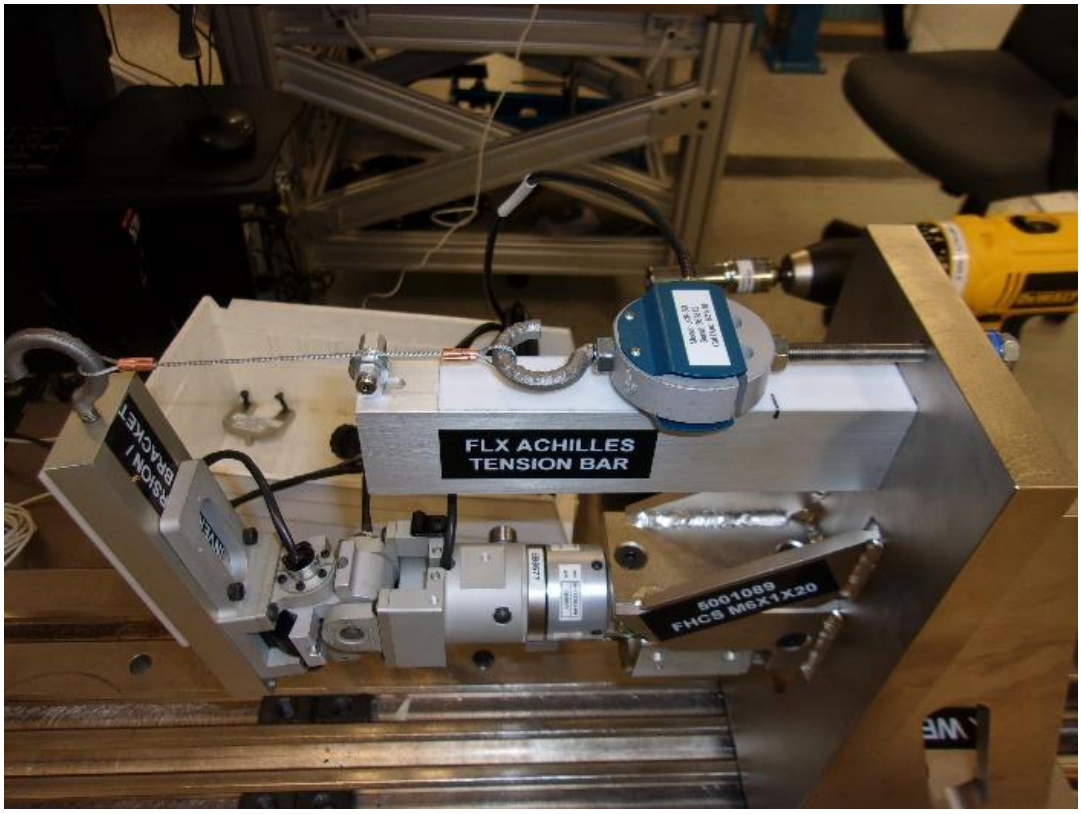

Figure 109. Example of Achilles cable tension setting kit

10.1.1.2 Instrumentation

1. Instrumentation to measure impact velocity.
2. Accelerometer for measuring the deceleration of the pendulum, mounted with its sensitive axis in line with the outermost radius of the impact surface.
3. Lower tibia 5 axis load cell (F_x, F_y, F_z, M_x, M_y) (IH-11820J)
4. Three ankle rotary potentiometers (X, Y, Z axis) (9945)
5. Achilles cable tension load cell

10.1.1.3 Definition of Foot Positions

The sign convention utilized during testing follows the standardized dummy coordinate system listed in the SAE Information Report J211, and is shown in Figure 110 for a right foot. The foot is at 0º plantarflexion and dorsiflexion when the bottom of the foot sole plate is 90º relative to the Y-Z plane. The foot is at 0º inversion and eversion when the bottom of the foot sole plate is 90º relative to the X-Z plane. The foot is at 0º rotation about the Z-axis when the midline of the foot sole plate is 90º relative to the Y-Z plane. When the ankle is at 0° dorsiflexion, inversion/eversion, and about the Z-axis, this is defined as the 'zero position'. Neutral position of the foot is defined as the ankle resting on the plantarflexion bumper, 0º inversion/eversion, and 0º rotation about the Z-axis.

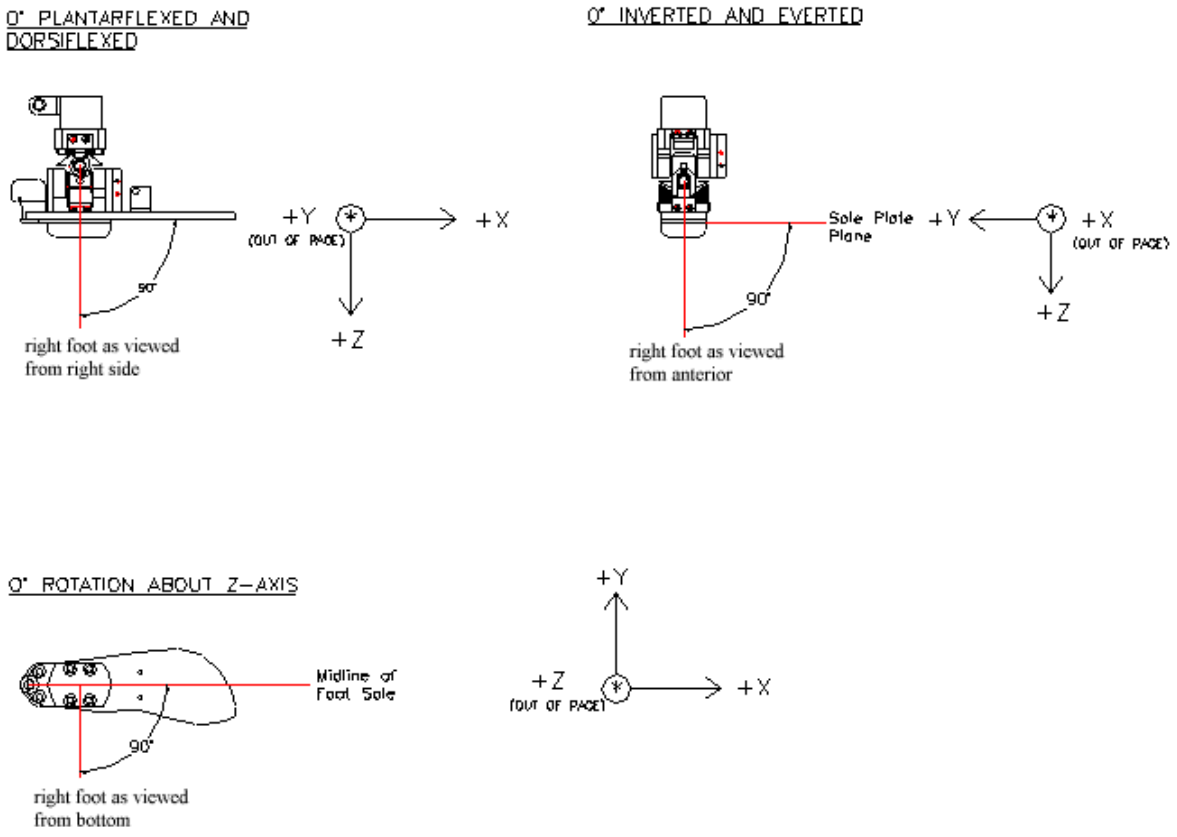

Figure 110. Definition of foot positions (shown for a right foot)

10.1.1.4 Ankle Potentiometer Zeroing Procedure

Before conducting any of the dynamic impact tests, it was necessary to determine the voltage outputs of the individual ankle potentiometers when the ankle is held in the 'zero position'. The zero position potentiometer

voltage values, along with the rotational calibration values in degrees per volt, were later used to determine the angular position of the foot relative to the tibia.

First, the potentiometers were electrically centered so they did not pass through the dead band area to allow proper signals to be collected during dynamic impact test. The foot rested approximately in the zero position. Any offsets that were already being applied to the potentiometers were removed.

NOTE: *Y-axis potentiometer were mounted on the same side as the eversion bumper* (Figure 111).

Figure 111. Y-axis potentiometer orientation

The potentiometer body was rotated until the voltage was 0 ± 0.25V and secure in place. The ankle zeroing bracket was used to hold the ankle in the zero position (Figure 112). ***NOTE:*** *Ankle zeroing bracket may have some freedom to rotate about certain axes. Orientation was centered before tightening hardware.* All offsets were removed from the three ankle potentiometers. The potentiometer offsets were then recorded and applied. Offsets were verified as correct by re-running the ankle potentiometer zeroing procedure which should report that X, Y, and Z orientation is 0 ± 0.05°.

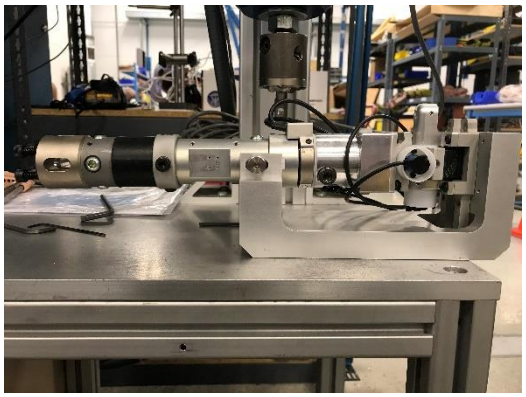

Figure 112. Lower leg assembled into ankle zeroing bracket

10.1.2 Achilles Cable Tension Setting Procedure

The THOR-05F lower leg was designed with an adjustable Achilles tendon cable which can change the engagement point of the Achilles relative to the ankle rotation angle. It was designed to have little to no resistance in the neutral position. The following procedure describes the adjustment of the Achilles spring cable tension using a fixture that is integrated with the same leg mounting bracket used in other lower leg tests.

10.1.2.1 Materials

1. THOR-05F lower leg assembly (474-5500-1/2)
2. Rigid fixture for ball of foot testing
3. Inversion/eversion test bracket (APPENDIX 3)
4. Achilles adjustment kit (TH-1603-0685)
5. Mechanism to pull cable

10.1.2.2 Instrumentation

1. Tension load cell
2. Y-axis ankle potentiometer
3. X-axis ankle potentiometer (for orientation)
4. Z-axis ankle potentiometer (for orientation)

10.1.2.3 Procedure

1. The ankle potentiometer zeroing procedure was first performed and offsets were properly applied.
2. The tibia skin, tibia guard, upper tibia compliant bushing assembly, molded shoe, and the front W50-61042 BHCS that attaches the lower tibia shaft to the lower tibia load cell were removed.
3. Lower leg assembly was mounted to the rigid fixture (Figure 113).

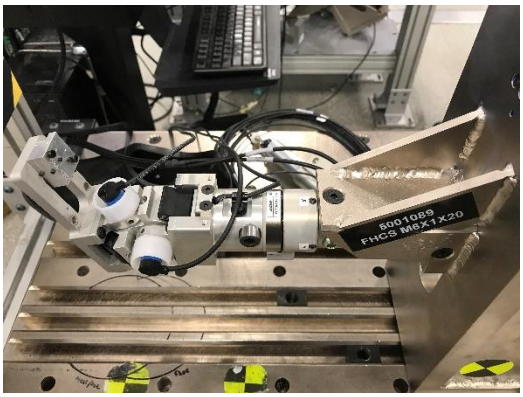

Figure 113. Lower leg mounted on rigid fixture

4. The adjustment nut was tightened on the Achilles assembly until there was no slack in the cable with the leg resting in the neutral position against the plantar flexion bumper. ***NOTE:*** *No slack should be achieved when the plastic primary load washer (474-5529) is flush with the top of the Achilles spring housing (474-5525).* Using two 8 mm thin-profile wrenches, the adjustment nut was locked in this position using the jam nut.
5. The inversion/eversion test bracket was attached to the bottom of the foot bone using four SHCS M4x0.7x20 (Figure 114).

Figure 114. Inversion/eversion test bracket attached to foot bone for Achilles procedure

6. The load cell guide bar was mounted onto the rigid fixture with the PTFE (Teflon®) pad facing up.
7. The hook was attached to the top of the inversion/eversion bracket and the threaded rod attached to the Achilles load cell was inserted through the hole in the rigid fixture. The thrust bearing was placed over the threaded rod, followed by the hex nut.
8. Foot hook was linked to tension load cell hook using the pull wire assembly and the wire was guided though the pulley (Figure 115). ***NOTE***: *The pull wire assembly had zero tension on it with the foot resting in the neutral position.*

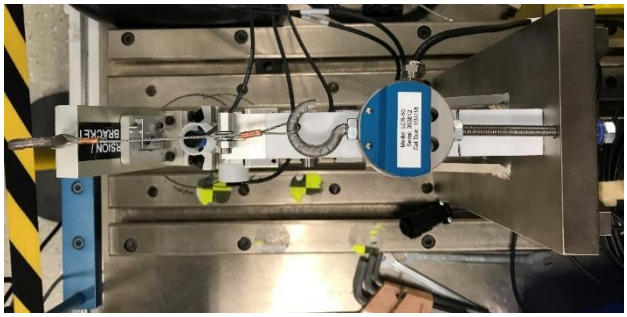

Figure 115. Example of Achilles tension setting apparatus

9. Pre-test voltage readings were acquired. The ankle orientation was adjusted so the X and Z-axis are 0 ± 0.2°.
10. Once the test was triggered, the pull mechanism was used to pull the foot hook past 0° dorsiflexion and then returned to the neutral position. Rate of pull was between 0.5 and 3.0°/sec at a consistent speed.
11. The load measured by the tension load cell while crossing 0° dorsiflexion at the rate of pull was 15.0 ± 6.0 N. If necessary, loosen (if tension is too high) or tighten (if tension is too low) the Achilles adjustment nut and repeat the test.

10.2 Axial Heel Impact

10.2.1 Methods

10.2.1.1 Test Setup

The ATD leg was separated just proximal to the femur load cell, and held in a custom-built fixture that allowed for uniaxial compression of the tibia, foot and ankle. The foot, tibia, and knee were left assembled and utilized during the experiment. The overall test setup is shown in Figure 116. The back of the fixture was rigid and did not allow for significant movement, while the footplate moved superiorly, compressing the foot and leg. The fixture was aligned such that the center of the ram was aligned through the center of the ankle and midline of the tibia using a laser guide. Two ratchet straps were used to support the mass of the leg so that it did not fall after the event. A 28.4 kg pneumatic ram was utilized as the energy into the system.

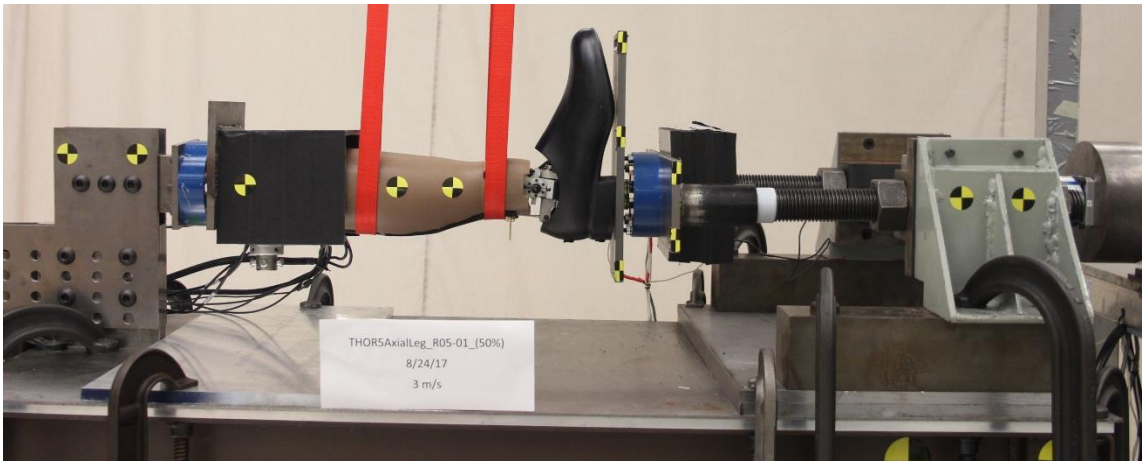

Figure 116. Axial heel impact fixture setup

10.2.1.2 Instrumentation

A total of 35 channels of data were recorded for each test, including both internal ATD channels along with external instrumentation on the test device. External instrumentation included a linear displacement potentiometer (Penny Giles, UK, Model #SLS190) on the impacting ram along with a single axis accelerometer (Endevco, CA, Model #7264c) and a 6-axis load cell attached to the impact face (RA Denton Inc, Rochester, MI). Attached under the loading footplate were a single axis load cell (Interface Model #1210AF-5K, Scottsdale, AZ) and a set of three single axis accelerometers (Endevco, CA, Model #7264c). Finally, another single axis load cell (Interface Model #1210AF-5K, Scottsdale, AZ) was placed at the proximal end of the fixture between the knee cup and the attachment plate.

Internally, the THOR-05F had the following instrumentation:

- 6-Axis Femur load cell (Humanetics Model # IH-11510J-PR)
- 5-Axis Upper Tibia load cell (Humanetics Model # IH-11520J-PR)
- 5-Axis Lower Tibia load cell (Humanetics Model # IH-11530J-PR)
- 3-Axis Ankle rotary potentiometer (Novotechnik, Model # Vert-x-13e-5v)
- 1-Axis Knee potentiometer (Servo, Model # 150-0121V-DN)

The upper and lower tibia load cells were used to measure the force transmitted through the tibia during the event, while the ankle potentiometers would verify any motion which occurred. Additionally, the two uniaxial external load cells were used to determine the amount of pre-tensioning that was placed through the tibia prior to the impact event. To track displacements using TEMA software (Image Systems Motion Analysis, Sweden), fiducials were placed on the footplate, rigid fixture, and on the tibia itself.

10.2.1.3 Pre-test

Before the test, an axial pre-compression of half of the specimen's body weight (233 N) was applied to the foot of the tibia. Teflon and oil were used to ensure that this pre-compression system did not bind and interfere with the test. Additionally, a 6" x 6" piece of polyurethane foam (3" thick) (polyurethane, McMaster-Carr part 86375K154) was placed between the impactor and the footplate. These mechanisms are shown in Figure 117.

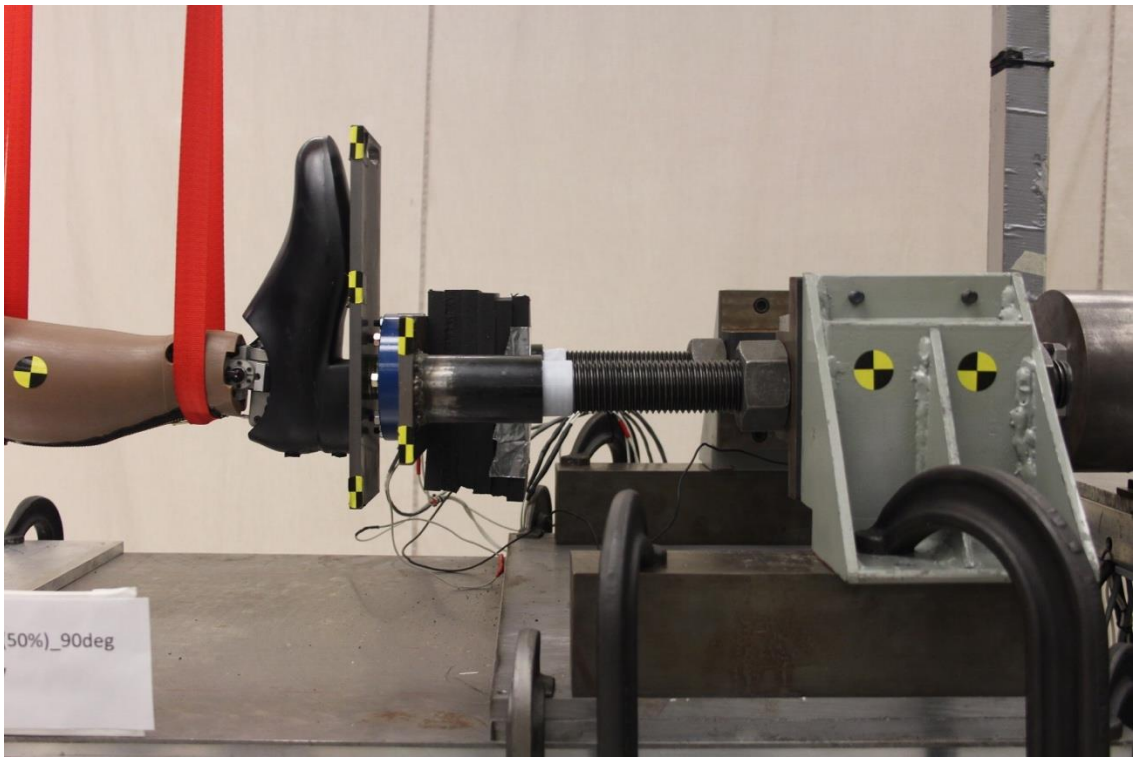

Figure 117. Pretensioning setup for Axial Heel Impact

The input energy for the test was applied by striking a 28.4 kg mass into the pre-compressed tibia's foot plate at 3.1 m/sec (achieved velocities are shown in Table 50). An accelerometer located on the impacting ram was used to verify the correct energy was applied to the system. Contact switch was attached to metal tapes on the impactor surface and the foam to trigger the event and this corresponded to time zero for all data including sensors and high-speed cameras.

It is important to note that for the three tests, the orientation of the lower tibia shaft was rotated with respect to the internal lower tibia load cell such that there was no interference between the Achilles load cell and the shaft of the tibia during compression of the softer bumper. Figure 116 and Figure 117 show a rotated test, but it is important to note that it is an internal change deep to the skin of the THOR-05F.

Table 50. Resulting velocities of the three axial heel impact tests

Test ID	AxialLegR05	AxialLegR06	AxialLegR07
Impact velocity	3.09 m/s	3.05 m/s	2.98 m/s

10.2.2 Results

The responses of the axial heel impact test are shown in Figure 118 through Figure 122. The BioRank for this test condition is 1.96, corresponding to "good" biofidelity.

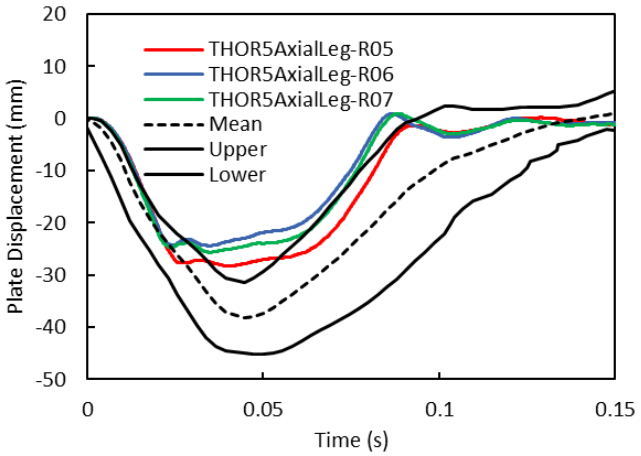

Figure 118. Impact plate displacement of the axial heel impact test

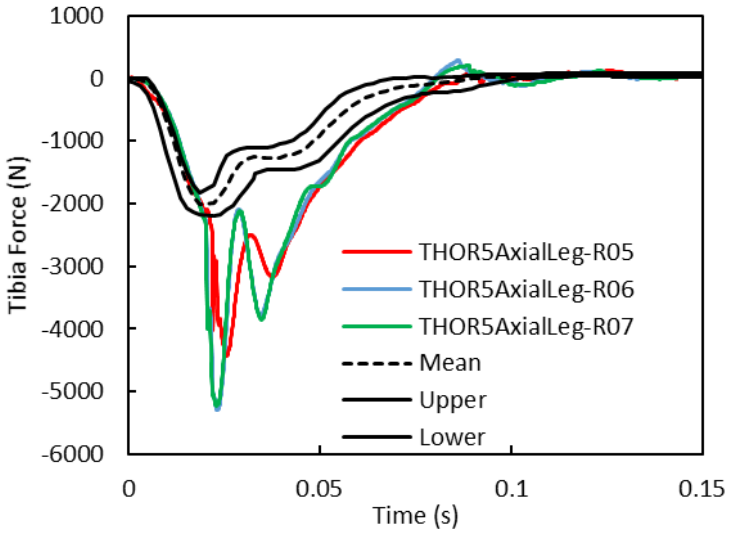

Figure 119. Lower tibia force Fz of the axial heel impact test

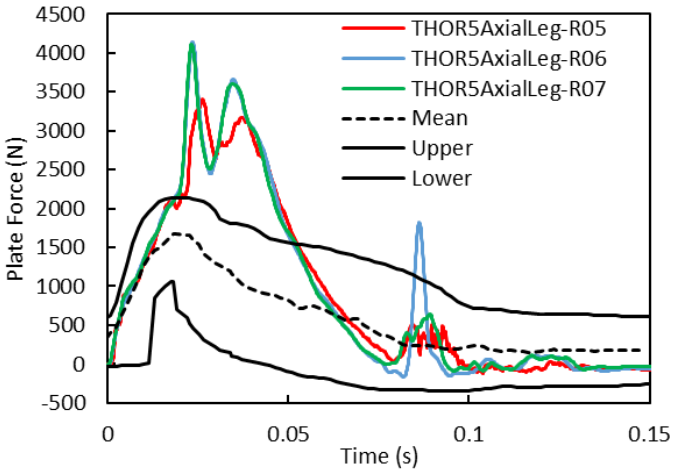

Figure 120. Impact plate force of the axial heel impact test

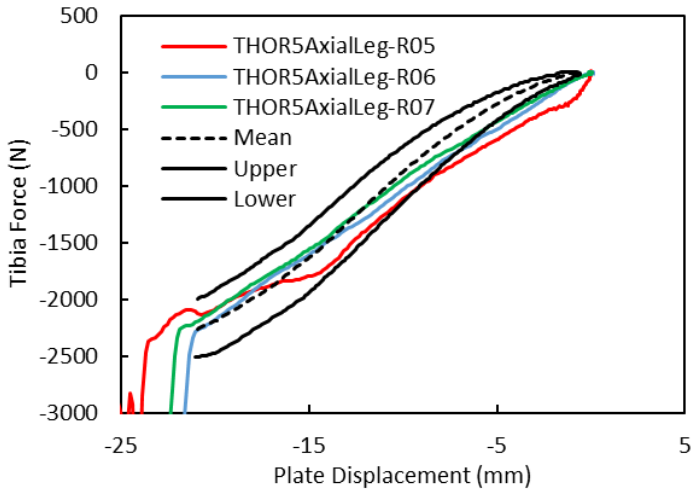

Figure 121. Lower tibia force vs plate displacement of the axial heel impact test

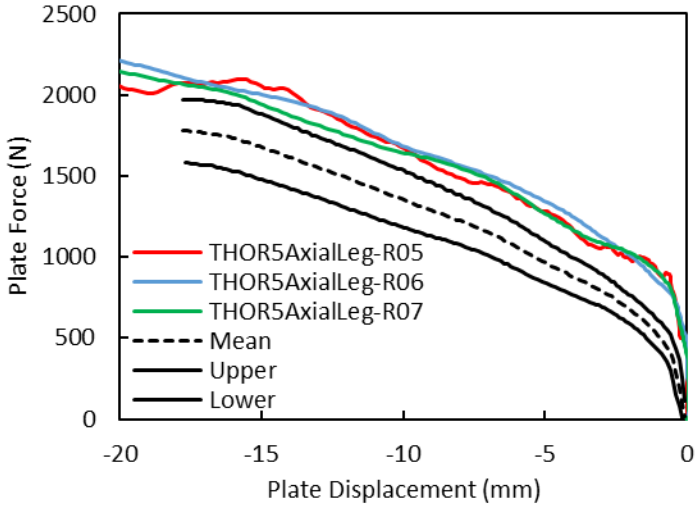

Figure 122. Plate force vs plate displacement of the axial heel impact test

10.3 Ball of Foot (BOF) Impact

10.3.1 Methods

10.3.1.1 Materials

6. THOR-05F lower leg assembly (474-5500-1/2)
7. Dynamic impactor (Figure 106)
8. Rigid fixture for ball of foot testing

10.3.1.2 Instrumentation

1. Instrumentation to measure impact velocity consists of a light trap and evenly spaced mechanical vanes that generate square electrical pulses for velocity calculation.
2. Accelerometer for measuring the deceleration of the pendulum, mounted with its sensitive axis in line with the outermost radius of the impact surface.
3. Lower tibia load cell (F_x, F_z, M_y) (IH-11820J)
4. X-axis ankle potentiometer (for orientation)

5. Y-axis ankle potentiometer
6. Z-axis ankle potentiometer (for orientation)

10.3.1.3 Test Procedure

1. The lower leg assembly was inspected for damage. The molded shoe (474-5903-1/2), ankle dorsi stop (474-5807) and the Achilles tube assembly were inspected for tears, permanent deformations, or separation.
2. The leg was soaked in a controlled environment at a temperature between 20.6° to 22.2°C (69° to 72°F) and a relative humidity from 10 to 70% for a period of at least 4 hours prior to testing. The test environment had the same temperature and humidity as the soak environment.
3. The Ankle Rotary Potentiometer zeroing Procedure was conducted.
4. The Achilles Cable Adjustment Procedure was conducted.
5. Make sure the tibia compliant element assembly at the lower flange joint is removed, which can be done by removing the two modified M6 plunger pins bolts (474-5512), the M6x10 FHCS, and the M6x10 BHCS.
   NOTE: *Unlike the THOR-50M, the Achilles assembly stays attached to the leg.*
6. The lower leg was mounted to the rigid fixture such that the Y-Z plane of the lower leg was horizontal and the toes were pointing upward using four M6x1x20 FHCS (Figure 123). ***NOTE***: *Needed to remove the front W50-61042 modified BHSS that attaches the 474-5540-(1/2) lower tibia shaft to the lower tibia load cell in order to mount the leg to the rigid fixture.*

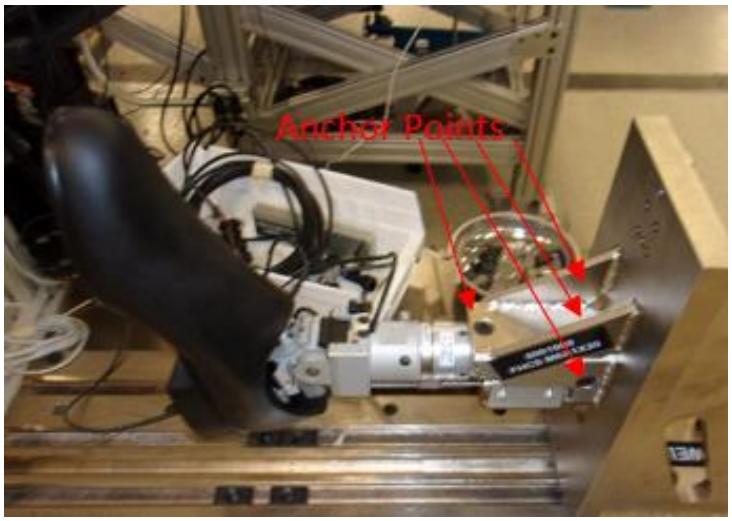

Figure 123. Example of BOF setup

7. With the pendulum arm vertical within ± 0.5°, the point of impact was 110 ± 1 mm above the longitudinal centerline of the lower leg (Figure 124). A self-leveling laser line was used in this process.

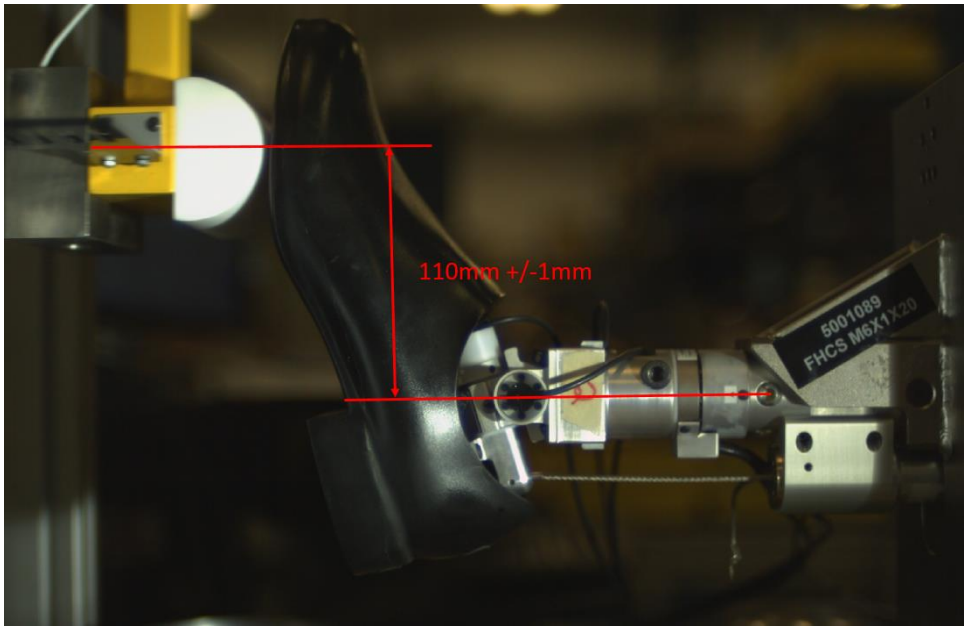

Figure 124. BOF impact height

8. Pre-test voltages were acquired. With the ankle resting in the neutral position, the X and Z-axis ankle potentiometers were oriented to 0 ± 0.2°.
9. The rigid fixture was positioned so the foot was just barely touching the impactor with the pendulum arm vertical ± 0.5° (Figure 125). The rigid fixture was secured. ***NOTE***: *Longitudinal centerline of the dynamic impactor was parallel to the X-Z plane of the lower leg when the impactor was just barely touching the shoe.*

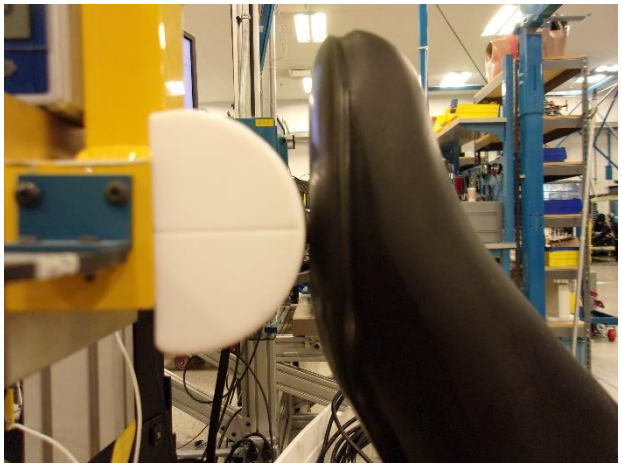

Figure 125. Pendulum just barely touching foot in neutral position at vertical

10. At least 20 milliseconds of pre-time zero data and 100 milliseconds of post-time zero data was recorded.
11. At least 30 minutes had passed since the last ball of foot test on the same shoe, dorsi bumper, or Achilles assembly (including break-in).
12. The pendulum was raised ~89.5° from vertical to generate an impact velocity of 5.0 m/s. Actual

velocities achieved are shown in Table 51.

13. Allow one break-in test before evaluating.

Table 51. Resulting velocities of the three right and three left Ball-of-Foot tests

Test ID	663	664	665	697	698	699
Impact velocity	5.02 m/s	5.02 m/s	5.02 m/s	5.02 m/s	5.02 m/s	5.03 m/s

10.3.1.4 Data Processing

1. The polarity conventions and data acquisition system conformed to the latest requirements of SAE Recommended Practice J211.
2. Data channel offset was removed, but ankle rotational potentiometer was not zeroed; per SAE J211 Section 8.4.3, the normalized value of a stable pre-test section of data was set to the proper initial value for the transducer.
3. Time zero (T_0) was defined when the accelerometer with a CFC-1000 response mounted on the pendulum rose through the 1g level.
4. Channels were filtered based on the CFC filter classes listed in Table 52.
5. The initial foot position prior to time zero (T_0) was determined.
6. The time history of the ankle resistive moment was calculated:

$$Left: M_{ANKL} = M_{yTBLL} - (0.0864m \times F_{xTBLL})$$

$$Right: M_{ANKR} = M_{yTBLR} - (0.0864m \times F_{xTBLR})$$

Table 52. Ball of foot data channels (same for left and right)

Item #	Channel Description	Filter Class	Comments
1	Pendulum Acceleration	CFC-180	
2	Lower Tibia Force, X-axis	CFC-600	
3	Lower Tibia Force, Z-axis	CFC-600	
4	Lower Tibia Moment, Y-axis	CFC-600	
5	Ankle Rotation, X-axis	CFC-180	
6	Ankle Rotation, Y-axis	CFC-180	
7	Ankle Rotation, Z-axis	CFC-180	
8	Ankle Resistive Moment	N/A	Calculated

10.3.2 Results

The force vs deflection response at 5 m/s impact speed is shown in Figure 126. The BioRank is 1.16, corresponding to “good” biofidelity.

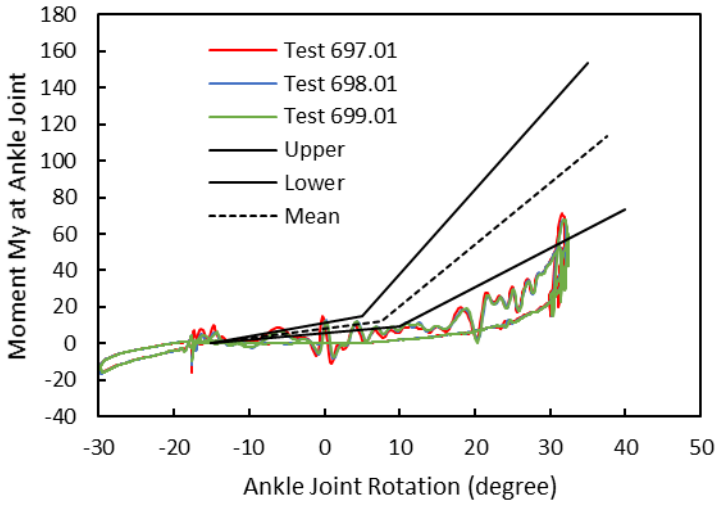

Figure 126. Force vs deflection response of the ball of foot impact test at 5 m/s

10.4 Dynamic Inversion and Eversion

10.4.1 Methods

10.4.1.1 General Test Overview

Each test was initiated by impacting a steel plate using a pneumatic ram that forces the foot holder assembly to rotate as seen in Figure 127. The loading objective of each test was to achieve a rotational velocity of the footplate of 1000 degrees per second. A fixture was designed to force rotation about the subtalar joint axis in this series of tests. A simplified model of the fixture done using MSC Adams (MSC Software, Newport Beach, California) is shown in Figure 128.

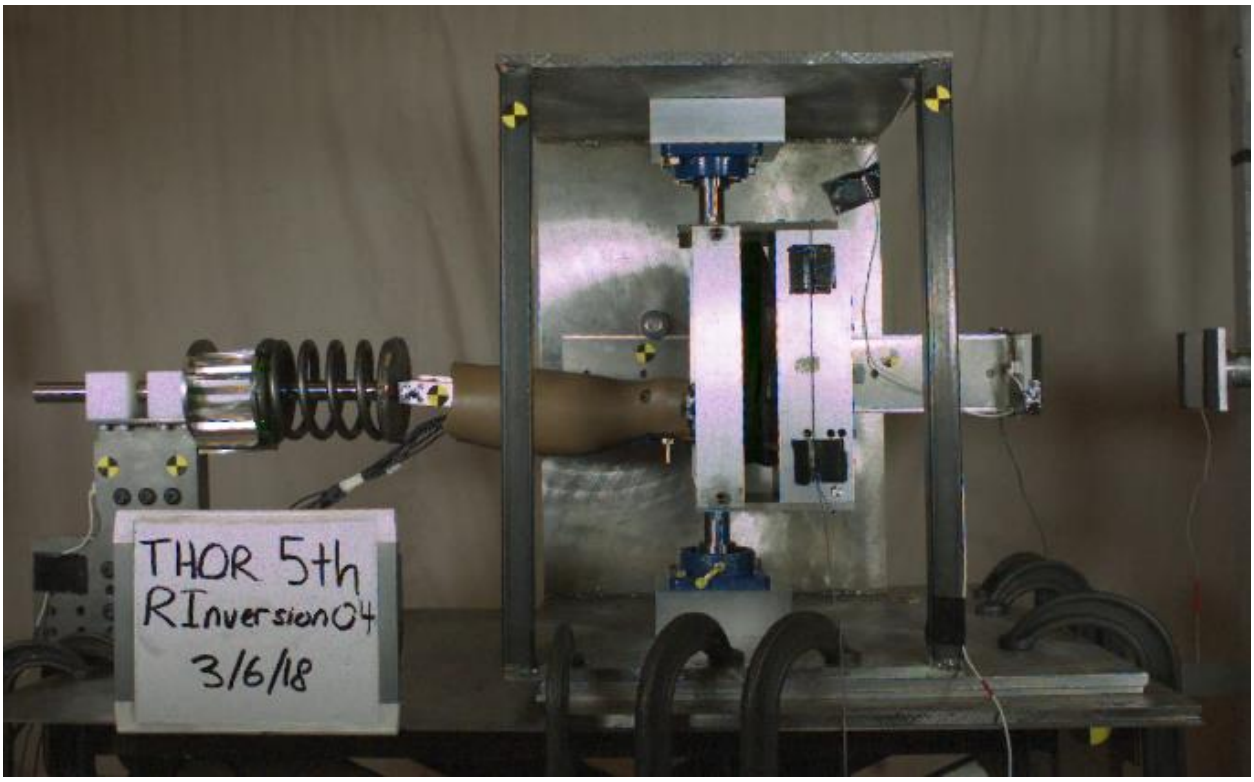

Figure 127. Physical test setup for inversion/eversion testing

The back of the fixture was designed to be compliant, in order to simulate the mass of the thigh and pelvis resisting the impact load as it propagates superiorly from the ankle up through the entire lower extremity. To accomplish this, a spring in series with aluminum honeycomb was placed at the proximal end of the tibia. This part of the fixture saw little deflection and the honeycomb did not crush.

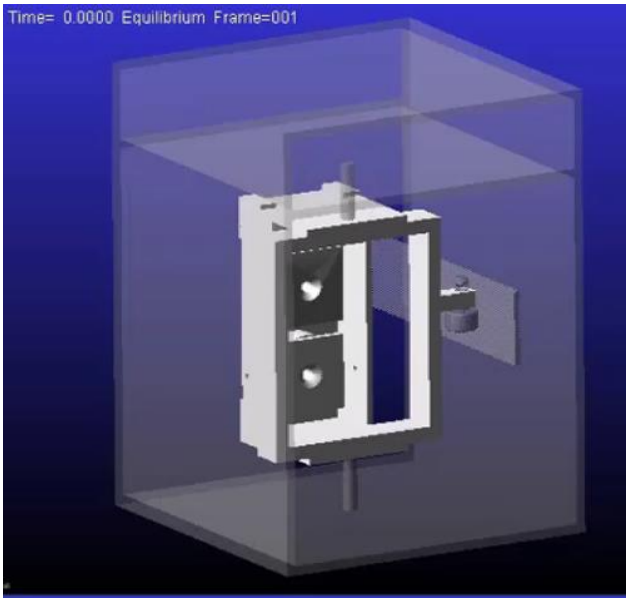

Figure 128. Virtual model of inversion/eversion testing fixture

10.4.1.2 Instrumentation

1. Input Instrumentation
    a. Light trap on the pneumatic impactor to define the speed of the ram at impact to the inversion/eversion fixture
    b. Accelerometers located on the impactor ram faceplate, the cam and housing of the fixture to help define the motion of the linear structures
    c. Angular rate sensor located on the footplate to define the rotational velocity of the footplate during the test.
2. THOR-05F Internal instrumentation
    a. Lower Tibia 5-Axis load cell (Fx, Fy, Fz, Mx and My)
    b. Upper Tibia 5-Axis load cell (Fx, Fy, Fz, Mx and My)
    c. Rotary potentiometers in the ankle to measure rotation about X, Y and Z-Axes

10.4.1.3 Test Procedure

1. The mass of the impacting pneumatic ram to 28.4 kg
2. The Inversion/Eversion fixture (Figure 128) was placed on the table in front of the impacting ram
3. The pneumatic ram was aligned with the cam/piston portion of the test fixture.
4. Laser levels were used to align the ram with the center of the leg/foot of the ATD and through the center of rotation of the ankle (Mx).
    a. The leg was placed with the toes of the foot pointed superiorly for the inversion based test
    b. The leg was placed with the toes pointing inferiorly for the eversion based test
5. The ankle was set in a resting position with the tibia centered over the ankle so that there was no initial subtalar joint angle (i.e. neutral plain without inversion or eversion). The foot was also placed perpendicular to the tibia to ensure a neutral position (i.e. neutral plane without plantar flexion or dorsiflexion).
6. Inserted the cam/piston portion into the support frame
7. Used 18" zip-ties and double-sided tape to secure the shoe of the ATD to the footplate system. This ensured the foot did not move vertically during the tests.
8. Used the laser levels to confirm the center of rotation of the ankle was still in alignment with the center of the tibia.
9. The proximal end of the tibia was mounted to the fixture through a stiff spring (McMaster-Carr part 96485k432) and Hexcel (3" honeycomb at 11/16" cell, 3000 series aluminum) in series. These tests were performed with no pre-load on the leg.
10. A high-speed camera (1,000 frames per second) was placed perpendicular to center of rotation of the ankle of the THOR-05F.
11. All instrumentation was checked for proper strain relief to prevent failures from pinched or pulled cables.
12. Velocities of the impacting ram are given in Table 53 and Table 54.

Table 53. Velocities achieved in the three inversion tests

Test ID	Inversion02	Inversion03	Inversion04
Impact velocity	3.32 m/s	3.34 m/s	3.30 m/s

Table 54. Velocities achieved in the three eversion tests

Test ID	Eversion01	Eversion02	Eversion03
Impact velocity	3.28 m/s	3.24 m/s	3.24 m/s

10.4.1.4 Data Processing

1. Data was collected at 20000 Hz using a TDAS system. Video was recorded at 1000 frames per second.
2. Time zero (T_0) was defined when the impactor contacted the cam piston, which applied the motion to the bottom of the foot.
3. All data were filtered according to J211 standards.

10.4.2 Inversion Results

To determine the time zero for the BioRank evaluation, the deflection of the test data was aligned with the deflection corridor mean at 1-degree rotation, the time coincident with the corridor time zero was defined as the time zero for the test data. The BioRank for this test condition is 1.68, corresponding to "good" biofidelity. The responses of the inversion tests are shown in Figure 129 through Figure 131.

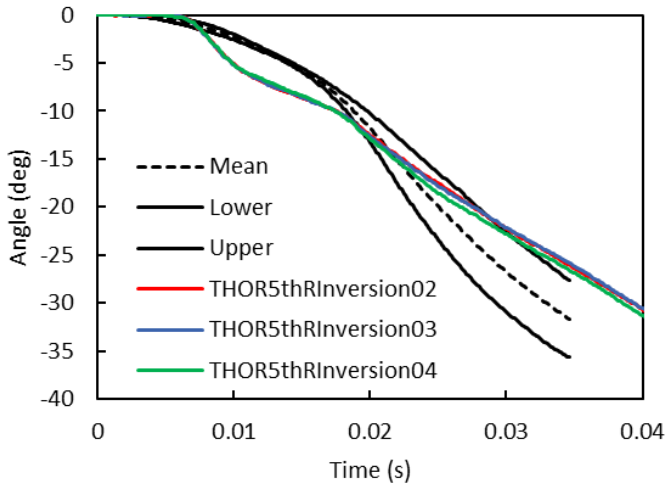

Figure 129. Ankle rotation in the dynamic inversion test

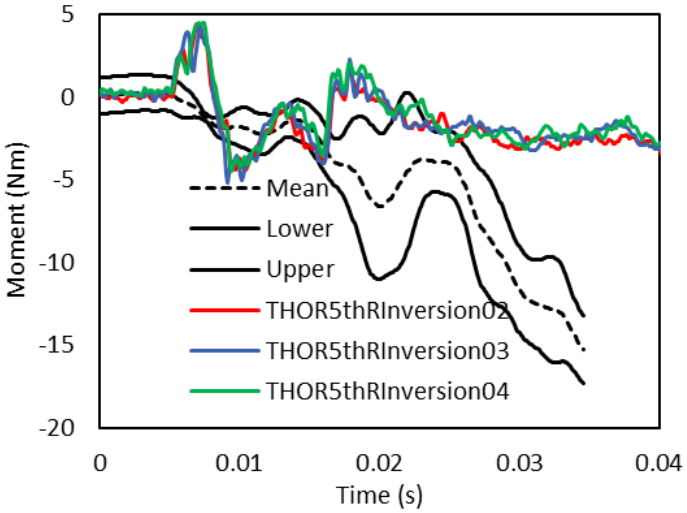

Figure 130. Moment at ankle joint center in the dynamic inversion test

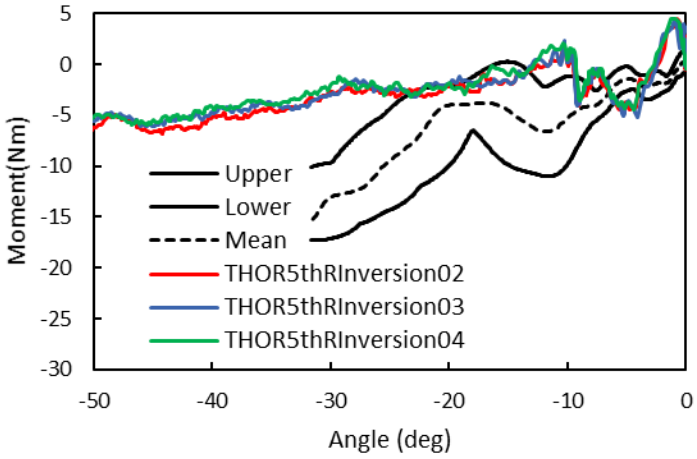

Figure 131. Moment at ankle joint vs rotation in the dynamic inversion test

10.4.3 Eversion Results

The time zero was determined in the same way as the dynamic inversion test. The test condition biofidelity is 1.24, corresponding to "good" biofidelity. The responses of the dynamic eversion test are shown in Figure 132,

Figure **133** and Figure 134.

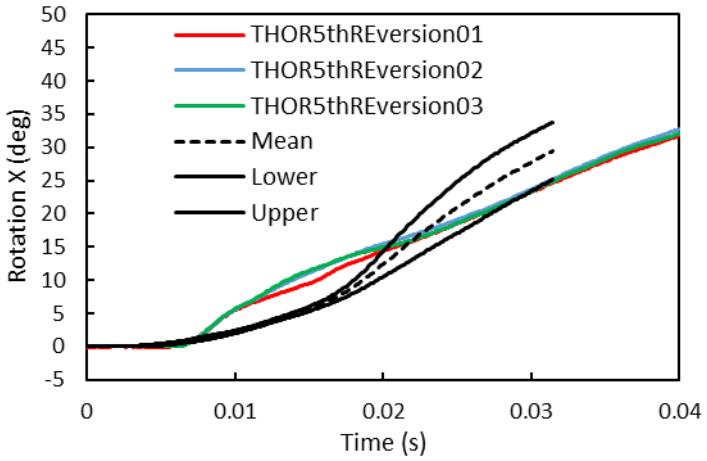

Figure 132. Ankle rotation in the dynamic eversion test

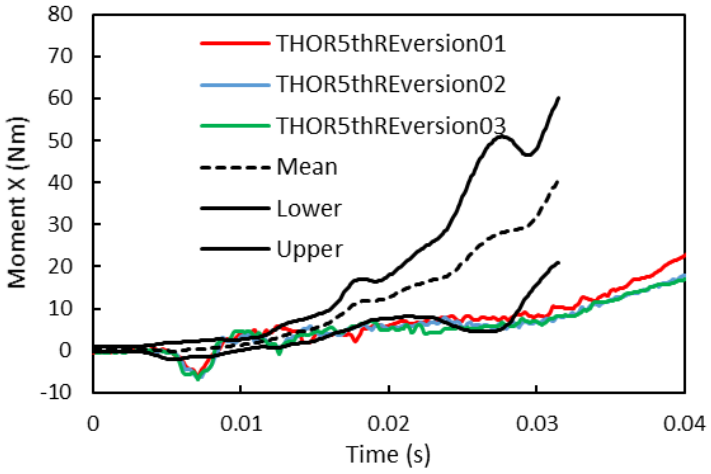

Figure 133. Moment at ankle joint center in the dynamic eversion test

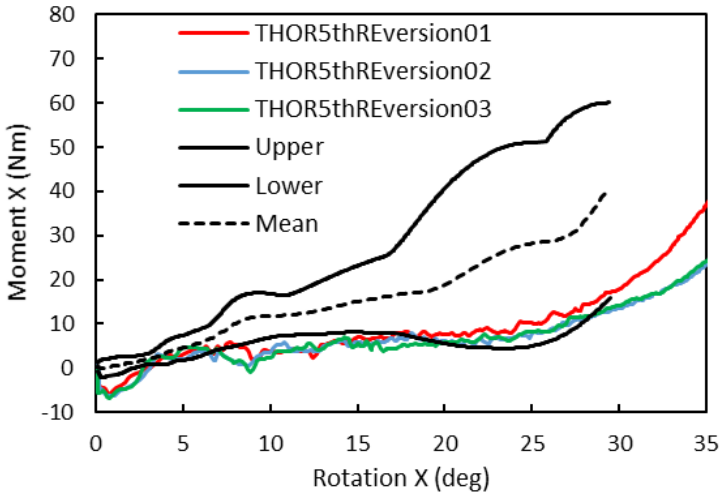

Figure 134. Moment at the ankle joint center vs rotation in the dynamic eversion test

10.5 Lower Extremity Biofidelity Summary

The lower extremity BioRank scores are summarized in Table 55. The lower extremity body region BioRank is 1.47, corresponding to "good" biofidelity.

Table 55. Lower extremity biofidelity summary

	SM	*P*	*RMS*
Axial Heel Impact			**1.94**
Tibia Force Z	4.68	0.84	4.76
Impact Plate Force	1.21	0.16	1.22
Impact Plate Displacement	1.02	0.01	1.02
Tibia Force Z vs plate displacement	0.72	NA	0.72
Impact plate force vs plate displacement	2.00	NA	2.00
Dynamic Dorsiflexion			**1.16**
Moment Y vs Rotation Y	1.16	NA	1.16
Dynamic Inversion			**1.58**
Rotation X	1.12	0.06	1.13
Moment X	2.16	0.15	2.17
Moment X vs Rotation X	1.45	NA	1.45
Dynamic Eversion			**1.19**
Rotation X	1.32	0.22	1.34
Moment X	1.26	0.17	1.27
Moment X vs Rotation X	0.96	NA	0.96
Lower Extremity Overall BioRank			**1.47**

11 Full Body Sled Test

11.1.1 Methods

11.1.1.1 Test Setup

The full body sled evaluation (also known generally as the “Gold Standard” test) consists of a 30 km/h frontal crash pulse, using a simplified sled buck, to study the torso and shoulder kinematic response in a frontal crash scenario (Figure 135). The ATD was seated forward-facing on a rigid flat seat and restrained in a right-front passenger configuration. The head and torso were supported using adjustable cables. The ATD used for this test condition was serial no. ED7441.

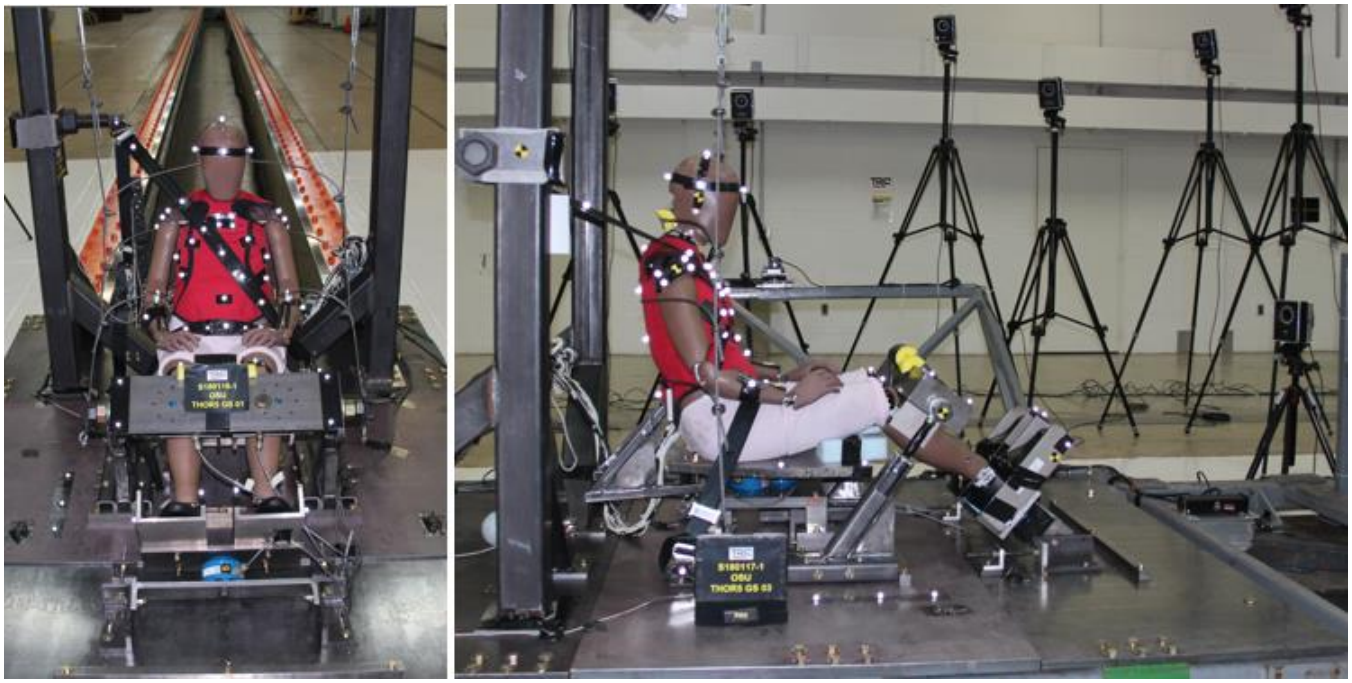

Figure 135. Pre-test positioning of THOR-05F on the sled buck

The restraint system included a 3-point lap and shoulder belt of standard webbing using separate belt segments of adjustable lengths. The belt system did not include a retractor. The shoulder belt was routed through a low friction D-ring and down to a custom belt load limiting device. The device, developed to limit the shoulder belt loads to 2 kilo-Newton tension, comprised of a 3/8” cell commercial grade aluminum honeycomb with seven active cells sandwiched between two aluminum plates and pulled using a cable connected to the shoulder belt on the other end (Figure 136).

Figure 136. Shoulder belt load limiting mechanism

For each of the four tests, the initial shoulder belt tension was adjusted to around 17 N, to ensure repeatable initial position of the belt with respect to each ATD and remove any slack. The shoulder belt was positioned to pass through the clavicle superiorly and exit on the lateral aspect of pelvis inferiorly. Pelvis and lower extremity motion were restricted using a combination of lap belt, rigid knee bolster and footrest which were adjusted to be in contact with the knees and feet of the ATD at the time of impact, but the forward torso movement was allowed.

The pre-test ATD positioning parameters are tabulated in Table 56. The ATD H-point was positioned such that the tibia and femur angles of around 36 and 13 degrees were achieved respectively. Upon positioning the lower body, the torso was positioned to obtain a target value of approximately 13 degrees. The resulting pre-test shoulder belt angle and location between the D-ring and head are tabulated in Table 57.

Table 56. ATD Positioning for full dummy sled test

Test ID	Torso Angle (deg)	Femur Angle (deg)	Tibia Angle (deg)
THOR5 GS01	14.2	14.5	36.0
THOR5 GS02	14.0	13.5	37.0
THOR5 GS03	13.0	11.5	35.0
THOR5 GS04	12.2	11.8	35.0

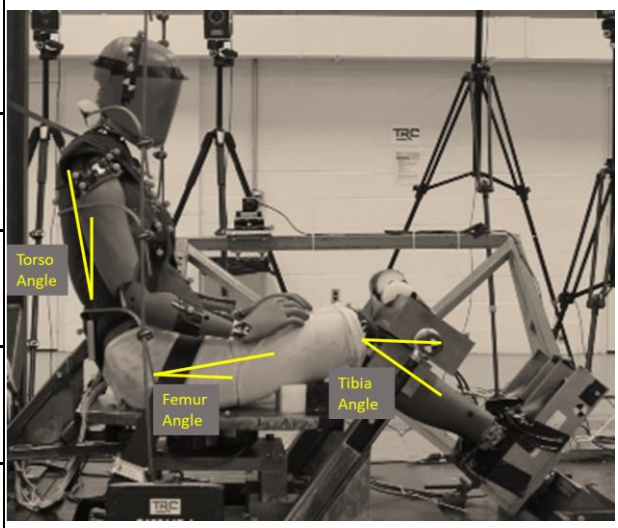

Table 57. Shoulder belt angle measured at sternum

Test ID	θ (deg)	X (mm)
THOR5 GS01	49.1	338
THOR5 GS02	49.2	324
THOR5 GS03	48.4	354
THOR5 GS04	48.5	325

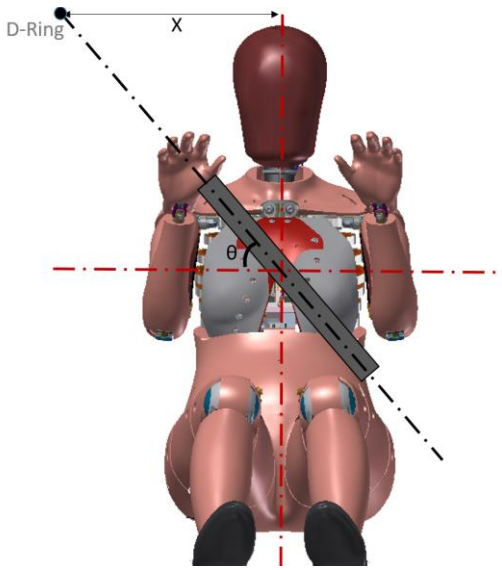

11.1.1.2 Instrumentation

On the sled buck, a total of six uniaxial load cells (Interface, Scottsdale, AZ, Model# 1100) including on the seat, one on each knee support plate, and one on the foot support plate measured forces. Three linear accelerometers (Endevco, CA, Model #7231c) accelerometers on the sled measured the acceleration of the sled. Seatbelt load cells (Measurement Specialties, now TE Connectivity, PA, Model #EL20) were affixed to the belt on the shoulder and lap of the ATD to measure belt forces.

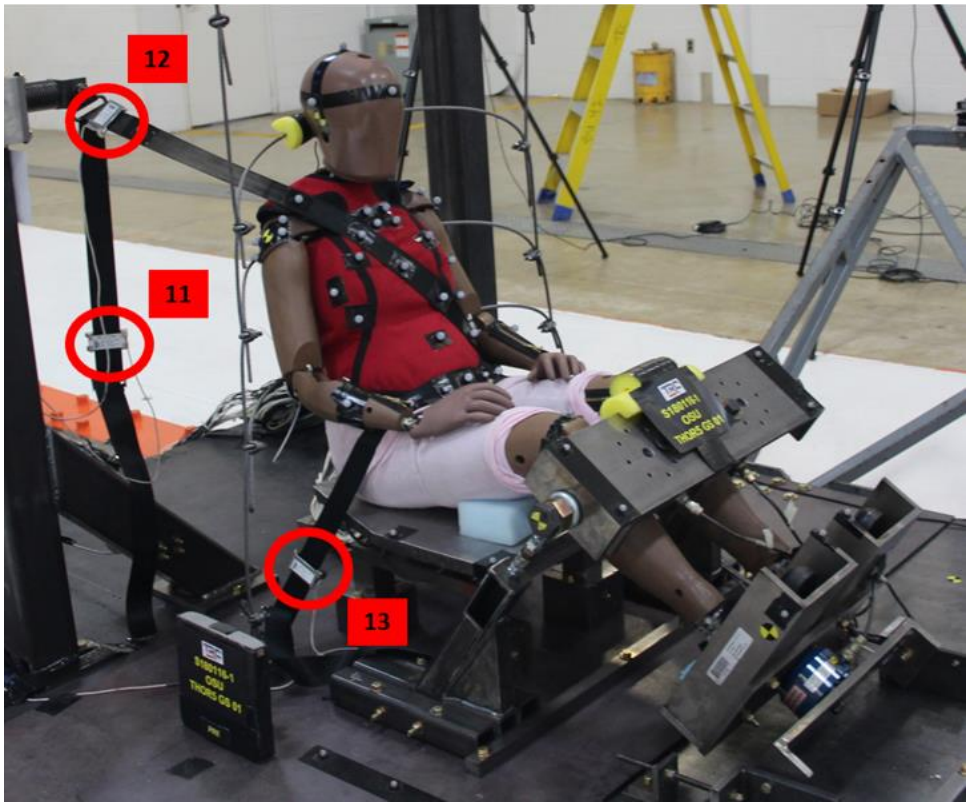

Figure 137. Belt load cells marked in red circles; numbers correspond to data channel entries in the data channels table; the load cell on shoulder belt (#12) was the primary load cell used to measure shoulder belt loads

Chest deflection was measured using four double-gimbaled Infrared Telescoping Rods for Assessment of Chest Compression (IR-TRACCs) mounted in the ATD thorax. These IR-TRACCs measured 3D deflection of the four quadrants of the anterior ribcage relative to the spine; upper IR-TRACCs at the level of T8 and lower IR-TRACCs at T12, approximately. A schematic of IR-TRACC locations is provided in Figure 138 and Table 58.

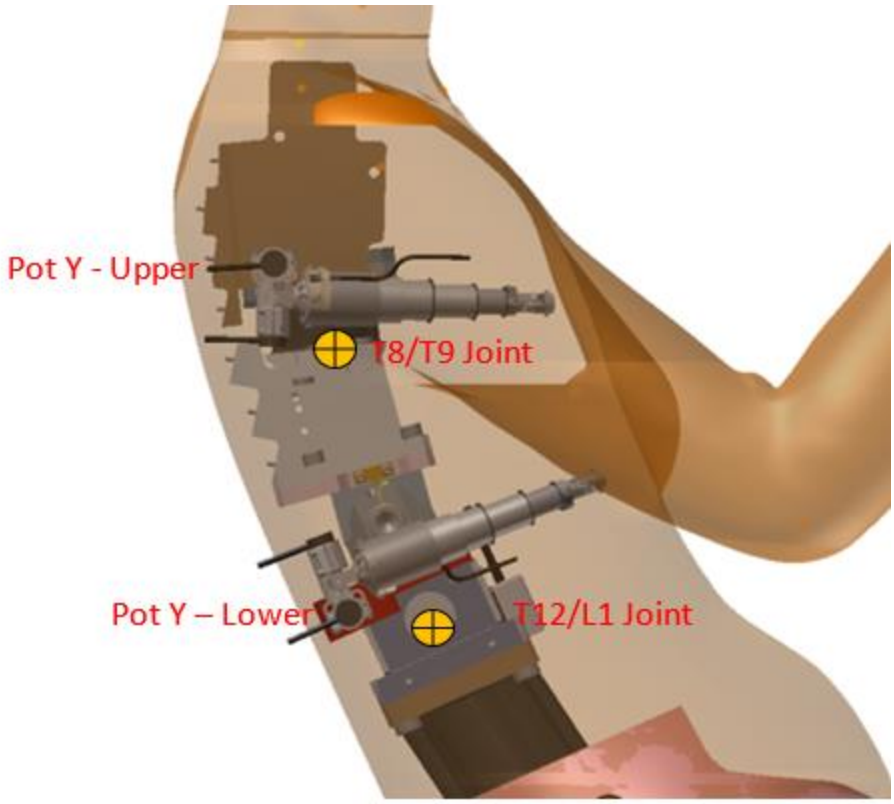

Figure 138. THOR-05F IR-TRACC Reference Position

Table 58. Coordinates of IR-TRACC position in UMTRO AMVO coordinate system (origin at hip joint center)

Position	X (mm)	Z (mm)
T8/T9 Joint	-196	273
T12/L1 Joint	-149	140
Pot Y - Upper	-223.7	309.2
Pot Y - Lower	-189.1	147.4

Data were acquired at a sampling frequency of 20,000 Hz and in the laboratory coordinate system (LCS), with the positive x-axis directed from posterior to anterior, positive y-axis directed from left to right, and positive z-axis directed from superior to inferior, per standard SAE-J211.

The kinematics of the ATD were studied using trajectories of several retroreflective targets obtained using a 16-camera, 1000 Hz motion capture cameras and data acquisition (VICON, Oxford, UK, Model Vantage) (Figure 139). These retroreflective targets were attached to the head, posterior aspect of spine, shoulders, anterior torso, pelvis and knees of the ATD. Additionally, test videos were recorded at 1000 frames per second using two on-board high-speed video cameras.

Figure 139. VICON cameras setup

Once the instrumentation was complete, a FARO Arm (FARO Technologies Inc., Florida) was used to document subject position in all three dimensions and locate the initial position of the some of the key landmarks on ATD and sled. Points were also taken for each of the VICON markers.

For all the tests, the chest jacket was used for accurate ATD representation and to take into account the influence of outer flesh/skin on the shoulder and thoracic response. In terms of input, all tests were conducted to target a 30kmph pulse. The resulting sled pulses from four tests are given in Figure 140.

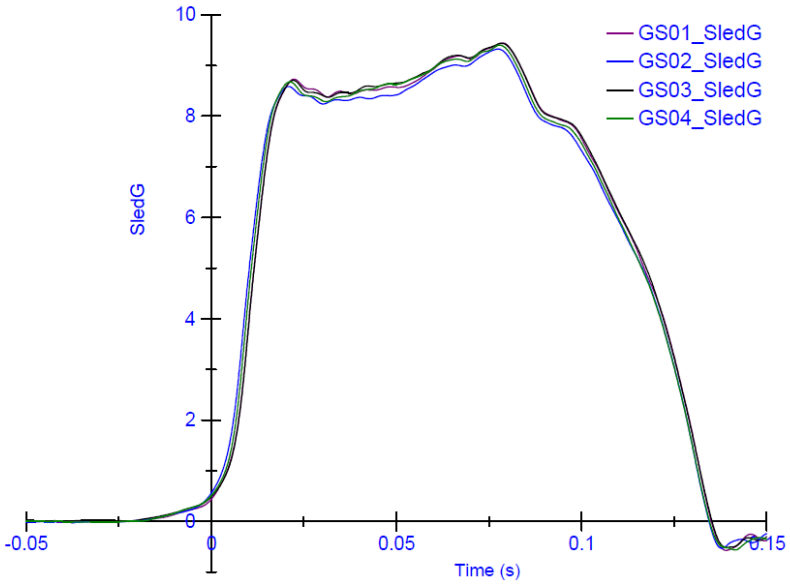

Figure 140. Sled pulses achieved for Gold Standard tests

11.1.2 Results

Responses are shown here for completeness but BioRank calculation was not performed for this test condition.

11.1.2.1 Displacement

The displacements in X, Y and Z directions of head, T1, T8, L2 and pelvis are shown in Figure 141. through Figure 155.

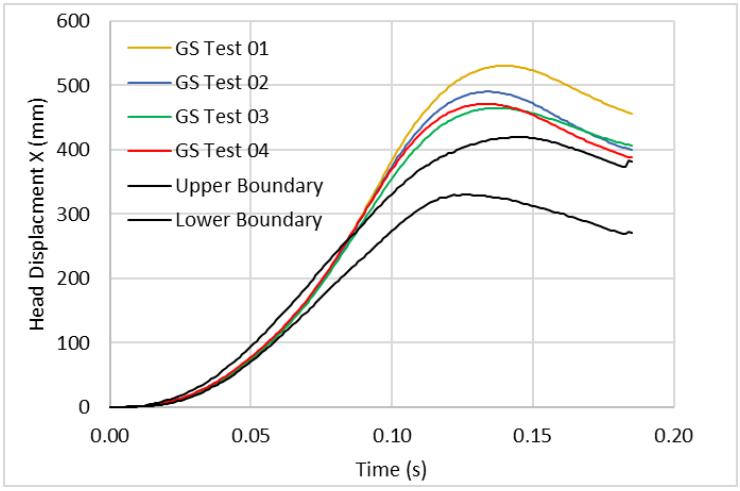

Figure 141. Head displacement X of the 30 km/h sled test

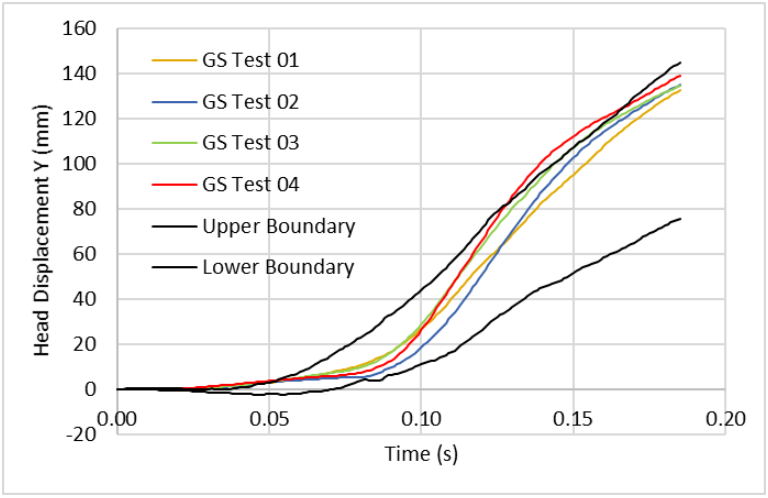

Figure 142. Head displacement Y of the 30 km/h sled test

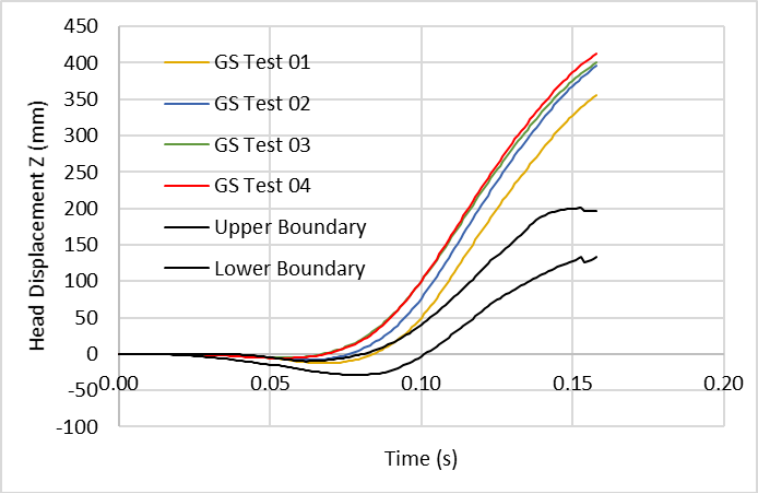

Figure 143. Head displacement Z of the 30 km/h sled test

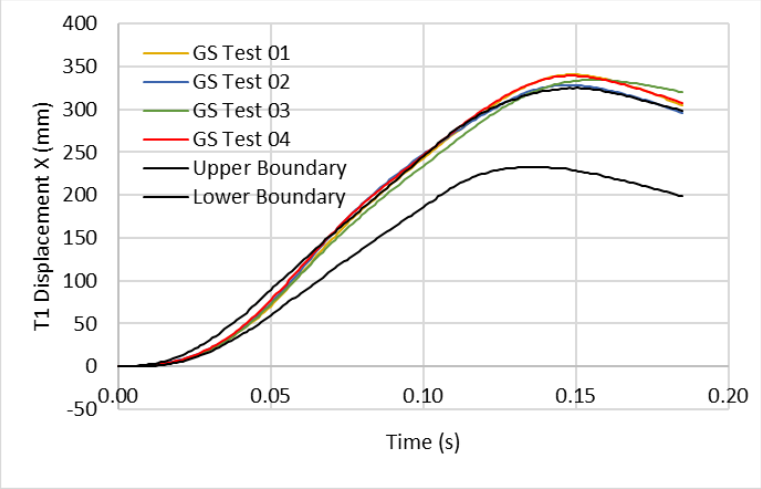

Figure 144. T1 displacement X of the 30 km/h sled test

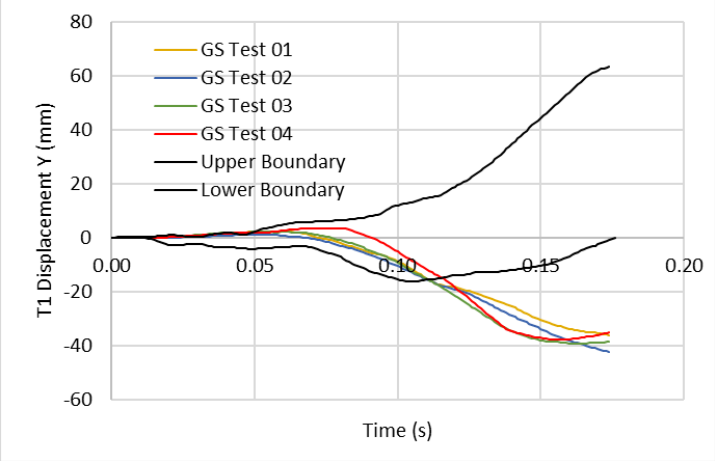

Figure 145. T1 displacement Y of the 30 km/h sled test

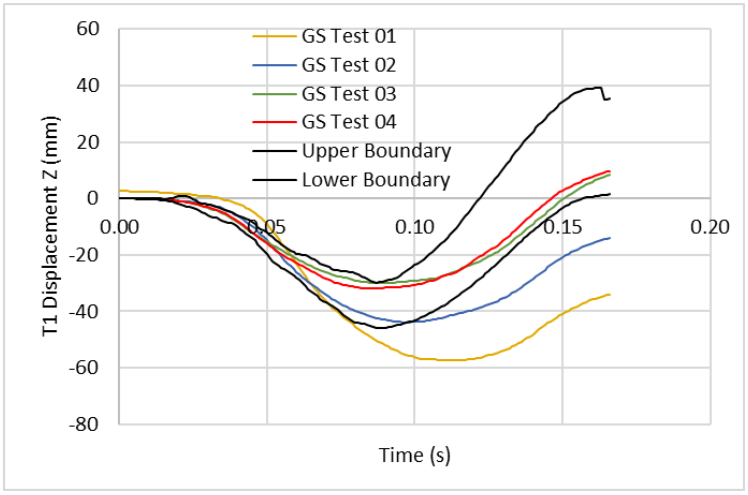

Figure 146. T1 Displacement Z of the 30 km/h sled test

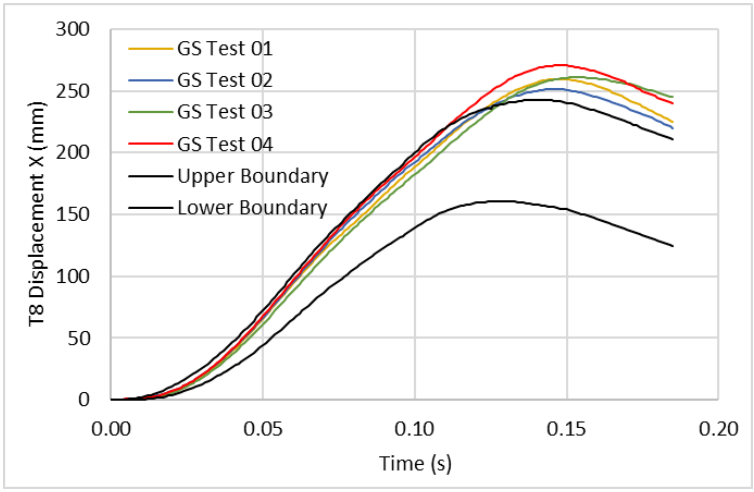

Figure 147. T8 displacement X of the 30 km/h sled test

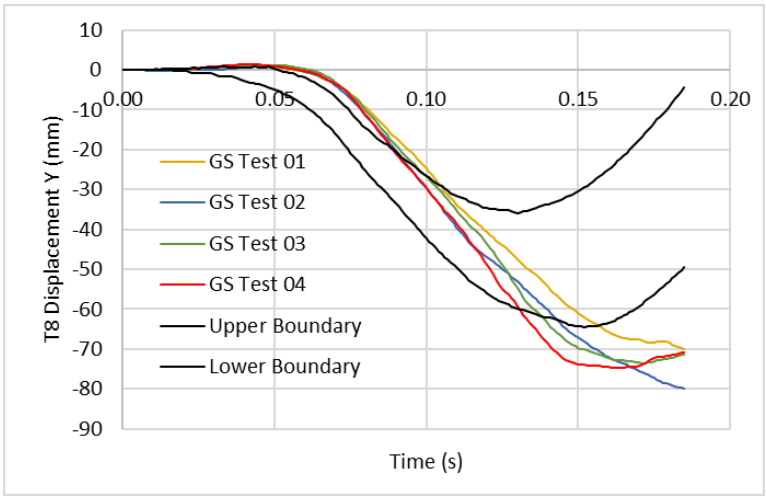

Figure 148. T8 displacement Y of the 30 km/h sled test

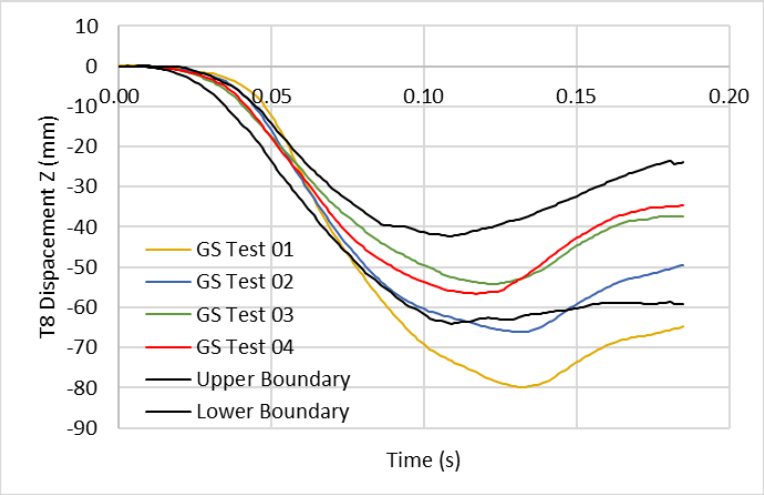

Figure 149. T8 displacement Z of 30 km/h sled test

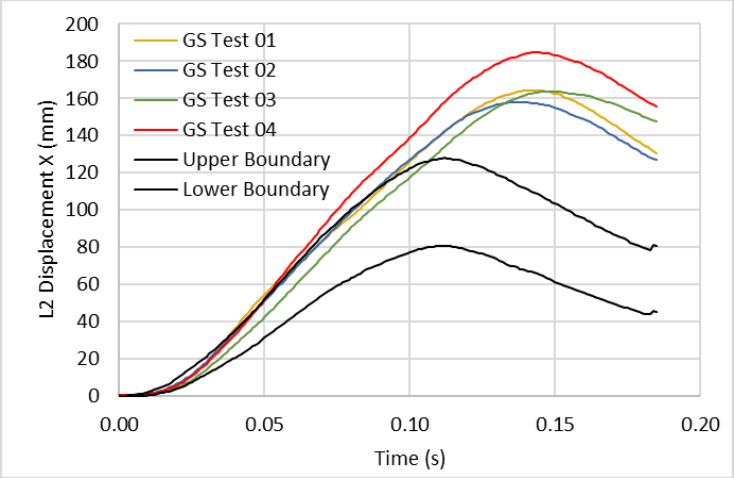

Figure 150. L2 displacement X of the 30 km/h sled test

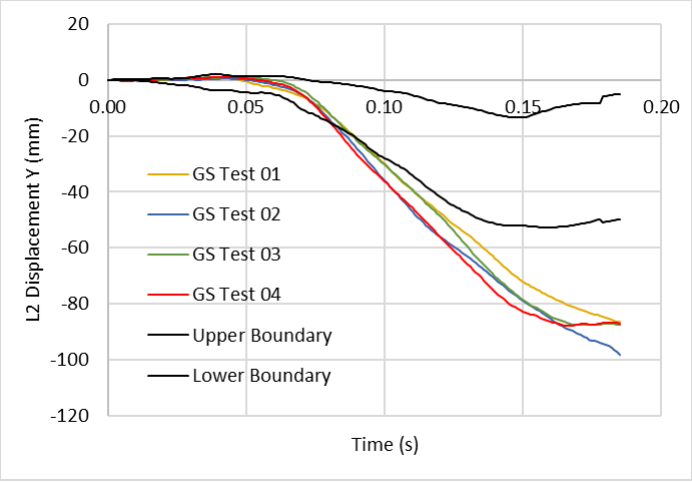

Figure 151. L2 Displacement Y of the 30 km/h sled test

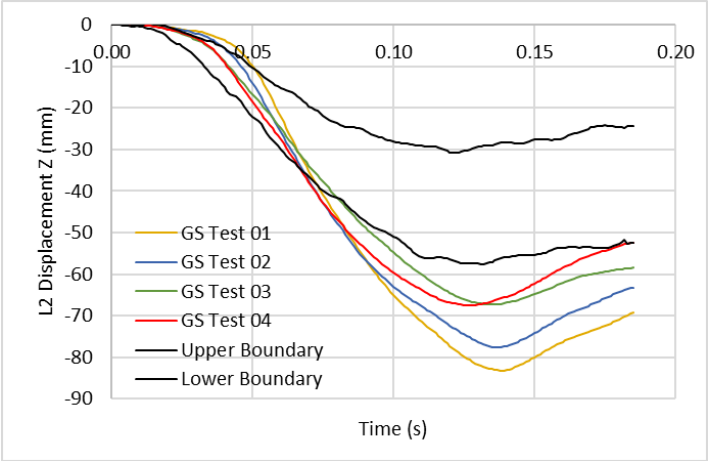

Figure 152. L2 displacement Z of the 30 km/h sled test

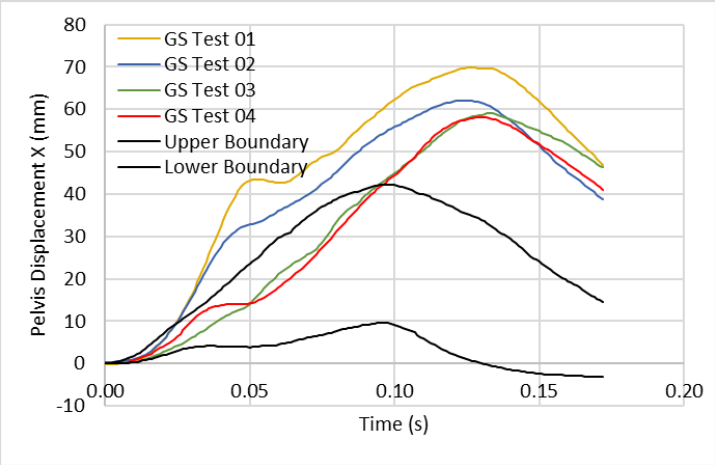

Figure 153. Pelvis displacement X of the 30 km/h sled test

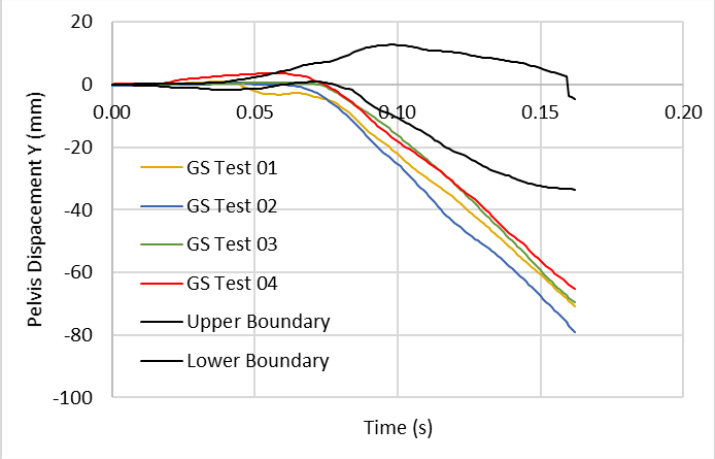

Figure 154. Pelvis displacement Y of 30 km/h sled test

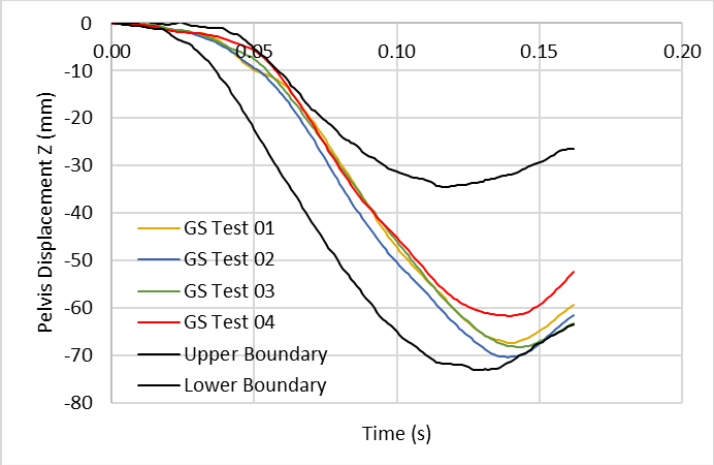

Figure 155. Pelvis displacement Z of 30 km/h sled test

11.1.2.2 Thorax Deflections

The thorax deflections of the IR-TRACCs of the THOR-05F are shown in Figure 156 through Figure 167.

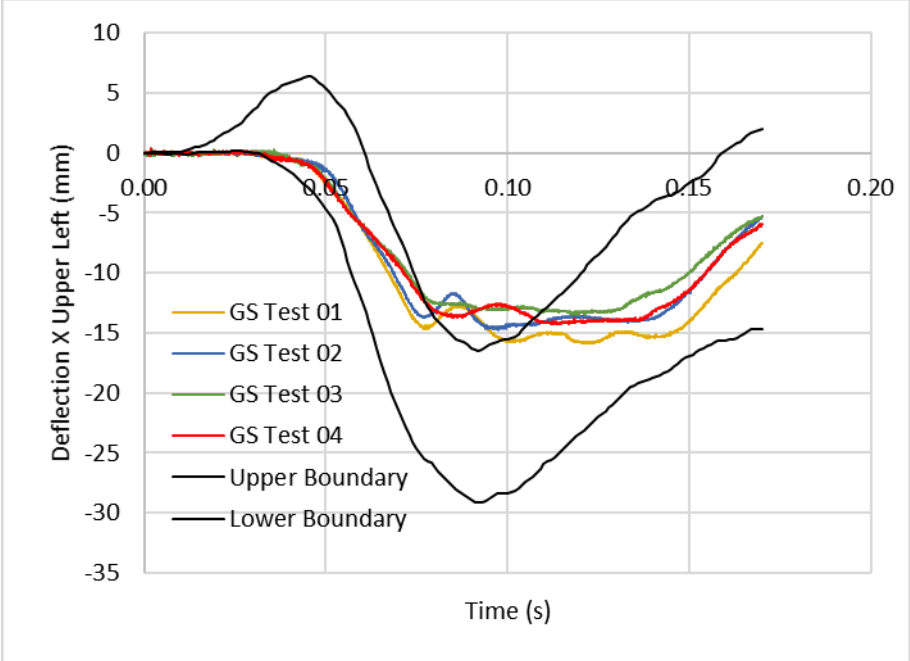

Figure 156. Chest deflection X at upper left chest position of the 30 km/h sled test

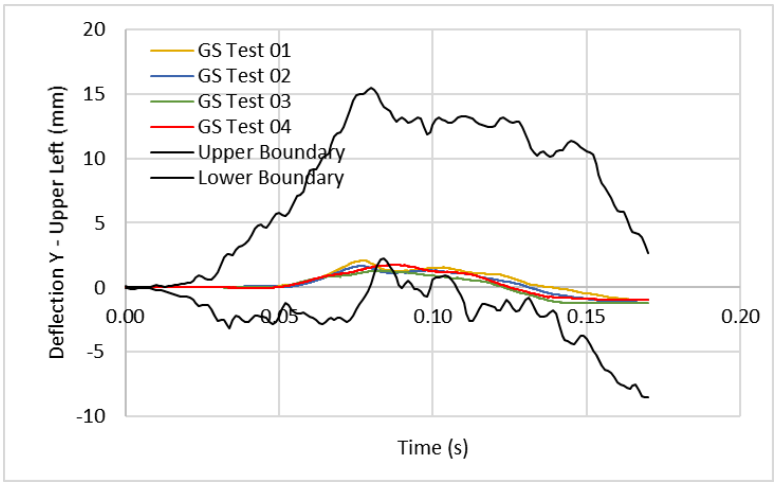

Figure 157. Chest deflection Y at upper left position of the 30 km/h sled test

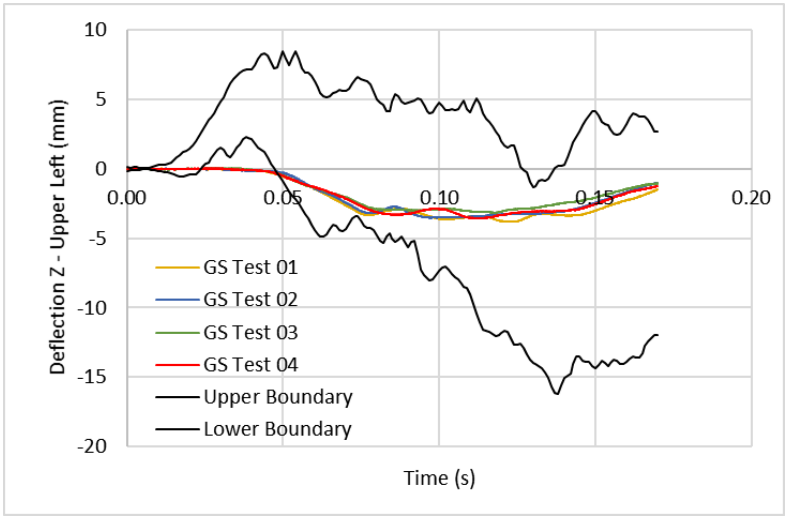

Figure 158. Chest deflection Z at upper left position of the 30 km/h sled test

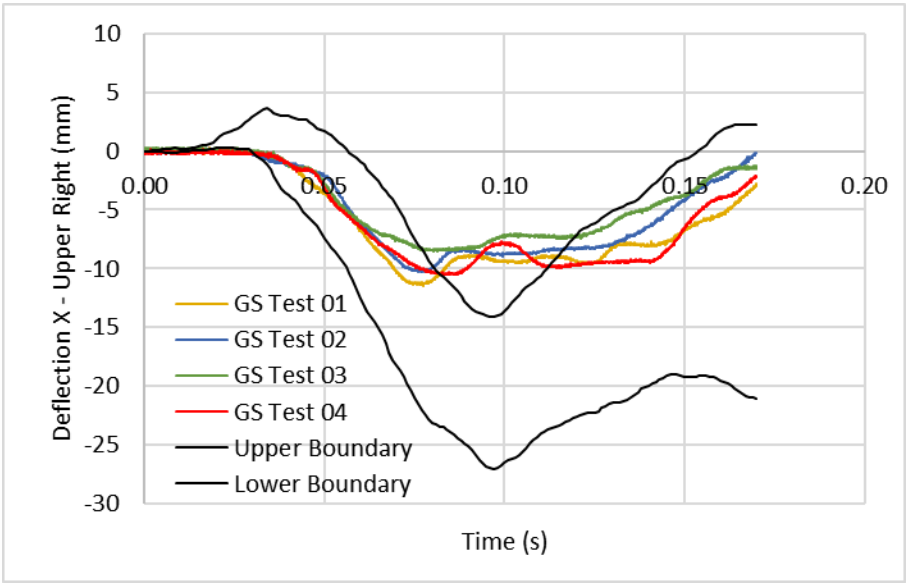

Figure 159. Chest deflection X at upper right position of the 30 km/h sled test

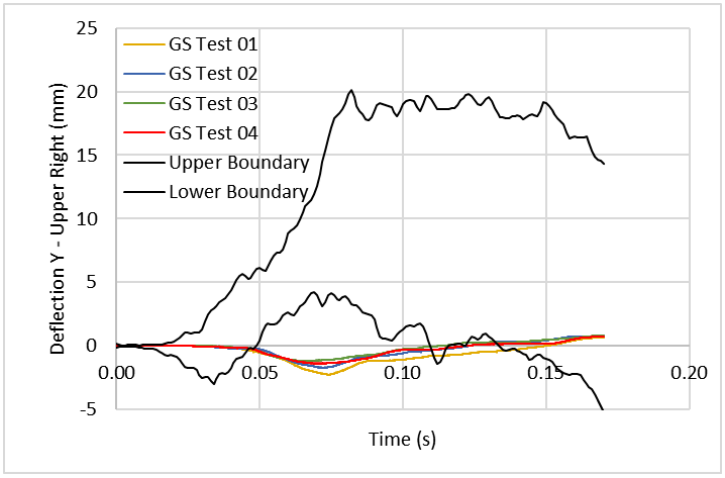

Figure 160. Chest deflection Y at upper right position of the 30 km/h sled test

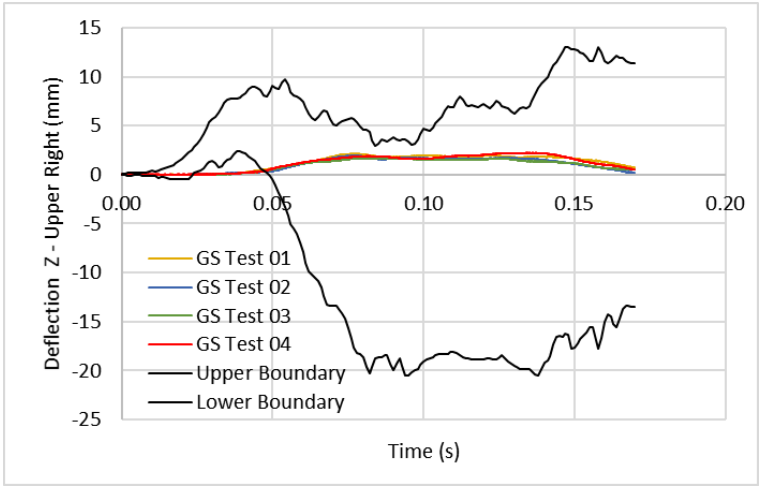

Figure 161. Chest deflection Z at upper right position of the 30 km/h sled test

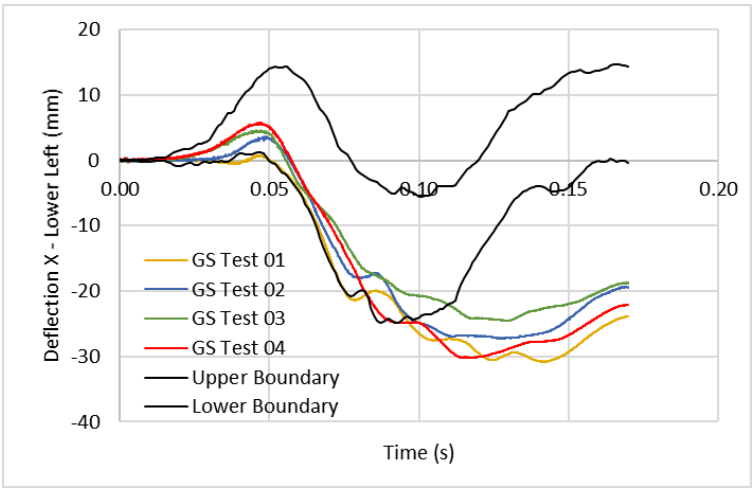

Figure 162. Chest deflection X at lower left position of the 30 km/h sled test

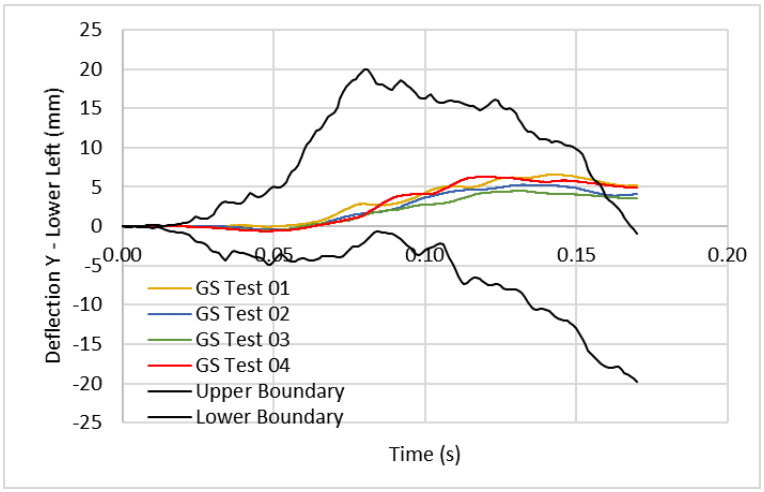

Figure 163. Chest deflection Y at lower left position of the 30 km/h sled test

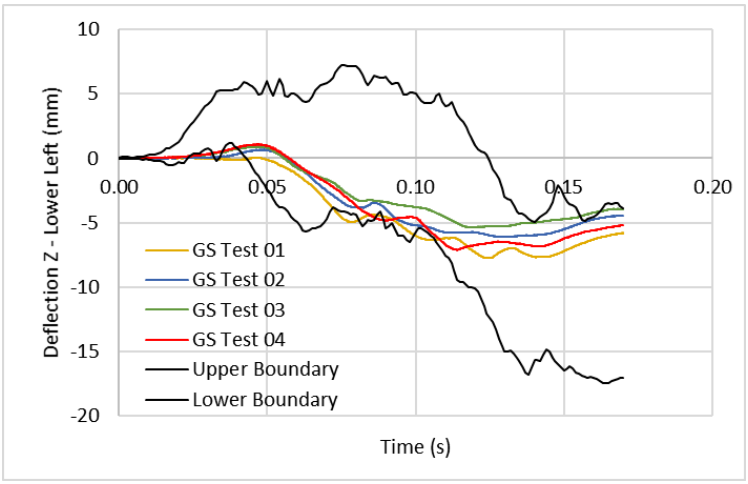

Figure 164. Chest deflection Z at lower left position of the 30 km/h sled test

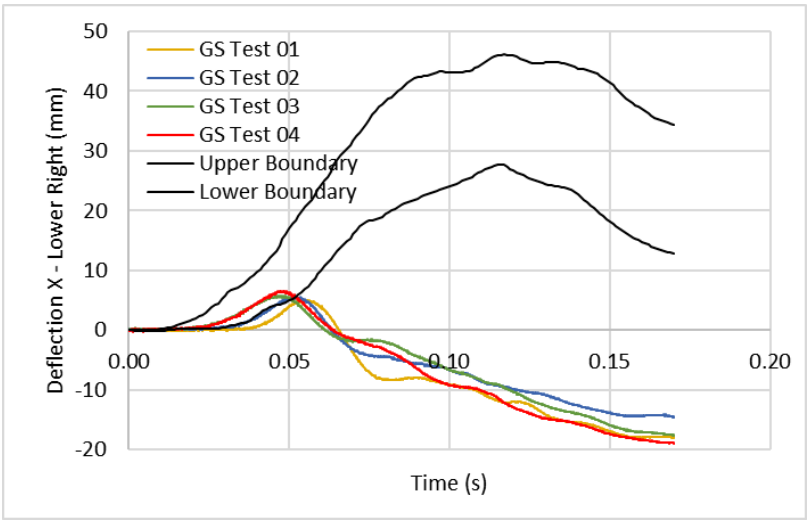

Figure 165. Chest deflection X at lower right position of the 30 km/h sled test

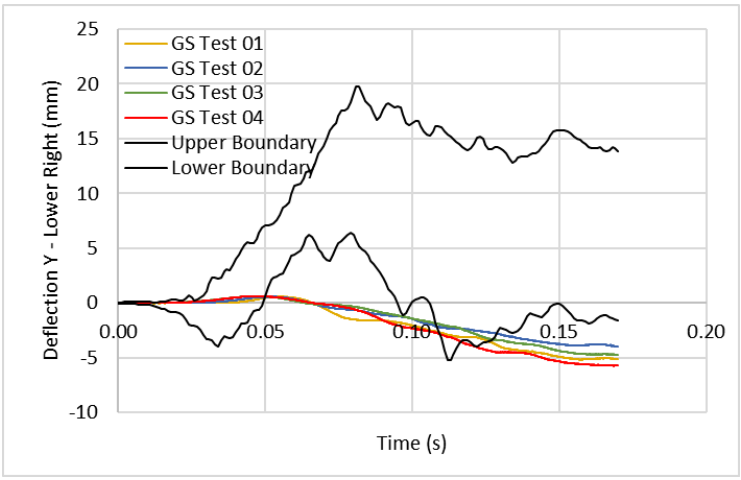

Figure 166. Chest deflection Y at lower right position of the 30 km/h sled test

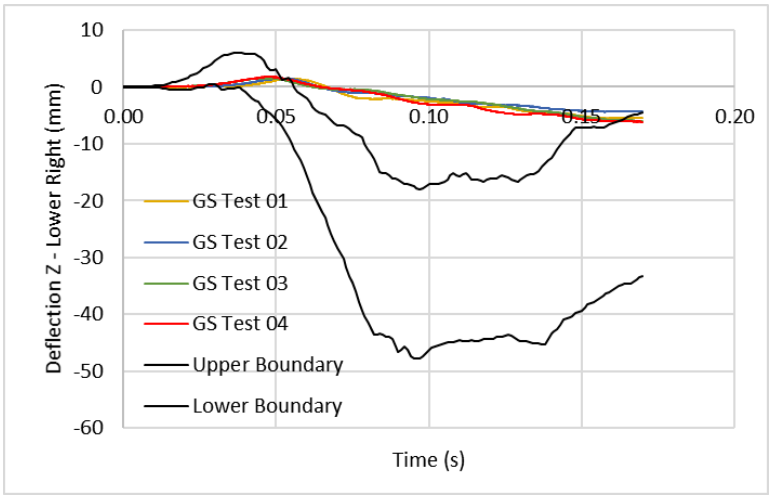

Figure 167. Chest deflection Z at lower right position of the 30 km/h sled test

11.1.2.3 Belt Force

The belt forces are shown in Figure 168 and Figure 169.

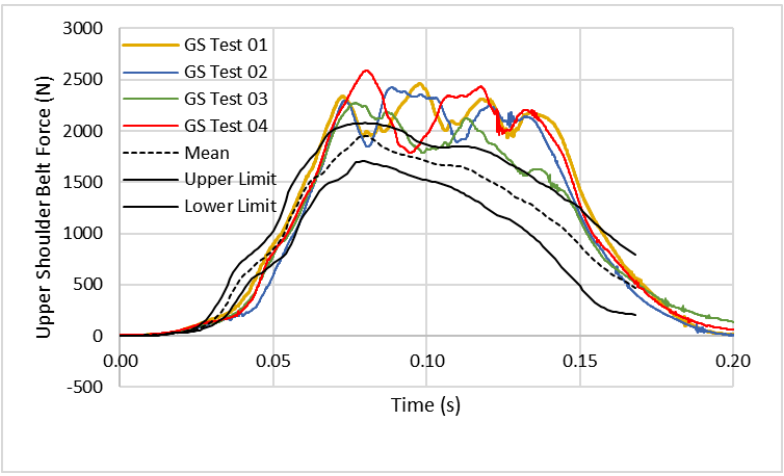

Figure 168. Upper shoulder belt force of 30 km/h sled test

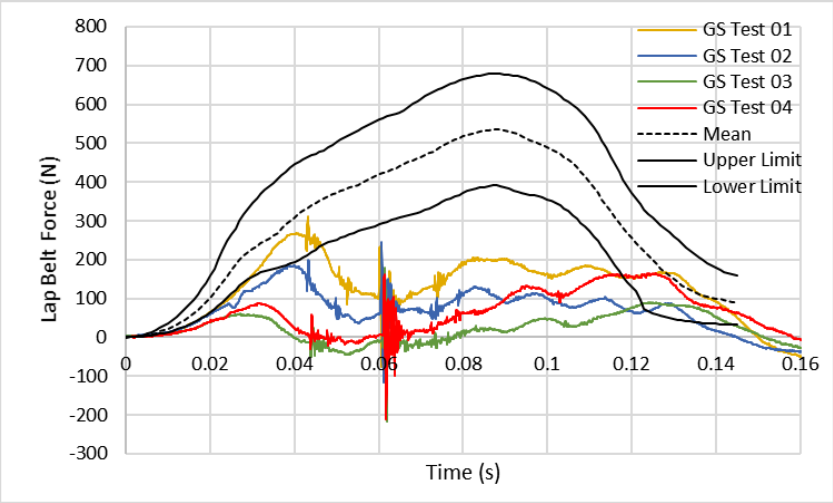

Figure 169. Lap belt force of 30 km/h sled test

11.1.2.4 Seat, Knee and Foot Force

The seat force, knee force and foot force are shown in Figure 170 through Figure 173.

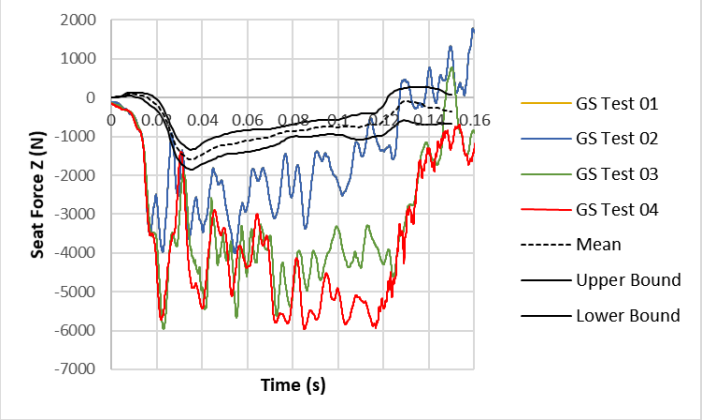

Figure 170. Seat force Z of 30 km/h sled test

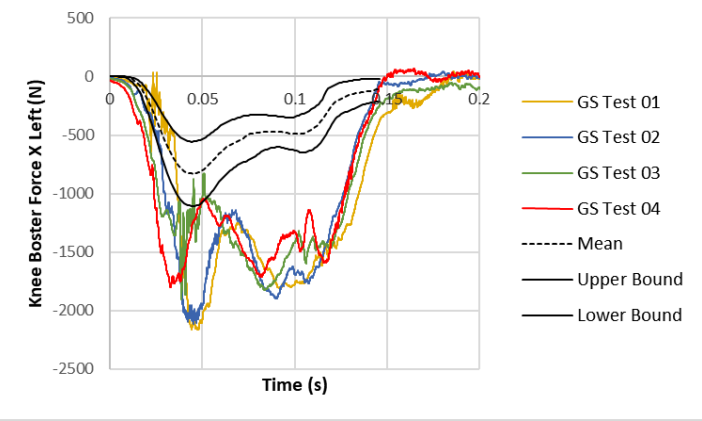

Figure 171. Knee bolster force X Left of 30 km/h sled test

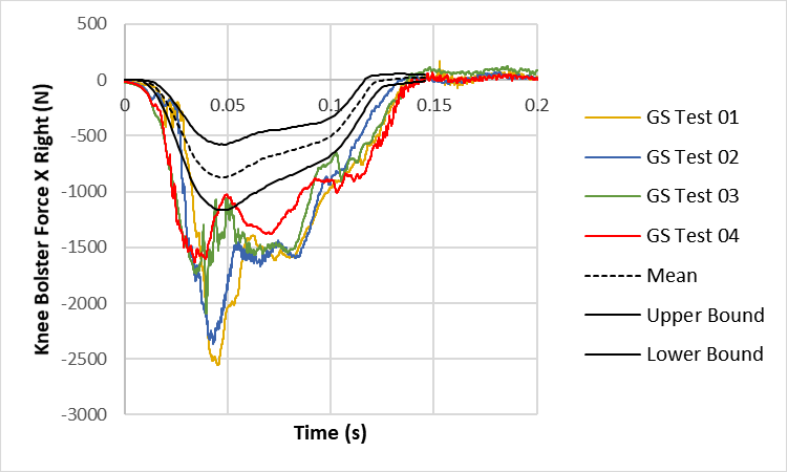

Figure 172. Knee bolster force X right of 30 km/h sled test

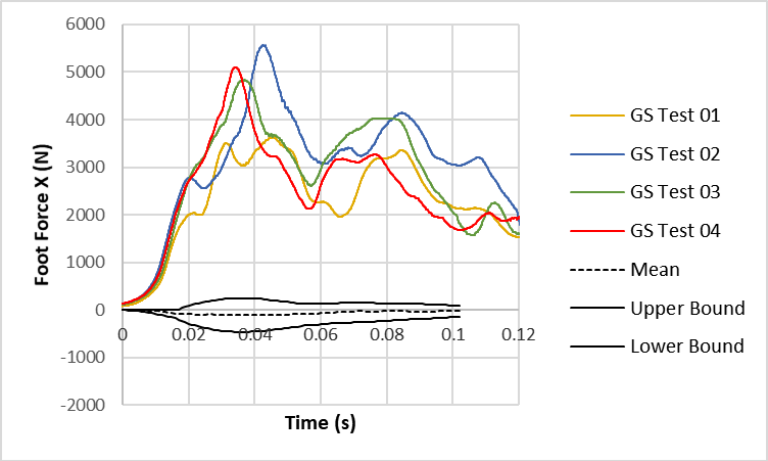

Figure 173. Foot force of 30 km/h sled test

12 Overall THOR-05F Biofidelity Summary

THOR-05F biofidelity was evaluated under twenty-three different test conditions. Only one dummy was tested in each of the twenty-three biofidelity tests. All three dummies were qualified using a subset of the test conditions, similar to the THOR-50M qualification procedures, to ensure the other two dummies had equivalent response to the dummy tested in these test conditions.

The dummy biofidelity is summarized in

Table 59. The overall ATD BioRank score of 1.51 represents “good” biofidelity of the dummy. The shoulder BioRank score is 0.81, corresponding to “excellent” biofidelity. Head, Thorax, Knee-Thigh-Hip and Lower Extremity BioRank scores are 1.32, 1.42, 1.31 and 1.47 respectively, corresponding to “good” biofidelity. The neck and abdomen BioRank are 2.20 and 2.03 respectively, corresponding to “marginal” biofidelity. The ATD withstood a minimum of three tests in each biofidelity test condition without damage. The repeatability of the ATD was reasonable for the limited tests conducted to date.

Table 59. Summary of body region BioRank

Body Region	BioRank	Biofidelity
Head	1.43	Good
Neck	2.20	Marginal
Shoulder	0.81	Excellent
Thorax	1.42	Good
Abdomen	2.03	Marginal
Knee-Thigh-Hip	1.31	Good
Lower	1.47	Good
Overall	**1.52**	**Good**

13 References

Gehre, C., Gades, H. and Wernicke, P. 2009. Objective rating of signals using test and simulation responses. Proceedings of the 21st International Technical Conference on the Enhanced Safety of Vehicles, Seoul, Korea.

Lee, E,. Parent, D.P., Craig, M.J., McFadden, J. and Moorhouse, K. 2019. Biomechanical response requirements manual: THOR 5th percentile female NHTSA advanced frontal dummy, Revision 2. DOT XXX XXX.

Lamielle, S., Vezin, P., Verriest, J.P., Petit, P., et al. 2008. 3D Deformation and dynamics of the human cadaver abdomen under seatbelt loading. Stapp Car Crash Journal, Vol. 50. SAE Paper # 2008-22-0011.

Parent, D., Craig, M., Moorhouse, K. 2017. Biofidelity evaluation of the THOR and Hybrid III 50th percentile male frontal impact anthropomorphic test devices. Stapp Car Crash Journal, Vol. 61, pp. 227-276.

Rhule, H., Donnelly, B., Moorhouse, K., Kang, Y.S., 2013. A methodology for generating objective targets for quantitively assessing the biofidelity of the crash test dummies. Proceedings of the 23rd ESV, Seoul, Korea.

Rhule, H., Moorhouse, K., Stricklin, J. 2018 Update to NHTSA's biofidelity ranking system, Proceedings of IRCOBI conference.

Schneider, L. W., Robbins, D. H., Pflug, M. S., and Snyder, R. G. 1983. Development of anthropometrically based design specifications for an advanced adult anthropometric dummy family, Volume 1. University of Michigan Transportation Research Institute, Report No. UMTRI-83-53-1.

Thunnissen, J., Wismans, J., Ewing, C.L., Thomas D.J., 1995. Human Volunteer Head-Neck Response in Frontal Flexion: A New Analysis. Thirty-ninth Stapp Car Crash Conference, San Diego, California, November 8-10, SAE Paper # 952721.

Uriot, J., Potier, P., Baudrit, P., Trosseille, X., Richard, O. and Douard, R., 2015. Comparison of HII, HIII and THOR dummy responses with respect to PMHS sled tests. Proceedings of IRCOBI Conference.

Wang, Z., McInnis, J., Benfant L., Feng, Z. and Lee, E. 2017. THOR 5th percentile female ATD design. Proceedings of the 25th International Technical Conference on the Enhanced Safety of Vehicles, Detroit, Michigan, USA.

14 Appendices

14.1 Appendix 1 – Neck Moment OC Calculations

THOR Neck OC Moment and Force Calculation

By Jerry Wang, PhD, Nov 17, 2011

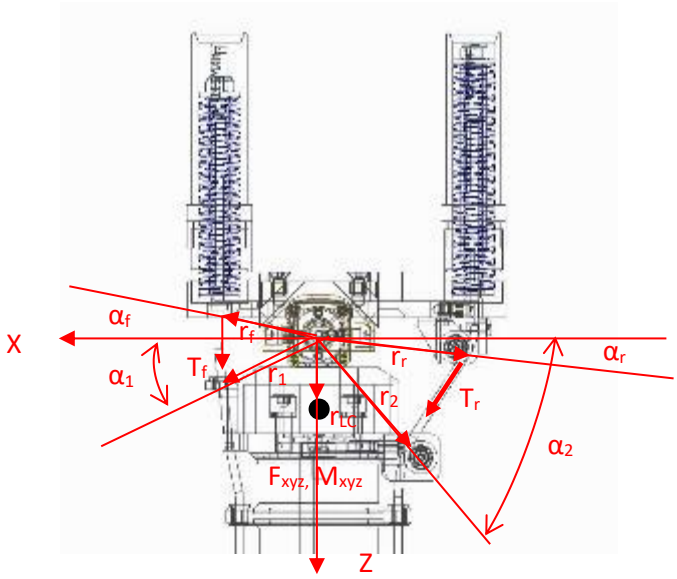

Figure 174. Neck Zero position

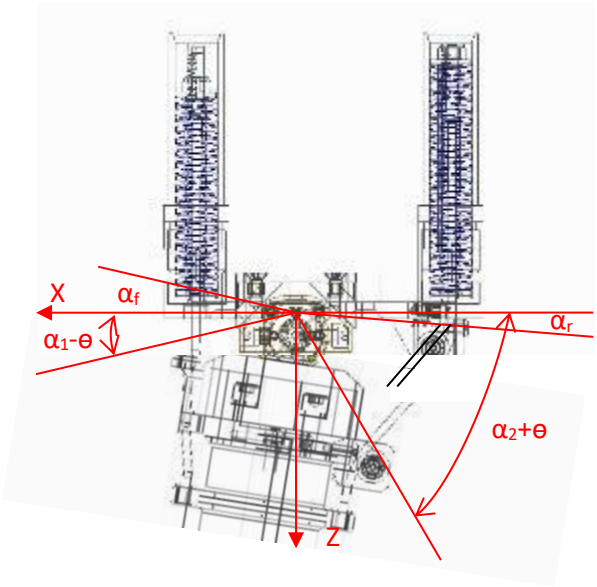

Figure 175. Position at any time point

Notes:

Neck rotary pot polarity:

Positive – hold neck, and push the head rearward

Negative – hold neck, and push the head forward

Spring load cells:

Rear Spring load cell: positive when bend head forward

Front Spring load cell: positive when bend head rearward

Upper neck load cell:

Fx: positive when hold neck and push head rearward

Fy: positive when hold neck and push head toward left

Fz: negative when push head downward

Mx: positive when hold neck and push head toward left

My: negative when hold neck and push head rearward

Mz: positive when twist the head in clock wise (nose toward right)

Notations:

V_0 – Voltage of OC pot at zero position, OC pot reading when head base plate is parallel to the load cell

V_t – Voltage of OC pot at time t

V_{FX} – Load cell Fx sensitivity

V_{FY} – Load cell Fy sensitivity

V_{FZ} – Load cell Fz sensitivity

V_{MX} – Load cell Mx sensitivity

V_{MY} – Load cell My sensitivity

V_{MZ} – Load cell Mz sensitivity

S_{oc} – OC pot sensitivity

$SF_{X,Y,Z}$ – sensitivities for lower neck load cell $F_{X,Y,Z}$

$SM_{X,Y,Z}$ – sensitivities for lower neck load cell $M_{X,Y,Z}$

S_f –sensitivity of frontal spring load cell

S_r – sensitivity of rear spring load cell

θ - OC joint rotations from zero position

r_r - distance between OC center to the rear cable contact point at head (measure from CAD design)

r_1 - distance between OC center to the rear cable contact point at neck (measure from CAD design)

r_f - distance between OC center to the front cable contact point at head (measure from CAD design)

r_2 - distance between OC center to the front cable contact point at neck (measure from CAD design)

r_{LC} – distance between OC center to the upper neck load cell neutral axis (measure from CAD design)

α_f – constant angle as shown (measurement from CAD design)

α_1 – constant angle as shown (measurement from CAD design)

α_r – constant angle as shown (measurement from CAD design)

α_2 – constant angle as shown (measurement from CAD design)

Step #1

Record V_0 of OC pot at zero position

Step #2

Trigger and record all data channels

Step #3

Calculate OC joint rotation from zero position, and moment arm angles

$\theta = Soc * (V_t - V_0)$, **do not zero OC pot data**

Step #4, Zero all load cell data at time zero

$F_{LCX}=V_{FX}*S_{FX}$

$F_{LCY}=V_{FY}*S_{FY}$

$F_{LCZ}=V_{FZ}*S_{FZ}$

$M_{LCX}=V_{MX}*S_{MX}$

$M_{LCY}=V_{MY}*S_{MY}$

$M_{LCZ}=V_{MZ}*S_{MZ}$

Step #5, Calculate the force and moment at OC

Transfer load cell readings from neck coordinate system to head coordinate system

$\overrightarrow{F_{LCH}} = \overrightarrow{T_{NH}} * \overrightarrow{F_{LC}}$

$\overrightarrow{M_{LCH}} = \overrightarrow{T_{NH}} * \overrightarrow{M_{LC}}$

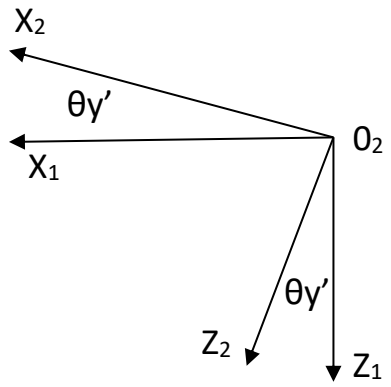

Figure 176. Coordinate rotation from neck to head

$$\begin{pmatrix} x1 \\ y1 \\ z1 \end{pmatrix} = \begin{Bmatrix} \cos(\theta x1x2) & \cos(\theta x1y2) & \cos(\theta x1z2) \\ \cos(\theta y1x2) & \cos(\theta y1y2) & \cos(\theta y1z2) \\ \cos(\theta z1x2) & \cos(\theta z1y2) & \cos(\theta z1z2) \end{Bmatrix} \begin{pmatrix} x2 \\ y2 \\ z2 \end{pmatrix}$$

$$T_{NH} = \begin{Bmatrix} \cos(\theta x1x2) & \cos(\theta x1y2) & \cos(\theta x1z2) \\ \cos(\theta y1x2) & \cos(\theta y1y2) & \cos(\theta y1z2) \\ \cos(\theta z1x2) & \cos(\theta z1y2) & \cos(\theta z1z2) \end{Bmatrix} = \begin{Bmatrix} \cos\theta & 0 & cos(90-\theta) \\ 0 & 0 & 0 \\ cos(90+\theta) & 0 & \cos\theta \end{Bmatrix} = \begin{Bmatrix} \cos\theta & 0 & \sin\theta \\ 0 & 1 & 0 \\ -sin\theta & 0 & \cos\theta \end{Bmatrix}$$

The LC force transferred to head coordinate system.

$F_{LCHX} = F_{LCX}\cos\theta + F_{LCZ}\sin\theta$

$F_{LCHY} = F_{LCY}$

$F_{LCHZ} = -F_{LCX}\sin\theta + F_{LCZ}\cos\theta$

$M_{LCHX} = M_{LCX}\cos\theta + M_{LCZ}\sin\theta$

$M_{LCHY} = M_{LCY}$

$M_{LCHZ} = -M_{LCX}\sin\theta + M_{LCZ}\cos\theta$

Calculate T_f components in head coordinate system

$$\vec{\boldsymbol{T}}_f = T_f * \overrightarrow{\boldsymbol{N}_f}$$

$$\overrightarrow{\boldsymbol{N}_f} = \frac{\overrightarrow{r_1} - \overrightarrow{r_f}}{|\overrightarrow{r_1} - \overrightarrow{r_f}|}$$

$$\overrightarrow{r_f} = r_f * \cos(90 + \alpha_f)\,\hat{x} + r_f * \sin(90 + \alpha_f)\,\hat{z} = r_f * \cos(\alpha_f)\,\hat{x} - r_f * \sin(\alpha_f)\,\hat{z}$$

$$r_{fx} = r_f * \sin(90 + \alpha_f) = r_f * \cos(\alpha_f)$$

$$r_{fz} = r_f * \cos(90 + \alpha_f) = -r_f * \sin(\alpha_f)$$

$$\overrightarrow{r_1} = r_1 * \sin[90 - (\alpha_1 - \theta)]\,\hat{x} + r_1 * \cos[90 - (\alpha_1 - \theta)]\,\hat{z}$$

$$= r_1 * \cos(\alpha_1 - \theta)\,\hat{x} + r_1 * \sin(\alpha_1 - \theta)\,\hat{z}$$

$$r_{f1} = |\overrightarrow{r_f} - \overrightarrow{r_1}| = \sqrt{[r_f * \cos(\alpha_f) - r_1 * \cos(\alpha_1 - \theta)]^2 + [r_f * \sin(\alpha_f) + r_1 * \sin(\alpha_1 - \theta)]^2}$$

$$\boldsymbol{N}_{fx} = \frac{r_1 * \cos(\alpha_1 - \theta) - r_f * \cos(\alpha_f)}{r_{f1}}$$

$$\boldsymbol{N}_{fz} = \frac{r_1 * \sin(\alpha_1 - \theta) + r_f * \sin(\alpha_f)}{r_{f1}}$$

$$T_{fx} = T_f * N_{fx}$$

$$T_{fy} = 0$$

$$T_{fz} = T_f * N_{fz}$$

Calculate T_r components in head coordinate system

$$\vec{\boldsymbol{T}}_r = T_r * \overrightarrow{\boldsymbol{N}_r}$$

$$\overrightarrow{\boldsymbol{N}_r} = \frac{\overrightarrow{r_2} - \overrightarrow{r_r}}{|\overrightarrow{r_2} - \overrightarrow{r_1}|}$$

$$\overrightarrow{r_r} = r_r * \sin[-(90-\alpha_r)]\hat{x} + r_r * \cos[-(90-\alpha_r)]\,\hat{z}$$

$$= -r_r * \cos(\alpha_r)\,\hat{x} + r_r * \sin(\alpha_r)\,\hat{z}$$

$$r_{rx} = -r_r * \cos(\alpha_r)$$

$$r_{rz} = r_r * \sin(\alpha_r)$$

$$\overrightarrow{r_2} = r_2 * \sin\{-[90-(\alpha_2+\theta)]\}\,\hat{x} + r_2 * \cos\{-[90-(\alpha_2+\theta)]\}$$

$$= -r_2 * \cos(\alpha_2+\theta)\,\hat{x} + r_2 * \sin(\alpha_2+\theta)\,\hat{z}$$

$$r_{r2} = |\overrightarrow{r_r} - \overrightarrow{r_2}| = \sqrt{[-r_r * \cos(\alpha_r) + r_2 * \cos(\alpha_2+\theta)]^2 + [r_r * \sin(\alpha_r) - r_2 * \sin(\alpha_2+\theta)]^2}$$

$$N_{rx} = \frac{-r_2 * \cos(\alpha_2+\theta) + r_r * \cos(\alpha_r)}{r_{r2}}$$

$$N_{rz} = \frac{r_2 * \sin(\alpha_2+\theta) - r_r * \sin(\alpha_r)}{r_{r2}}$$

$$T_{rx} = T_r * N_{rx}$$

$$T_{ry} = 0$$

$$T_{rz} = T_r * N_{rz}$$

$$\vec{\boldsymbol{F}}_{OC} = -(\vec{\boldsymbol{F}}_{LC} + \vec{T}_r + \vec{T}_f)$$

This above force is the force applied to the head, the reaction force applied to the neck is:

$$\vec{\boldsymbol{F}}_{OC} = \vec{\boldsymbol{F}}_{LC} + \vec{T}_r + \vec{T}_f$$

i.e.

$$F_{OCx} = F_{LCHx} + T_{rx} + \mathrm{T_{fx}}$$

$$F_{OCy} = F_{LCy}$$

$$F_{OCz} = F_{LCHz} + T_{rz} + \mathrm{T_{fz}}$$

$$\overrightarrow{r_{LC}} = r_{LC} * sin\theta\,\hat{x} + r_{LC} * cos\theta\,\hat{z}$$

i.e.

$r_{LCz} = r_{LC} * sin\theta$

$r_{LCz} = r_{LC} * cos\theta$

Calculate the Moment at OC in head coordinate system

$\overrightarrow{\boldsymbol{M}_{OC}} = -(\overrightarrow{\boldsymbol{M}_{LCH}} + \overrightarrow{r_{LC}} \otimes \overrightarrow{\boldsymbol{F}_{LCH}} + \overrightarrow{r_r} \otimes \overrightarrow{\boldsymbol{T}_r} + \overrightarrow{r_f} \otimes \overrightarrow{\boldsymbol{T}_f})$

The above moment is the moment applied to the head, the reaction moment applied to the neck is

$\overrightarrow{\boldsymbol{M}_{OC}} = \overrightarrow{\boldsymbol{M}_{LCH}} + \overrightarrow{r_{LC}} \otimes \overrightarrow{\boldsymbol{F}_{LCH}} + \overrightarrow{r_r} \otimes \overrightarrow{\boldsymbol{T}_r} + \overrightarrow{r_f} \otimes \overrightarrow{\boldsymbol{T}_f}$

$= M_{LCHx}\hat{x} + M_{LCHy}\hat{y} + M_{LCHz}\hat{z} + (r_{LCx}\hat{x} + r_{LCz}\hat{z}) \otimes (F_{LCHx}\hat{x} + F_{LCHy}\hat{y} + F_{LCHz}\hat{z})$

$+(r_{rx}\hat{x} + r_{rz}\hat{z}) \otimes (T_{rx}\hat{x} + T_{rz}\hat{z}) + (r_{fx}\hat{x} + r_{fz}\hat{z}) \otimes (T_{fx}\hat{x} + T_{fz}\hat{z})$

$= (M_{LCHx} - r_{LCz} * F_{LCHy})\,\hat{x}$

$+(M_{LCHy} - r_{LCx} * F_{LCHz} + r_{LCz} * F_{LCHx} - r_{rx} * T_{rz} + r_{rz} * T_{rx} - r_{fx} * T_{fz} + r_{fz} * T_{fx})\,\hat{y}$

$+(M_{LCHz} + r_{LCx} * F_{LCHy})\,\hat{z}$

i.e.

$M_{OCx} = M_{LCHx} - r_{LCz} * F_{LCHy}$

$M_{OCx} = M_{LCX}\cos\theta + M_{LCZ}\sin\theta - r_{LC} * cos\theta * F_{LCy}$

$M_{OCy} = M_{LCHy} - r_{LCx} * F_{LCHz} + r_{LCz} * F_{LCHx} - r_{rx} * T_{rz} + r_{rz} * T_{rx} - r_{fx} * T_{fz} + r_{fz} * T_{fx}$

$= M_{LCHy} - r_{LC} * sin\theta * (-F_{LCX}\sin\theta + F_{LCZ}\cos\theta) + r_{LC} * cos\theta * (F_{LCX}\cos\theta + F_{LCZ}\sin\theta) - r_{rx} * T_{rz} + r_{rz} * T_{rx} - r_{fx} * T_{fz} + r_{fz} * T_{fx}$

$= M_{LCHy} + r_{LC} * F_{LCX} * sin^2\theta - r_{LC} * F_{LCZ} * sin\theta * \cos\theta + r_{LC} * F_{LCX} * cos^2\theta + r_{LC} * F_{LCZ} * \sin\theta * cos\theta - r_{rx} * T_{rz} + r_{rz} * T_{rx} - r_{fx} * T_{fz} + r_{fz} * T_{fx}$

$M_{OCy} = M_{LCy} + r_{LC} * F_{LCX} - r_{rx} * T_{rz} + r_{rz} * T_{rx} - r_{fx} * T_{fz} + r_{fz} * T_{fx}$

Figure 177. Constants for neck moment calculations.

Additional simplifications if necessary for M_{OCy}

$= M_{LCy} + r_{LC} * F_{LCX} + r_r * \cos(\alpha_r) * T_{rz} + r_r * \sin(\alpha_r) * T_{rx} - r_f * \cos(\alpha_f) * T_{fz} - r_f * \sin(\alpha_f) * T_{fx}$

$= M_{LCy} + r_{LC} * F_{LCX} + r_r * T_{rz} * \cos\alpha_r + r_r * T_{rx} * \sin\alpha_r - r_f * T_{fz} * \cos\alpha_f - r_f * T_{fx} * \sin\alpha_f$

$\boldsymbol{M_{OCy} = M_{LCy} + r_{LC} * F_{LCX} + r_r * (T_{rz} * \cos\alpha_r + T_{rx} * \sin\alpha_r) - r_f * (T_{fz} * \cos\alpha_f + T_{fx} * \sin\alpha_f)}$

$M_{OCz} = M_{LCHz} + r_{LCx} * F_{LCHy}$

$M_{OCz} = -M_{LCX}\sin\theta + M_{LCZ}\cos\theta + r_{LC} * sin\theta * F_{LCy}$

14.2 Appendix 2 – Pendulum Effective Mass Calculation

Objective: Effective pendulum mass of 3.00 ± 0.02 kg (6.614 ± 0.044 lbs).

The effective pendulum mass is the total mass attached to the lower one-third of the pendulum arm. The pendulum arm must be ~47.6" in length and be made out of 1" x 1" x 1/8" aluminum with a density of ~2.7g/cm^3. The pendulum must have a lower block that is welded to the impact end of the pendulum arm which is used for attaching the impact face and ballast necessary to meet the mass specification. Since the lower block is welded to the pendulum arm, the mass of the lower one-third of the pendulum arm must be approximated:

Cross Sectional Area of Square Tubing: (1" x 1") – (.75" x .75") = .4375 in^2

Volume of Pendulum Arm: (.4375 in^2) * (47.6") = 20.825 in^3 (341.26 cm^3)

Mass of Pendulum Arm: (341.26 cm^3) * (2.7 g/cm^3) = 921.4 grams

1/3 Mass of Pendulum Arm: 921.4 grams / 3 = 307 grams (.307 kg)

½ Mass of the Pendulum Arm (For Reference): 921.4 grams / 2 = 461 grams (.461 kg)

Measure the mass of the pendulum arm assembly as described in Figure 178.

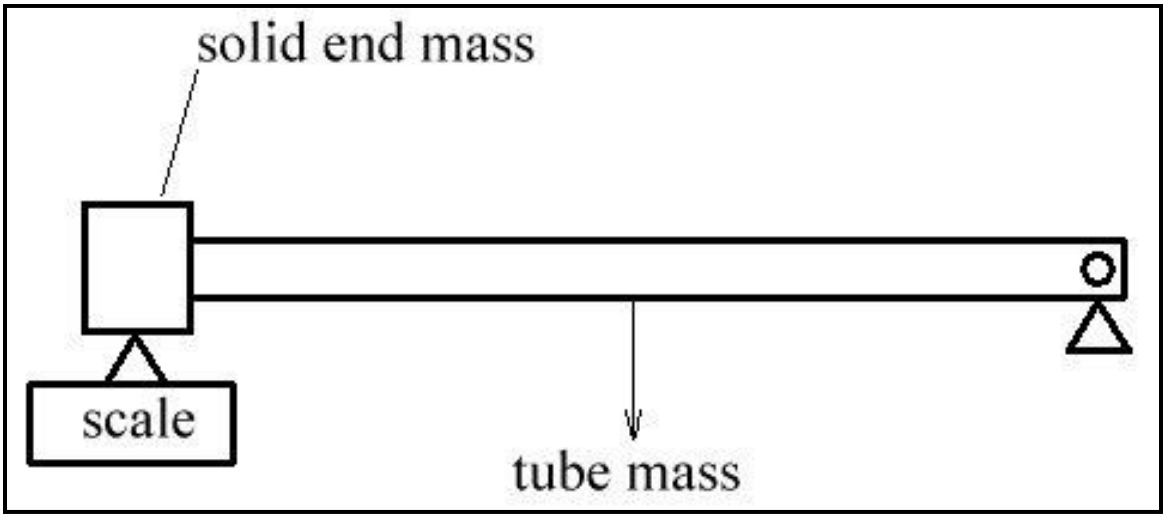

Figure 178. Pendulum arm mass measurement

The measurement read by the scale will be equal to the mass of the solid end plus ½ of the mass of the pendulum arm. In order to get the effective pendulum mass, subtract half of the pendulum arm mass (461 kg) and add the one-third mass of the pendulum arm (.307 kg). Essentially, subtracting .154 kg from the measured value. Adjust the ballast mass as necessary to meet the mass specification (3.00 ± 0.02 kg).

14.3 APPENDIX 3 – Inversion/Eversion Test Bracket Design

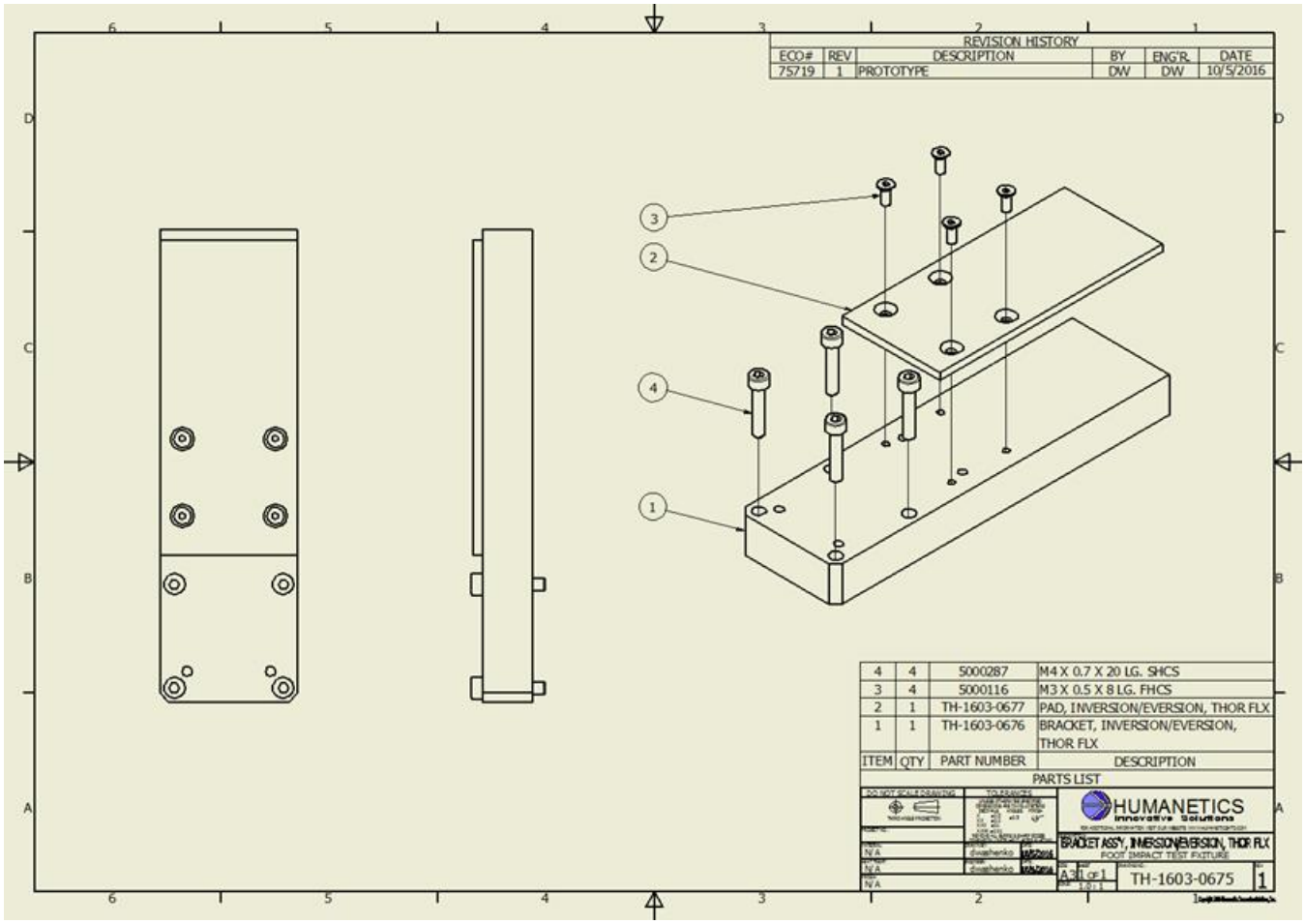

Figure 179. Inversion/eversion test bracket

14.4 APPENDIX 4 – Bolt Torque

Table 60. Bolt torque for metric fasteners

Diameter	Recommended Seatin						
	ISO 4762DIN 912		DIN 7984	ISO 10642DIN 7991		ISO 7380	
	Socket CapScrews		Low HeadSocket Cap Screws	Flat HeadCountersunk Socket Cap Screws		Button HeadSocket Cap Screws	
	10.9	12.9	10.9	10.9	12.9	10.9	12.9
M1.6	0.25	0.30					
M2	0.50	0.63					
M2.5	1.03	1.27					
M3	1.83	2.20	1.15	1.15	1.35	1.15	1.35
M4	4.27	4.83	2.70	2.70	3.10	2.70	3.10
M5	8.64	10.0	5.40	5.40	6.10	5.40	6.10
M6	14.7	16.8	9.15	9.15	10.5	9.15	10.5
M6.5							
M8	35.6	41.0	22.0	22.0	26.0	22.0	26.0
M10	70.6	81.0	44.0	44.0	52.0	44.0	52.0
M12	123	142	77.0	77.0	90.0	77.0	90.0
M13							
M14	195	226	122	122	143		
M16	305	350	190	190	225	190	225
M18	420	485	262				
M20	596	685	371	370	440		
M22	811	930					
M24	1031	1180					
M25							
M27	1508	1730					
M30	2048	2380					
M33	2787	3262					
M36	3580	4190					
M39	4633	5420					